CFD Modeling and Simulation of High Speed Reacting Flows: Theory

Tomasz (Tom) G. Drozda

tomasz.g.drozda@nasa.gov

Hypersonic Airbreathing Propulsion Branch

NASA Langley Research Center

Hampton Virginia

With contributions from Dr. Rob Baurle, Jeff White, and Dr. Phil Drummond.

Outline

- Introduction
- Governing Transport Equations
- Nondimensionalization
- Introduction to Modeling and Simulation
- Numerical Methods
- Example Applications

Hypersonic Airbreathing Propulsion Branch at NASA

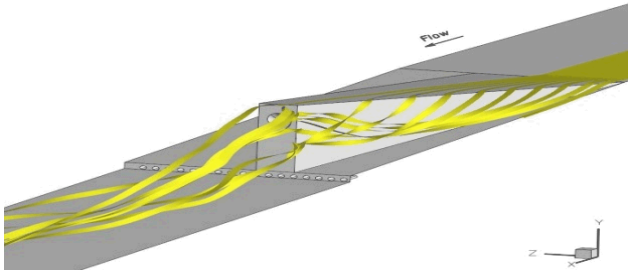

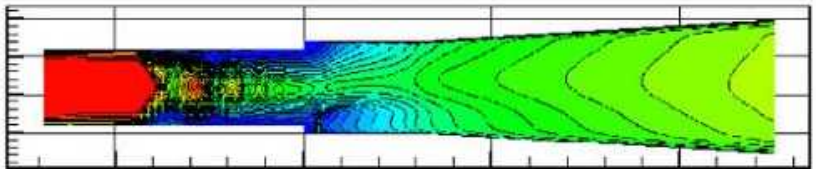

Physics Model Development, Numerical Methods, and Code Development

Experimental Airbreathing Propulsion

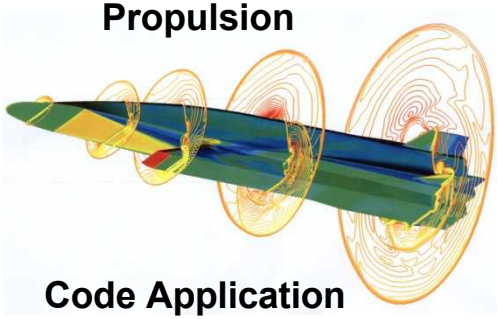

Code Application

MISSION

Conduct multidisciplinary research to develop advanced technology for hypersonic airbreathing propulsion systems for aerospace vehicles.

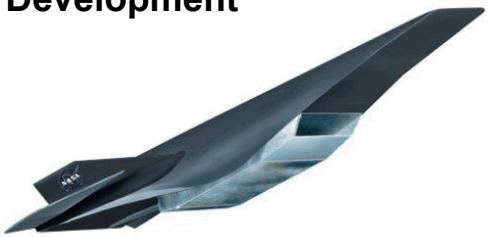

Vehicle Configuration Development and Optimization

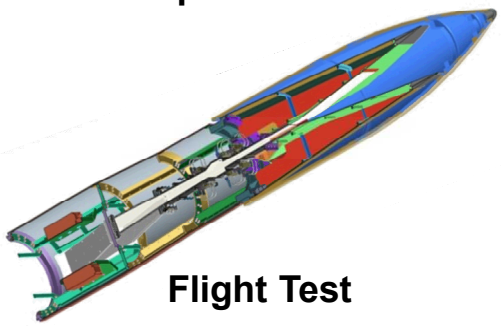

Flight Test

http://hapb-www.larc.nasa.gov

Introduction: High-Speed Atmospheric Flight

Hypersonic Vehicle Applications

- Military

(rapid response and strike on global scale)

- Aerospace

(safer and more affordable access to space)

- Civil Aviation

(point-to-point transport)

Types of Vehicle:

- Gliders (re-entry, unpowered cruise)
- Airbreathers (launch, cruise, re-entry)

Types of Hypersonic Propulsion:

- Ramjet (RJ) / Scramjet (SJ)
- Turbine-based combined cycle (TBCC)
- Rocket-based combined cycle (RBCC)
- Air-augmented or ducted rocket (DR)
- Rocket

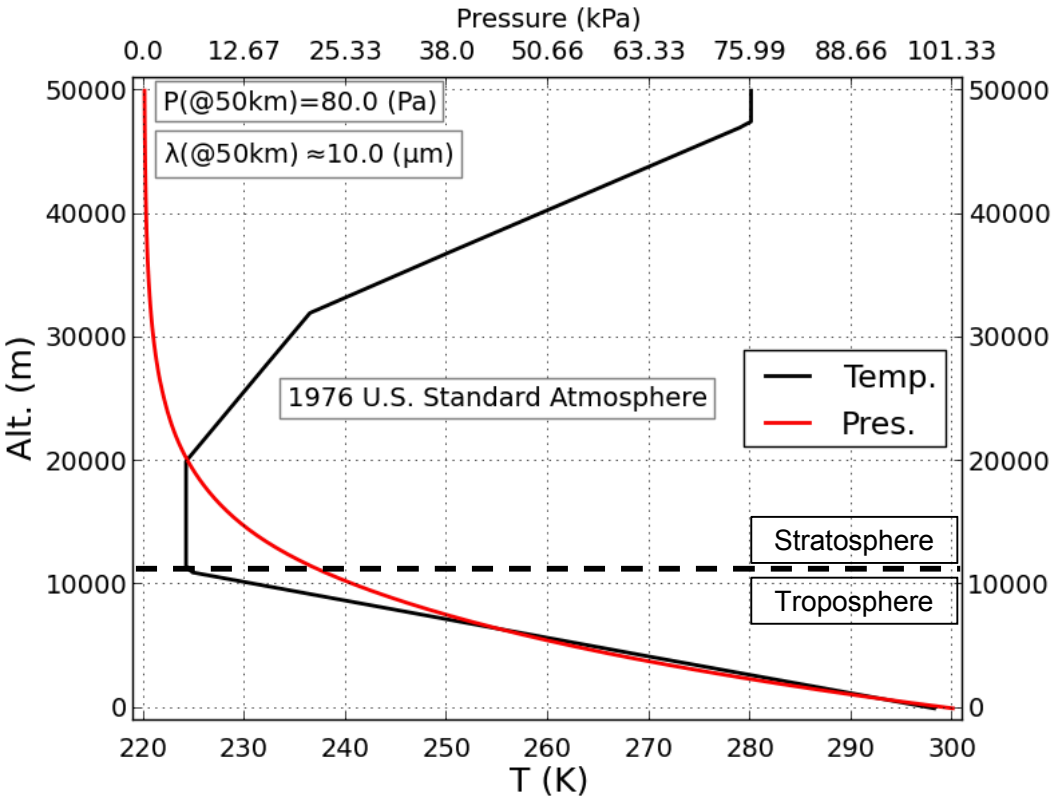

Main Benefit of Hypersonic Airbreathing Propulsion (oxidizer ~ 94% of propellant mass):

- Vehicle only needs to carry fuel for its propulsive needs, thereby
  - allowing for larger payloads or …
  - lighter vehicle (less structure to support weight) or …
  - more fuel for longer range

Hypersonic Access-to-Space Flight Trajectories

- Bernoulli's equation for a moving fluid gives rise to the *Dynamic Pressure*:

$$q_0(Pa) = \frac{\rho u^2}{2} = \frac{1}{2}\gamma p M_0^2$$

which is the kinetic component of the total pressure

- *q* is a useful aerodynamic parameter that is related to lift and drag forces of a vehicle:

$$L(N) = q_0\, C_L\, S$$
$$D(N) = q_0\, C_D\, S$$

- *When q* is too large, the structural forces and the drag can become excessive.
- When *q* is too small, the wing area required for controlled sustained flight may become too large

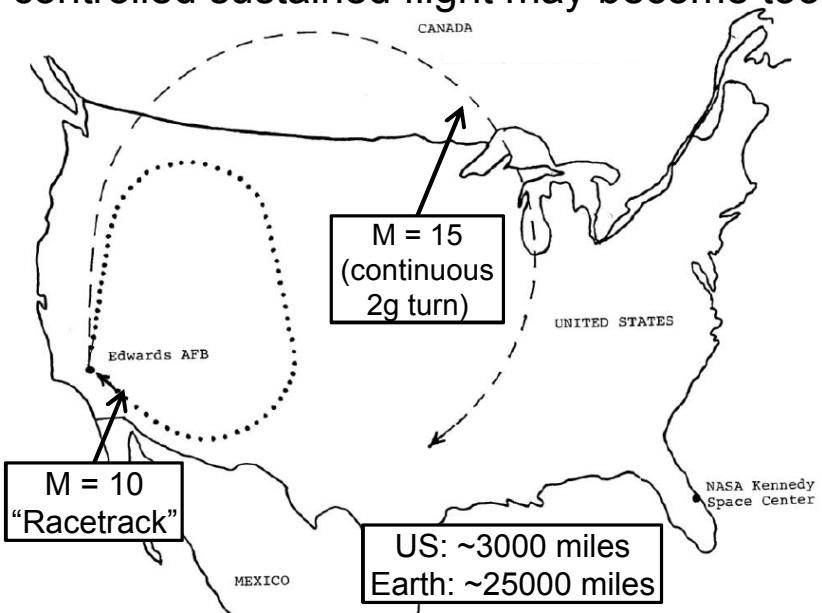

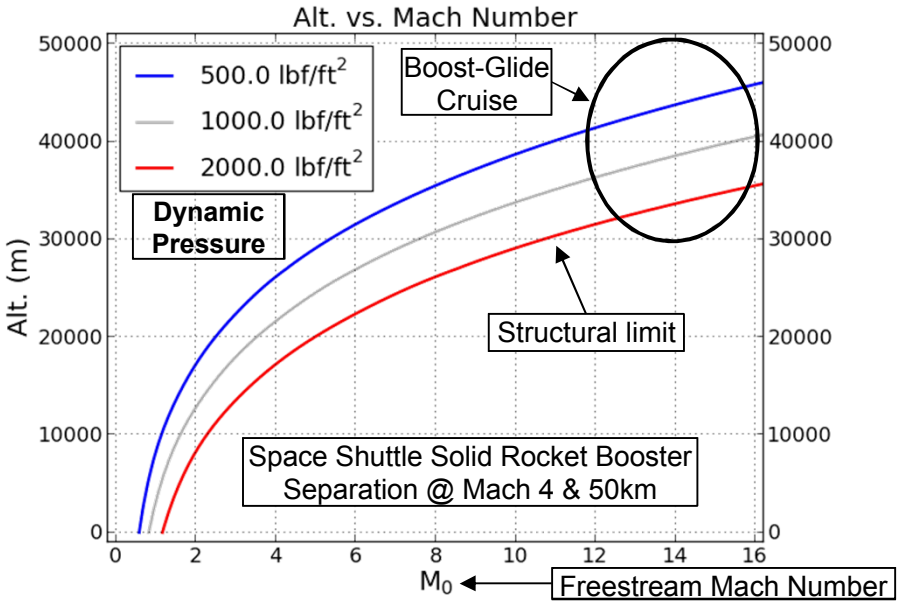

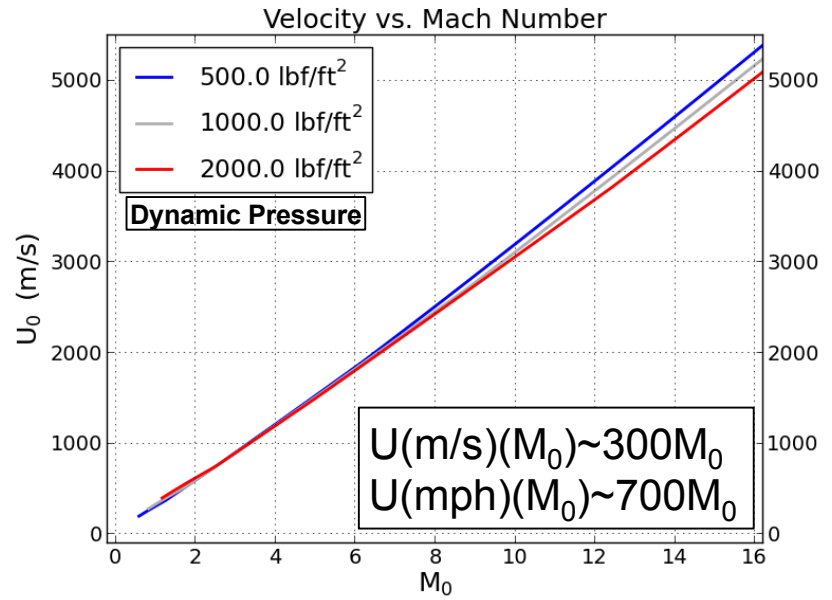

Mass Flow Rate and Engine Thrust

- Mass flow rate of air through the engine can also be related to the *Dynamic Pressure, q*:

$$\dot{m}_0 \left(\frac{kg}{s}\right) = \dot{m}_0'' A_0 = \frac{2q}{u_0} A_0$$

- And since mass flow rate through the engine is related to engine net thrust (obtained from the *conservation of momentum*), we obtain:

$$F(N) = (p_e - p_0)A_e + \frac{2q}{u_0} A_0 (u_e(1+f) - u_0)$$

- *Specific Impulse (Isp)* is a measure of how efficiently a vehicle uses its propellant to generate thrust:

$$I_{sp}(s) = \frac{F}{g\,\dot{m}_0\,f}$$

- One of the most important nondimensional parameters is the *Reynolds Number*:

$$Re = \frac{2\,q_0\,L}{u_0\,\mu_0}, \qquad Natural\ Transition\ for\ Re > 10^7$$

- *Re* indicates to the designer whether the boundary layers are laminar, transitional, or turbulent
  - Externally, *laminar boundary layers* are preferred due to lower skin friction and wall heat transfer
  - Internally, *turbulent boundary layers* are preferred due to greater resistance to flow separation

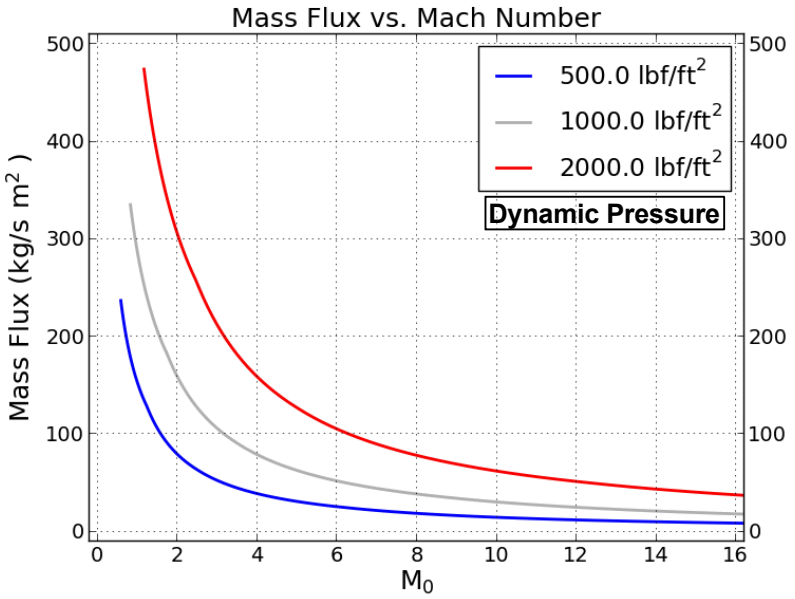

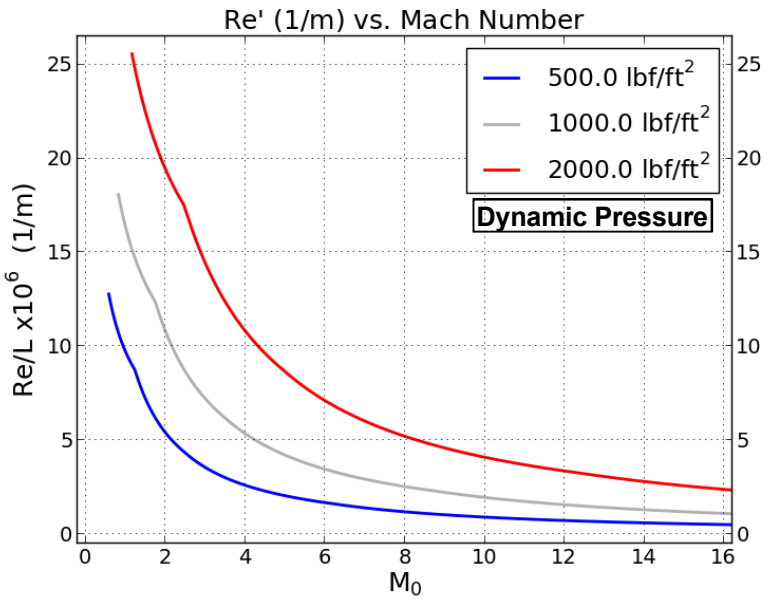

Aero-Thermodynamic Heating

- From the definition of total energy and static enthalpy, we have:

$$e^t = e + k = h - \frac{p}{\rho} + k = h^t - \frac{p}{\rho},$$

$$h = \sum_{\alpha} Y_{\alpha} \int_0^T dT' Cp_{\alpha}(T')$$

- If we stagnate the flow such that all of *k* is absorbed into the *h*, then the flow's temperature must rise. This new temperature of the stagnated flow is called *stagnation* or total temperature*.
  - In subsonic flows, the kinetic energy is small, and so the static and total temperatures are about the same
  - In supersonic flows, the kinetic energy is large, and the ratio of static and total temperatures depends on the Mach number:

$$\frac{T_t}{T} = \left(1 + \frac{k}{h}\right) = \left(1 + \frac{\gamma - 1}{2} M^2\right)$$

  - In hypersonic flows, the kinetic energy is >> than the enthalpy such that most of the flow's energy is in the kinetic form, e.g., at Mach 7, the kinetic energy is an order of magnitude larger than the enthalpy.
- Heating (and cooling) considerations drive material selection in high speed applications.

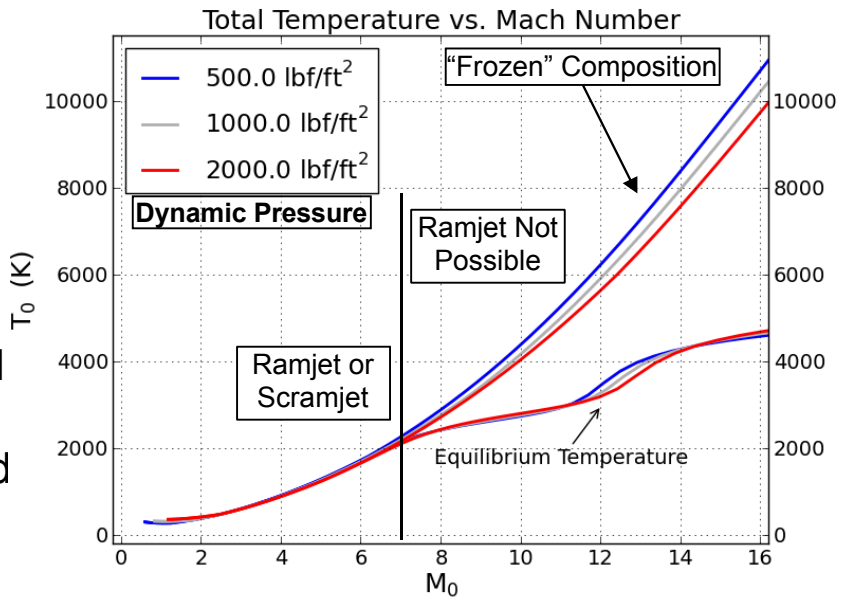

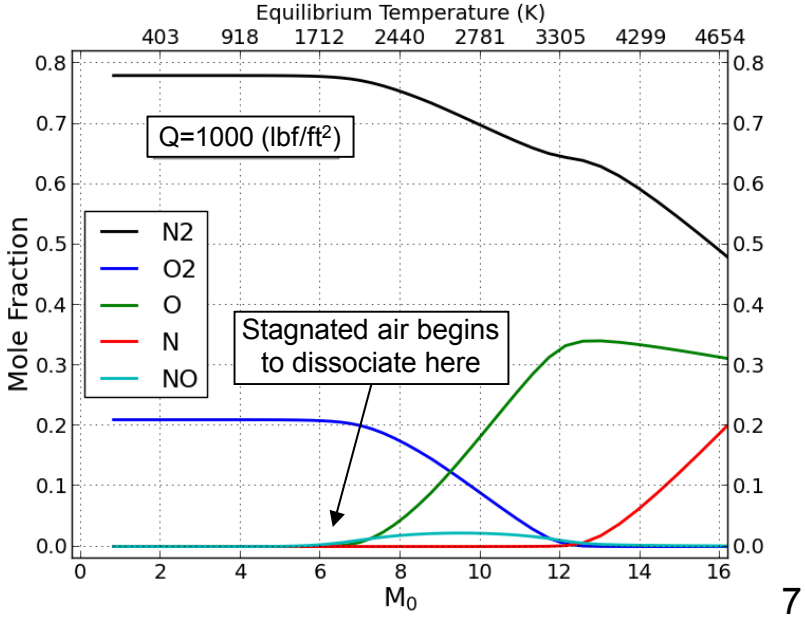

Problem Space Addressed by the CFD

Flight

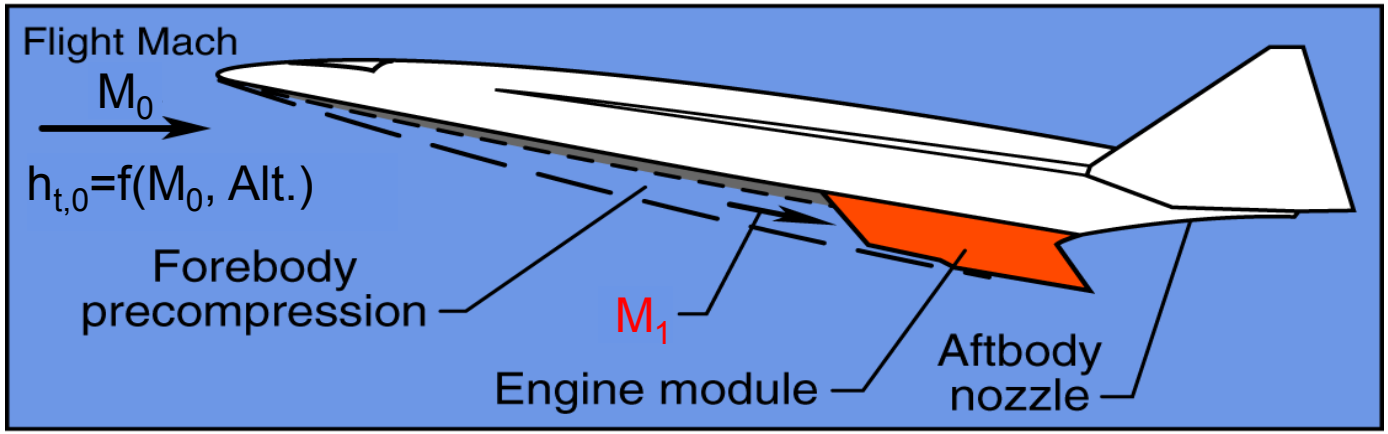

Simulation in ground facility

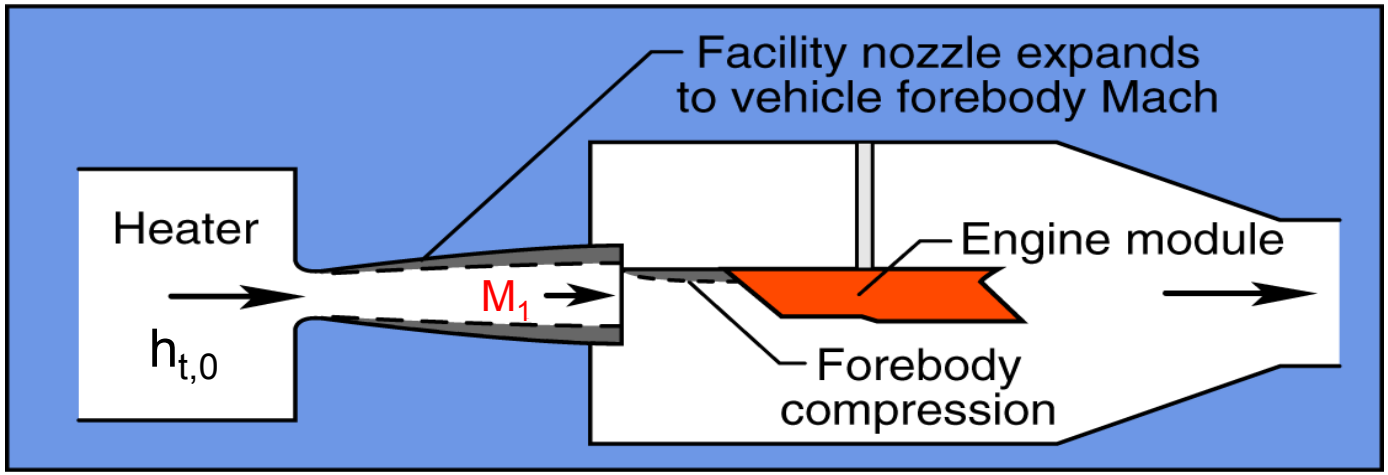

Hypersonic Research as an Aeroscience

M&S ($)
100s/year

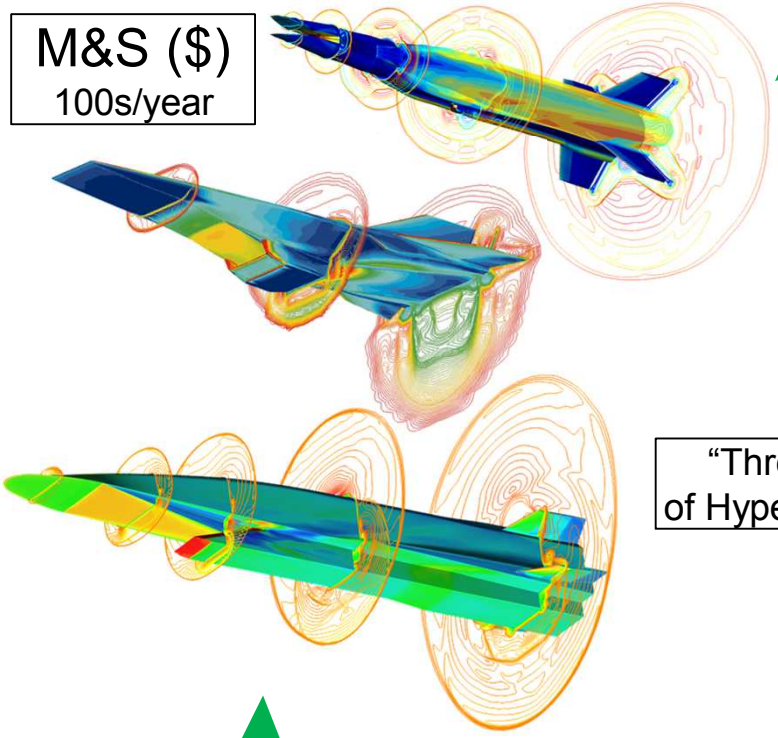

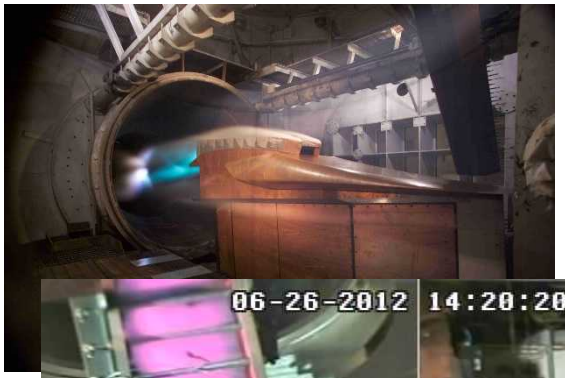

Ground Testing ($$$)
10/year

"Three Legged Stool" of Hypersonic Aeroscience

Flight Testing ($$$$$$)
1/year

Scramjet Propulsion System

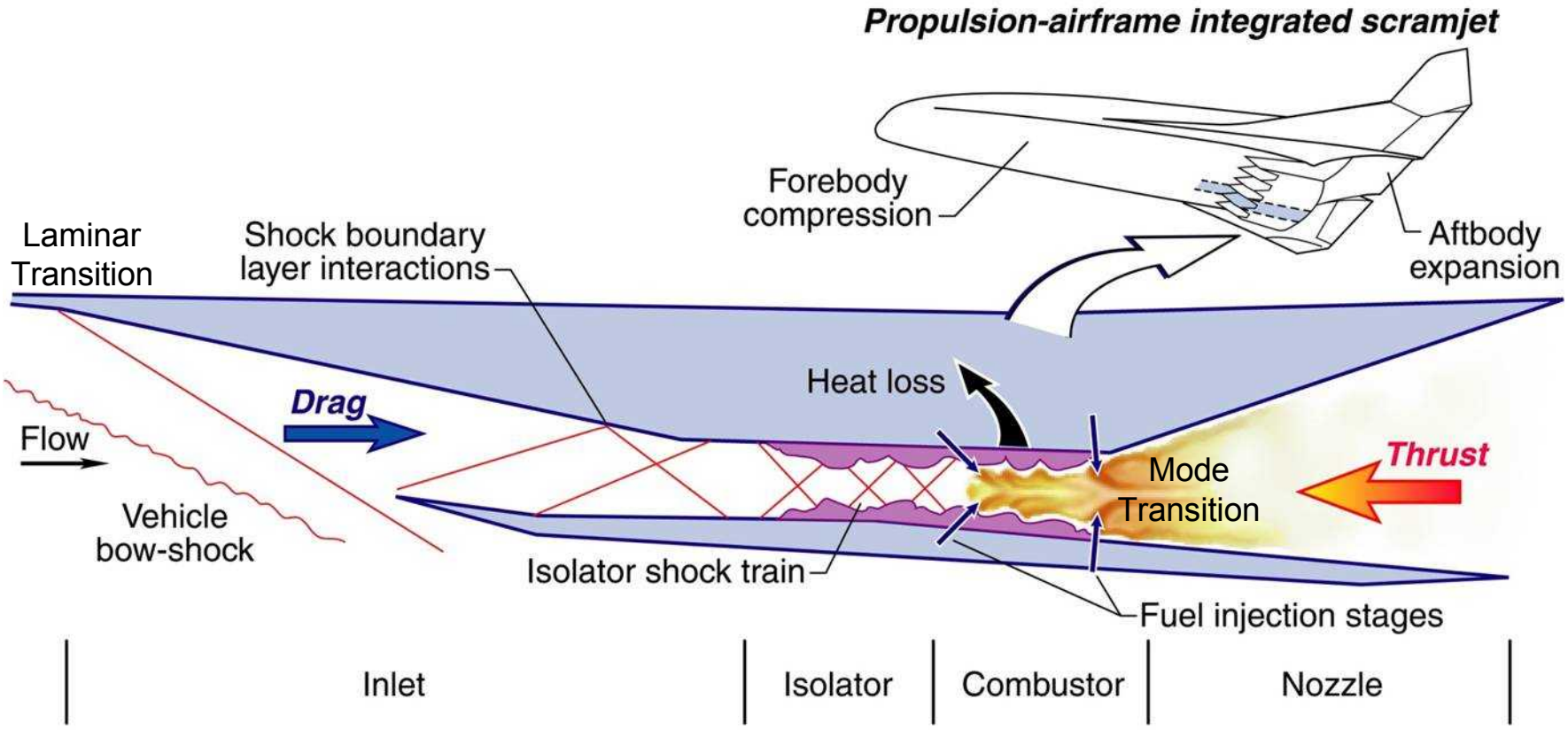

Anderson, J. D. "**Hypersonic and High Temperature Gas Dynamics**"
AIAA Education Series, 2006

Heiser, W. H. and Pratt, D. T. "**Hypersonic Airbreathing Propulsion**"
AIAA Education Series,1994

Role of CFD in Hypersonic Vehicle Development

- MODSIM will be increasingly relied upon for aero-propulsion system designs.
- Currently, 3-D CFD is already being used as a risk-mitigating and parameter exploration tool in design and analysis.
- CFD capabilities continue to improve via
  - More robust and efficient algorithms
  - More accurate physics models
  - Faster computers
- **More so than in low speed flows, CFD is playing a critical role in scramjet development**
  - Not possible to exactly reproduce hypersonic flight conditions at ground test facilities
    - CFD used to extrapolate results to flight
    - CFD used to examine test-media effects (e.g., vitiation) in ground facilities
  - Not possible to measure all relevant properties at ground test facilities
    - CFD used to “fill-in” gaps due to lack of measurements
    - CFD used to examine trends from perturbations made from a calibrated condition
  - Vehicle and engine size limited by the facility capabilities

In the future, CFD must evolve to a state capable of reliably certifying propulsion systems for flight

Governing Transport Equations

- Conservation of Mass

$$\frac{\partial \rho}{\partial t} + \frac{\partial \rho u_k}{\partial x_k} = 0,$$

- Einstein summation notation used, i.e.,

$$\frac{\partial u_k}{\partial x_k} = \frac{\partial u_1}{\partial x_1} + \frac{\partial u_2}{\partial x_2} + \frac{\partial u_3}{\partial x_3} = \frac{\partial u}{\partial x} + \frac{\partial v}{\partial y} + \frac{\partial w}{\partial z}.$$

- The RHS is zero except in multiphase flows, where it could contain terms describing the mass exchange between the phases.

Governing Transport Equations

- Conservation of Species Mass

$$\frac{\partial \rho Y_\alpha}{\partial t} + \frac{\partial \rho u_k Y_\alpha}{\partial x_k} = \frac{\partial J_{\alpha k}}{\partial x_k} + \dot{\omega}_\alpha, \qquad \alpha = 1, 2, \ldots N,$$

- Some properties

$$\sum_\alpha Y_\alpha = 1 \qquad \sum_\alpha J_{\alpha k} = \sum_\alpha Y_\alpha V_{\alpha k} = 0 \qquad \sum_{\alpha=1}^{N} \dot{\omega}_\alpha = 0.$$

- Sum over all of the species recovers the conservation of mass:

$$\sum_\alpha \left(\frac{\partial \rho Y_\alpha}{\partial t} \right) + \sum_\alpha \left(\frac{\partial \rho u_k Y_\alpha}{\partial x_k} \right) = \sum_\alpha \left(\frac{\partial}{\partial x_k} \left(\rho Y_\alpha V_{\alpha k} \right) \right) + \sum_\alpha \left(\dot{\omega}_\alpha \right)$$

Governing Transport Equations

- Species mass production rate

$$\dot{\omega}_\alpha = W_\alpha \sum_{i=1}^{K} (\nu''_{\alpha i} - \nu'_{\alpha i}) \left(k_i^f \prod_{\phi=1}^{N} [C_\phi]^{\nu'_{\phi i}} - k_i^b \prod_{\varphi=1}^{N} [C_\varphi]^{\nu''_{\varphi i}} \right)$$

$$k_i^f = A_i T^{\beta_i} \exp\left(\frac{-E_i}{R_u T}\right),$$

$$\sum_{\alpha=1}^{N} \nu'_{\alpha i} M_\alpha \longleftrightarrow \sum_{\alpha=1}^{N} \nu''_{\alpha i} M_\alpha, \qquad i = 1, 2, \ldots K,$$

$$[C_\alpha] = \frac{\rho Y_\alpha}{W_\alpha} = \rho Y_\alpha \sum_{\phi=1}^{N} \frac{Y_\phi}{W_\phi},$$

$$C_x H_y + \left(x + \frac{y}{4}\right) O_2 \rightarrow x CO_2 + \frac{y}{2} H_2O,$$

- Lu, T. & Law, C., "Toward Accommodating Realistic Fuel Chemistry in Large-Scale Computations," *Prog. Energy Combust. Sci.*, **2009**, *35*, 192-215.
- Pope, S. "Small Scales, Many Species and the Manifold Challenges of Turbulent Combustion," *Proc. Combust. Inst.*, **2013**, *34*, 1-31.
- Princeton Summer School on Combustion https://www.princeton.edu/cefrc/combustion-summer-school/lecture-notes/

Governing Transport Equations

- Species molecular diffusion

$$J_{\alpha k} = -\rho Y_\alpha V_{\alpha k},$$

- Fick's model

$$V^F_{\alpha k} = -\frac{D_\alpha}{Y_\alpha}\frac{\partial Y_\alpha}{\partial x_k} \qquad V^c_k = \sum_\alpha D_\alpha \frac{\partial Y_\alpha}{\partial x_k}$$

$$Le_\alpha = \frac{k}{\rho C p D_\alpha} = \frac{\kappa}{D_\alpha} = \frac{\text{rate of thermal diffusion}}{\text{rate of mass diffusion}},$$

$$Pr = \frac{C_p \mu}{k} = \frac{\text{rate of viscous diffusion}}{\text{rate of thermal diffusion}},$$

$$D = \frac{k}{\rho C p Le} = \frac{\mu}{\rho Pr Le} = \frac{\mu}{\rho Sc},$$

- Conservation of species mass fractions

$$\frac{\partial \rho Y_\alpha}{\partial t} + \frac{\partial \rho (u_k + V^c_k) Y_\alpha}{\partial x_k} = \frac{\partial}{\partial x_k}\left(\rho D_\alpha \frac{\partial Y_\alpha}{\partial x_k}\right) + \dot{\omega}_\alpha, \qquad \alpha = 1, 2, \ldots N.$$

Governing Transport Equations

- Conservation of momentum (Navier-Stokes Eqs.)

$$\frac{\partial \rho u_i}{\partial t} + \frac{\partial \rho u_k u_i}{\partial x_k} = -\frac{\partial p}{\partial x_i} + \frac{\partial \tau_{ik}}{\partial x_k} + \rho |g| \hat{n}_i \cdot \hat{n}_g$$

- Viscous stress tensor

$$\tau_{ij} = \mu \left(\frac{\partial u_i}{\partial x_j} + \frac{\partial u_j}{\partial x_i} \right) - \frac{2}{3} \mu \frac{\partial u_k}{\partial x_k} \delta_{ij}.$$

- Pressure (EoS)

$$p = \frac{\rho R_u T}{W_{mix}} = \rho R_u T \sum_{\alpha} \frac{Y_\alpha}{W_\alpha},$$

Governing Transport Equations

- Total energy

$$e^t = e + k = h - \frac{p}{\rho} + k = h^t - \frac{p}{\rho} = \sum_\alpha h_\alpha Y_\alpha - \frac{p}{\rho} + \frac{u_i u_i}{2},$$

- Conservation of total energy and heat flux vector

$$\frac{\partial \rho e^t}{\partial t} + \frac{\partial \rho u_k h^t}{\partial x_k} = \frac{\partial u_i \tau_{ik}}{\partial x_k} - \frac{\partial \dot{q}_k}{\partial x_k} + \rho u_k |g| \hat{n}_k \cdot \hat{n}_g.$$

$$\dot{q}_k = -k \frac{\partial T}{\partial x_k} + \rho \sum_\alpha h_\alpha Y_\alpha V_{\alpha k}.$$

- Conservation of enthalpy (typically solved for in low speed flows)

$$\frac{\partial \rho h}{\partial t} + \frac{\partial \rho (u_k + V_k^c) h}{\partial x_k} = \underbrace{\frac{\mathcal{D}p}{\mathcal{D}t} + \tau_{ik} \frac{\partial u_i}{\partial x_k}}_{\approx 0 \ if \ Mach < 0.3} + \frac{\partial}{\partial x_k} \left(\frac{k}{Cp} \frac{\partial h}{\partial x_k} \right) - \underbrace{\frac{\partial}{\partial x_k} \left(\frac{k}{Cp} \sum_\alpha \left(\frac{Le_\alpha - 1}{Le_\alpha} \right) h_\alpha \frac{\partial Y_\alpha}{\partial x_k} \right)}_{=0 \ if \ Le_\alpha = 1}.$$

Governing Transport Equations

$$\frac{\partial \rho u_k}{\partial x_k} = 0, \qquad \boxed{\rho u A = \dot{m}}$$

$$\frac{\partial \rho (u_k + V_k^c) Y_\alpha}{\partial x_k} = \frac{\partial}{\partial x_k}\left(\rho D_\alpha \frac{\partial Y_\alpha}{\partial x_k}\right) + \dot{\omega}_\alpha, \qquad \alpha = 1, 2, \ldots N.$$

$$V_k^c = \sum_\alpha D_\alpha \frac{\partial Y_\alpha}{\partial x_k}$$

$$\frac{\partial \rho u_k u_i}{\partial x_k} = -\frac{\partial p}{\partial x_i} + \frac{\partial \tau_{ik}}{\partial x_k} + \rho |g| \hat{n}_i \cdot \hat{n}_g \qquad \boxed{\rho u^2 A + pA = \mathcal{F}}$$

$$p = \frac{\rho R_u T}{W_{mix}} = \rho R_u T \sum_\alpha \frac{Y_\alpha}{W_\alpha}, \qquad \tau_{ij} = \mu\left(\frac{\partial u_i}{\partial x_j} + \frac{\partial u_j}{\partial x_i}\right) - \frac{2}{3}\mu \frac{\partial u_k}{\partial x_k}\delta_{ij}.$$

$$\frac{\partial \rho u_k h^t}{\partial x_k} = \frac{\partial u_i \tau_{ik}}{\partial x_k} - \frac{\partial \dot{q}_k}{\partial x_k} + \rho u_k |g| \hat{n}_k \cdot \hat{n}_g. \qquad \boxed{h + \frac{1}{2}u^2 = h^t}$$

$$\dot{q}_k = -k\frac{\partial T}{\partial x_k} + \rho \sum_\alpha h_\alpha Y_\alpha V_{\alpha k}.$$

- References

Panton, R.L., *Incompressible Flow*, John Wiley and Sons, New York, NY, 1984.

Williams, F.A., *Combustion Theory*, The Benjamin/Cummings Publishing Company, Menlo Park, CA, 2nd ed., 1985.

Turns, S.R., *An Introduction to Combustion: Concepts and Applications*, McGraw Hill, 2nd ed., 2000.

Kuo, K.K., *Principles of Combustion*, John Wiley and Sons, Hoboken, N.J., 2nd ed., 2005.

Warnatz, J., Maas, U., and Dibble, R.W., *Combustion*, Springer, Berlin, Germany, 4th ed., 2006.

Poinsot, T. and Veynante, D., *Theoretical and Numerical Combustion*, R.T. Edwards, Inc., Philadelphia, PA, 2nd ed., 2005.

Nondimensionalization

- Nondimensionalization
  - Identifies a minimum set of nondimensional groups
  - Helps to identify limiting behavior of a set of equations
  - Homogenizes the values of different quantities so the values are neither too small or too large
- For high speed flows it is convenient to use a combination of free stream and sonic nondimensionalization variables

$$t^* = \frac{tc_r}{l_r},\ x^* = \frac{x}{l_r},\ \rho^* = \frac{\rho}{\rho_r},\ u_i^* = \frac{u_i}{c_r},\ T^* = \frac{T}{T_r},\ p^* = \frac{p}{\rho_r c_r^2},\ e^{t*} = \frac{e^t}{c_r^2},\ h^* = \frac{h}{c_r^2},$$

$$\mu^* = \frac{\mu}{\mu_r},\ k^* = \frac{k}{k_r},\ D_\alpha^* = \frac{D_\alpha}{D_r},\ R^* = \frac{R}{R_r},\ W_\alpha^* = W_\alpha / W_r,$$

- With some reference quantities computed from other reference values:

$$c_r = \sqrt{\gamma_r R_r T_r},\ \gamma_r = \frac{Cp_r}{Cp_r - R_r},\ Cp_r = \sum_\alpha Y_{\alpha,r} Cp_\alpha(T_r),\ R_r = \frac{R_u}{W_r},\ W_r = \frac{1}{\sum_\alpha \frac{Y_{\alpha,r}}{W_\alpha}},$$

$$\mu_r = \mu(T_r),\ k_r = k(T_r),\ D_r = c_r l_r,$$

- Nondimensional parameters become

$$Re_r = \frac{\rho_r u_r l_r}{\mu_r},\ Fr_r = \frac{u_r}{\sqrt{l_r |g|}},\ M_r = \frac{u_r}{c_r},\ Pr_r = \frac{\mu_r Cp_r}{k_r},\ Le_r = \frac{k_r}{\rho_r Cp_r D_r},\ Sc_r = Pr_r Le_r,$$

Nondimensionalization

- Transport Equations for Mass, Momentum, and Energy

$$\frac{\partial \rho^*}{\partial t^*} + \frac{\partial \rho^* u_k^*}{\partial x_k^*} = 0.$$

$$\frac{\partial \rho^* Y_\alpha}{\partial t^*} + \frac{\partial \rho^* (u_k^* + V_k^{c*}) Y_\alpha}{\partial x_k^*} = \frac{\partial}{\partial x_k^*}\left(\rho^* D_\alpha^* \frac{\partial Y_\alpha}{\partial x_k^*}\right) + \frac{l_r}{\rho_r c_r}\dot{\omega}_\alpha,$$
$$= \frac{\partial}{\partial x_k^*}\left(\frac{\mu^*}{Sc_\alpha^*}\frac{\partial Y_\alpha}{\partial x_k^*}\right) + \frac{l_r}{\rho_r c_r}\dot{\omega}_\alpha, \qquad \alpha = 1, 2, \ldots N,$$

$$\frac{\partial \rho^* u_i^*}{\partial t^*} + \frac{\partial \rho^* u_k^* u_i^*}{\partial x_k^*} = -\frac{\partial p^*}{\partial x_i^*} + \frac{M_r}{Re_r}\frac{\partial}{\partial x_k^*}\left(\mu^*\left(\frac{\partial u_i^*}{\partial x_k^*} + \frac{\partial u_k^*}{\partial x_i^*}\right) - \frac{2}{3}\mu^*\frac{\partial u_j^*}{\partial x_j^*}\delta_{ik}\right) + \frac{M_r^2}{Fr_r^2}\rho^* \hat{n}_i \cdot \hat{n}_g$$

Re>>1 : Euler Eqs.

Fr>>1 : Neglect Buoyancy

$$\frac{\partial \rho^* e^{t*}}{\partial t^*} + \frac{\partial \rho^* (u_k^* + V_k^{c*}) h^{t*}}{\partial x_k^*} = \frac{M_r}{Re_r}\frac{\partial}{\partial x_k^*}\left(u_i^*\left(\mu^*\left(\frac{\partial u_i^*}{\partial x_k^*} + \frac{\partial u_k^*}{\partial x_i^*}\right) - \frac{2}{3}\mu^*\frac{\partial u_j^*}{\partial x_j^*}\delta_{ik}\right)\right)$$
$$+ \frac{M_r}{Re_r Pr_r}\frac{\partial}{\partial x_k^*}\left(\frac{\mu^*}{Pr^*}\frac{\partial h^*}{\partial x_k^*} - \frac{\mu^*}{Pr^*}\sum_\alpha\left(\frac{Le_\alpha^* - 1}{Le_\alpha^*}\right)h_\alpha^*\frac{\partial Y_\alpha}{\partial x_k^*}\right) + \frac{\partial \rho^* k^* V_k^{c*}}{\partial x_k^*} + \frac{M_r^2}{Fr_r^2}\rho^* u_k^* \hat{n}_k \cdot \hat{n}_g,$$

Nondimensionalization

- Nondimensional form of the species production rate
  - Difficult to implement in a solver
  - Reveals two more nondimensional groups

$$\frac{l_r}{\rho_r c_r}\dot{\omega}_{CO_2} = xW^*_{CO_2} Da \exp\left(\frac{-Ze}{T^*}\right)\rho^{*m+n} Y^m_{C_xH_y} Y^n_{O_2},$$

$$Da = \frac{l_r}{\rho_r c_r}\frac{W_r \rho_r^{m+n} A}{W^m_{C_xH_y} W^n_{O_2}},\ Ze = \frac{E_a}{R_u T_r},$$

- Damkohler number:
  - Da >> 1 leads to rapid reaction and near equilibrium chemical compositions.
  - Da << 1 leads to extinction
- Zeldovich number represents the nondimensional measure of the temperature sensitivity of the reaction

- One physical phenomena that can be studied using the Navier-Stokes equations is turbulence
  - Turbulence is multiscale, i.e., occurs over a range of length and time scales

  - Turbulence complicates other physical processes through non-linear interactions, e.g., combustion
  - Turbulence leads to complex flow behaviors, e.g., boundary layers.
- Range of turbulence scales is proportional to the Reynolds number
  - The range is too large to simulate numerically for engineering problems

$$\frac{\eta}{L} = Re^{-3/4}, \qquad \frac{t_\eta}{t_L} = Re^{-1/2},$$

Direct Numerical Simulation (DNS)

Large Eddy Simulation (LES)

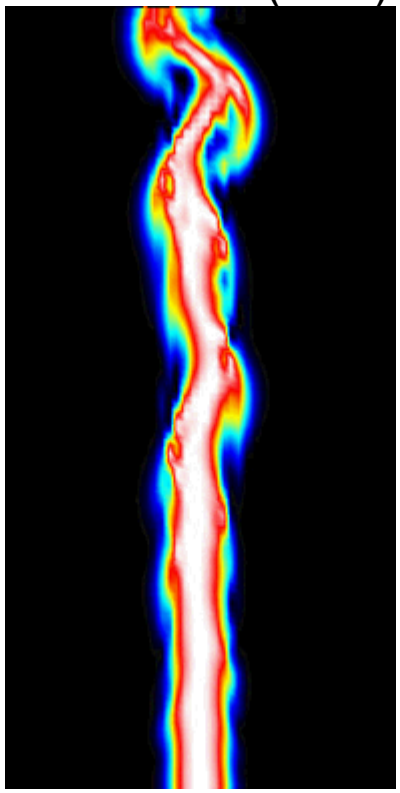

Reynolds-Averaged Simulation (RAS)

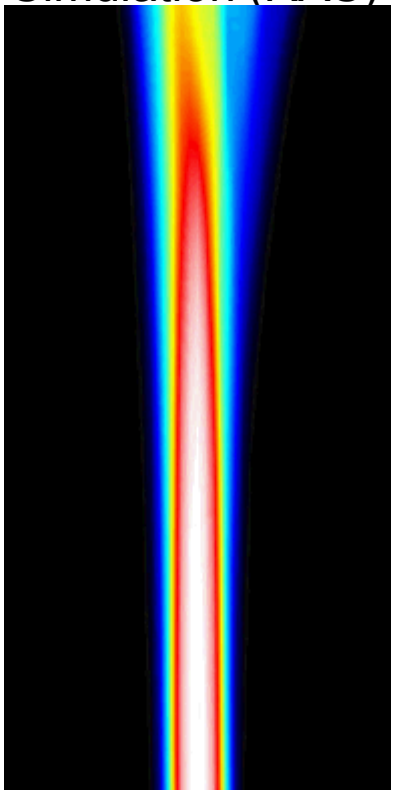

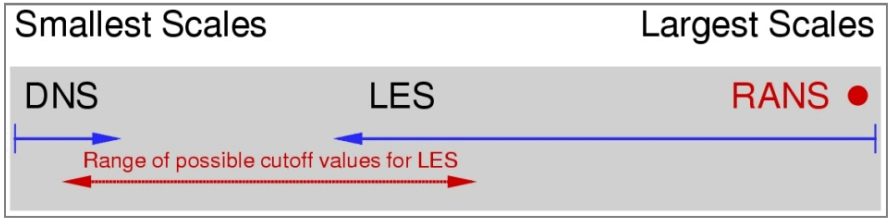

10 – 100 μm microseconds

10 – 100 cm milliseconds

- The range of turbulence scales must be reduced to allow for simulations

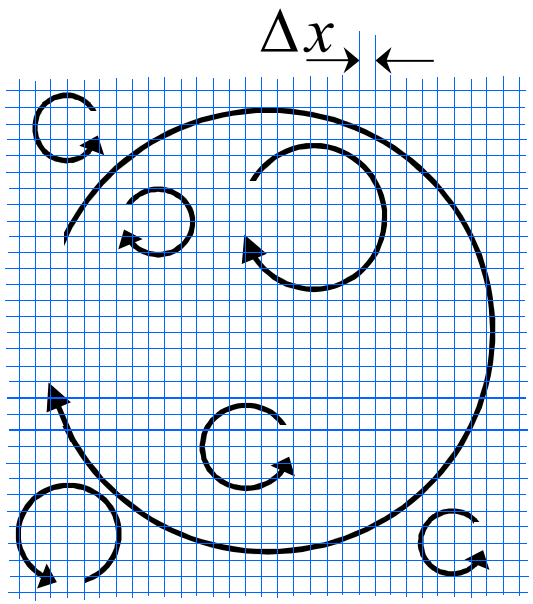

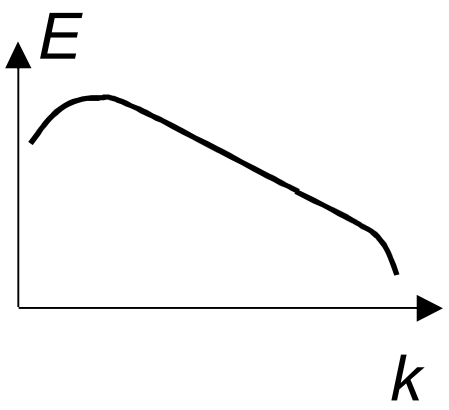

All scales resolved (DNS)

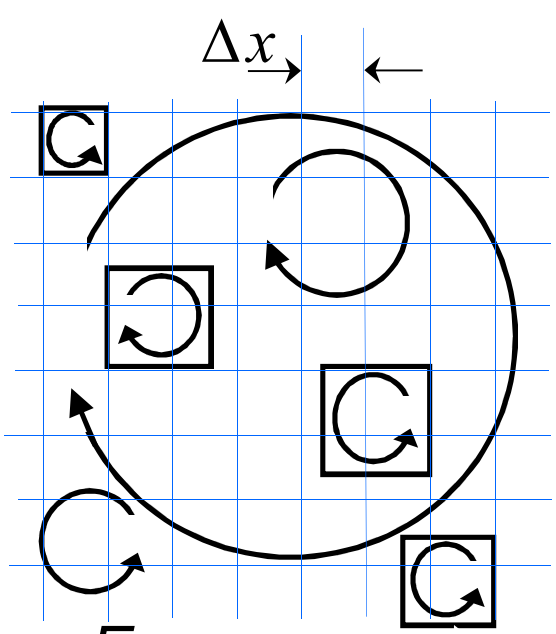

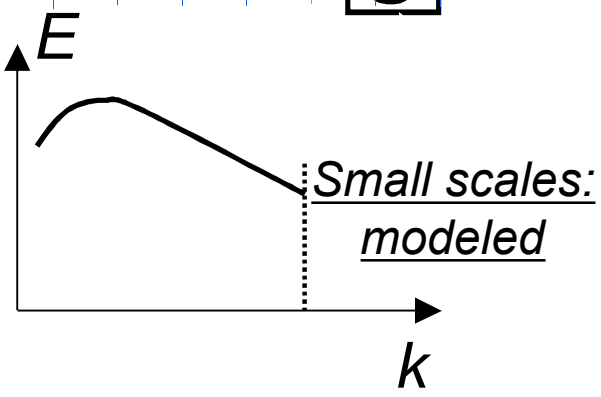

Large scales resolved (LES)

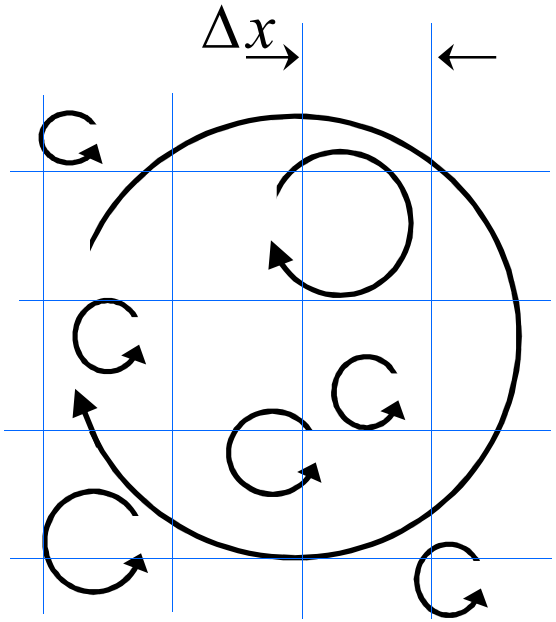

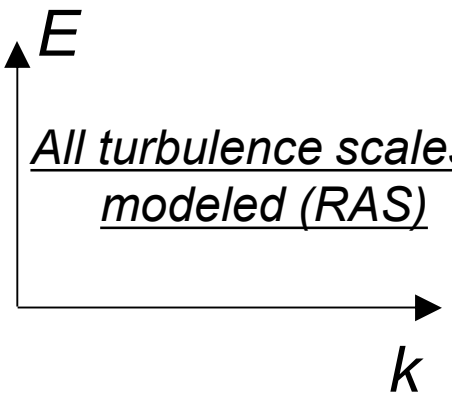

- The two most common scale-reduction strategies are the time-averaging and spatial-averaging (or filtering)
  - Time-averaging gives rise to Reynolds averaged simulations (RAS)

$$\overline{f}(x) = \lim_{T\to\infty} \int_{t}^{t+T} \mathrm{d}t'\, f(x,t'),$$

  - Filtering leads to large-eddy simulations (LES)

$$\overline{f}(x,t) = \int_{-\infty}^{+\infty} \mathrm{d}x'\, f(x',t)\mathcal{G}(x'-x),$$

- Favre average is useful in variable density flows and is defined as the density-weighted average.

$$\widetilde{f} = \frac{\overline{\rho f}}{\overline{\rho}}.$$

- Both of the above operators
  - produce the exact same (looking) set of governing equations although the interpretation and modeling strategies vary
  - **produce extra terms in the governing equations that require modeling**

- LES (or RAS) equations are:

$$\frac{\partial \overline{\rho}}{\partial t} + \frac{\partial \overline{\rho}\widetilde{u}_k}{\partial x_k} = 0, \qquad \overline{p} = \overline{\rho}\widetilde{RT} = \overline{\rho}\sum_\alpha \frac{Ru}{W_\alpha}\widetilde{Y}_\alpha\widetilde{T} + \underbrace{\overline{\rho}\sum_\alpha \frac{Ru}{W_\alpha}\left(\widetilde{Y_\alpha T} - \widetilde{Y}_\alpha\widetilde{T}\right)}_{\text{Scalar-Temperature Correlation}},$$

$$\frac{\partial \overline{\rho}\widetilde{Y}_\alpha}{\partial t} + \frac{\partial \overline{\rho}(\widetilde{u}_k + \widehat{V}_k^c)\widetilde{Y}_\alpha}{\partial x_k} = \frac{\partial}{\partial x_k}\left(\frac{\widehat{\mu}}{\widehat{Sc}_\alpha}\frac{\partial \widetilde{Y}_\alpha}{\partial x_k}\right) + \dot{\omega}_\alpha(\overline{p}, \widetilde{Y}_\alpha, \widetilde{T})$$

$$\underbrace{-\frac{\partial}{\partial x_k}\left(\overline{\rho u_k Y_\alpha} - \overline{\rho}\widetilde{u}_k\widetilde{Y}_\alpha\right)}_{\text{Turbulence Subgrid Flux}} + \underbrace{\left(\overline{\dot{\omega}_\alpha(p, Y_\alpha, T)} - \dot{\omega}_\alpha(\overline{p}, \widetilde{Y}_\alpha, \widetilde{T})\right)}_{\text{Turbulence Chemistry Interaction (TCI)}}, \qquad \alpha = 1, 2, \ldots N,$$

$$\frac{\partial \overline{\rho}\widetilde{u}_i}{\partial t} + \frac{\partial \overline{\rho}\widetilde{u}_k\widetilde{u}_i}{\partial x_k} = -\frac{\partial \overline{p}}{\partial x_i} + \frac{M_r}{Re_r}\frac{\partial}{\partial x_k}\left(\widehat{\mu}\left(\frac{\partial \widetilde{u}_i}{\partial x_k} + \frac{\partial \widetilde{u}_k}{\partial x_i}\right) - \frac{2}{3}\widehat{\mu}\frac{\partial \widetilde{u}_j}{\partial x_j}\delta_{ik}\right) - \underbrace{\frac{\partial}{\partial x_k}\left(\overline{\rho u_k u_i} - \overline{\rho}\widetilde{u}_k\widetilde{u}_i\right)}_{\text{Turbulence Subgrid Stress}}$$

$$\frac{\partial \overline{\rho}\widetilde{e^t}}{\partial t} + \frac{\partial \overline{\rho}(\widetilde{u}_k + \widehat{V}_k^c)\widetilde{h^t}}{\partial x_k} = \frac{M_r}{Re_r}\frac{\partial}{\partial x_k}\left(\widetilde{u}_i\left(\widehat{\mu}\left(\frac{\partial \widetilde{u}_i}{\partial x_k} + \frac{\partial \widetilde{u}_k}{\partial x_i}\right) - \frac{2}{3}\widehat{\mu}\frac{\partial \widetilde{u}_j}{\partial x_j}\delta_{ik}\right)\right) + \underbrace{\frac{M_r}{Re_r}\frac{\partial}{\partial x_k}\left(\overline{u_i\tau_{ik}} - \widetilde{u}_k\overline{\tau_{ik}}\right)}_{\text{Velocity-Shear Stress Correlation}}$$

$$+ \frac{M_r}{Re_r Pr_r}\frac{\partial}{\partial x_k}\left(\frac{\widehat{\mu}}{\widehat{Pr}}\frac{\partial \widetilde{h}}{\partial x_k} - \frac{\widehat{\mu}}{\widehat{Pr}}\sum_\alpha\left(\frac{\widehat{Le}_\alpha - 1}{\widehat{Le}_\alpha}\right)\widetilde{h}_\alpha\frac{\partial \widetilde{Y}_\alpha}{\partial x_k}\right) + \frac{\partial \overline{\rho}(\widetilde{k} + k)\widehat{V}_k^c}{\partial x_k}$$

$$\underbrace{-\frac{\partial}{\partial x_k}\left(\overline{\rho u_k h} - \overline{\rho}\widetilde{u}_k\widetilde{h}\right)}_{\text{Turbulence Subgrid Enthalpy Flux}} - \underbrace{\frac{\partial}{\partial x_k}\left(\overline{\rho u_k}\frac{\widetilde{u_i u_i}}{2} - \overline{\rho}\widetilde{u}_k\frac{\widetilde{u_i u_i}}{2}\right)}_{\text{Turbulence Subgrid Kinetic Energy Flux}}$$

- With the commonly found definitions

$$\tau(a,b) = \widetilde{a\,b} - \widetilde{a}\,\widetilde{b},$$

$$\tau(a,b,c) = \widetilde{a\,b\,c} - \widetilde{a}\tau(b,c) - \widetilde{b}\tau(a,c) - \widetilde{c}\tau(a,b) - \widetilde{a}\,\widetilde{b}\,\widetilde{c},$$

- The unclosed terms can be written as

$$\overline{\rho}\widetilde{u_k Y_\alpha} - \overline{\rho}\widetilde{u}_k\widetilde{Y}_\alpha = \overline{\rho}\tau(u_k, Y_\alpha),$$

$$\overline{\rho}\widetilde{u_k u_i} - \overline{\rho}\widetilde{u}_k\widetilde{u}_i = \overline{\rho}\tau(u_k, u_i),$$

$$\overline{\rho}\widetilde{u_k h} - \overline{\rho}\widetilde{u}_k\widetilde{h} = \overline{\rho}\tau(u_k, h),$$

$$\overline{\rho}\widetilde{u_k\frac{u_i u_i}{2}} - \overline{\rho}\widetilde{u}_k\widetilde{\frac{u_i u_i}{2}} = \frac{1}{2}\overline{\rho}\tau(u_k, u_i, u_i) - \overline{\rho}\widetilde{u}_i\tau(u_k, u_i).$$

- We either have to represent the above terms as functions of the variables we are solving for or derive the transport equations and solve for them
- If we derive the transport equation for any one of the above unclosed terms we'll find that additional, yet higher order terms appear in those equations. **This is referred to as the closure problem.**

- The most common closures used for the turbulence subgrid stresses and fluxes are the Boussinesq approximation (or gradient diffusion assumption)

$$\overline{\rho}\tau(u_k,u_i)-\frac{1}{3}\overline{\rho}\tau(u_j,u_j)\delta_{ik}=-\mu_t\left(\frac{\partial\widetilde{u}_i}{\partial x_k}+\frac{\partial\widetilde{u}_k}{\partial x_i}\right)-\frac{2}{3}\mu_t\frac{\partial\widetilde{u}_j}{\partial x_j}\delta_{ik},$$

$$\overline{\rho}\tau(u_k,Y_\alpha)=-\frac{\mu_t}{Sc_t}\frac{\partial\widetilde{Y}_\alpha}{\partial x_k},$$

$$\overline{\rho}\tau(u_k,h)=-\frac{\mu_t}{Pr_t}\frac{\partial\widetilde{h}}{\partial x_k},$$

$$\frac{1}{2}\overline{\rho}\tau(u_k,u_i,u_i)=-\frac{\mu_t}{\sigma_k}\frac{\partial k}{\partial x_k}$$

- In general
  - any correlations between molecular transport properties and transported quantities are neglected
  - the scalar-temperature correlations in the EoS are typically neglected
- In engineering applications
  - turbulence-chemistry interactions are often neglected
- So how do we obtain turbulence subgrid viscosity?

- Hierarchy of turbulence models

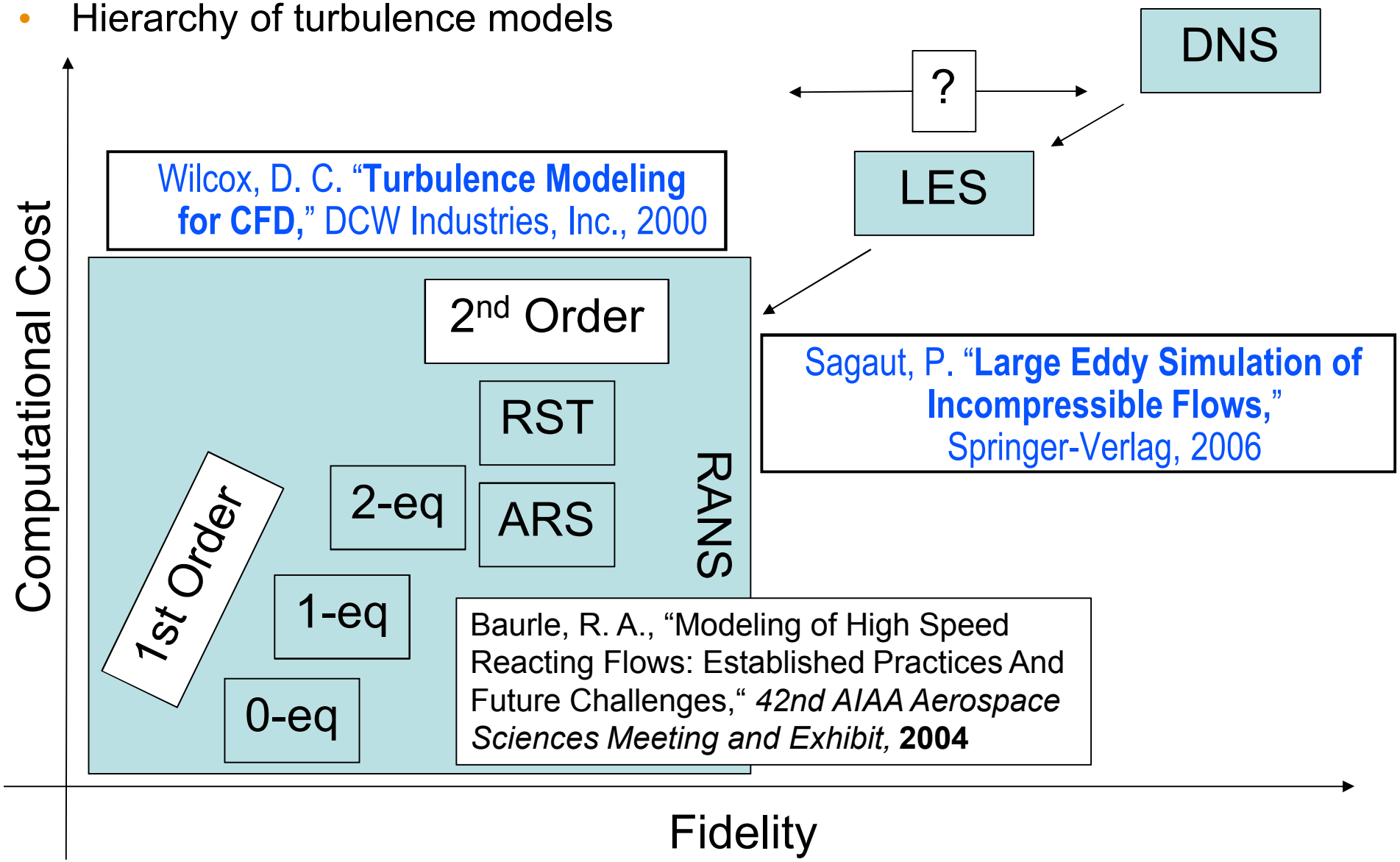

- Anyone getting started with LES should probably read:
  - Pope, S. B., "Ten Questions Concerning the Large-Eddy Simulation of Turbulent Flows," *New J. Phys.*, **2004**, *6*, 35.
- To get us started the most common model for the subgrid viscosity is the Smagorinsky model:

$$\mu_t = \overline{\rho} C_s^2 \Delta_L^2 |\widehat{S}|,$$

$$|\widehat{S}| = \sqrt{2\widehat{S}_{ij}\widehat{S}_{ij}},$$

$$\widehat{S}_{ij} = \frac{1}{2}\left(\frac{\partial \widetilde{u}_i}{\partial x_j} + \frac{\partial \widetilde{u}_j}{\partial x_i}\right),$$

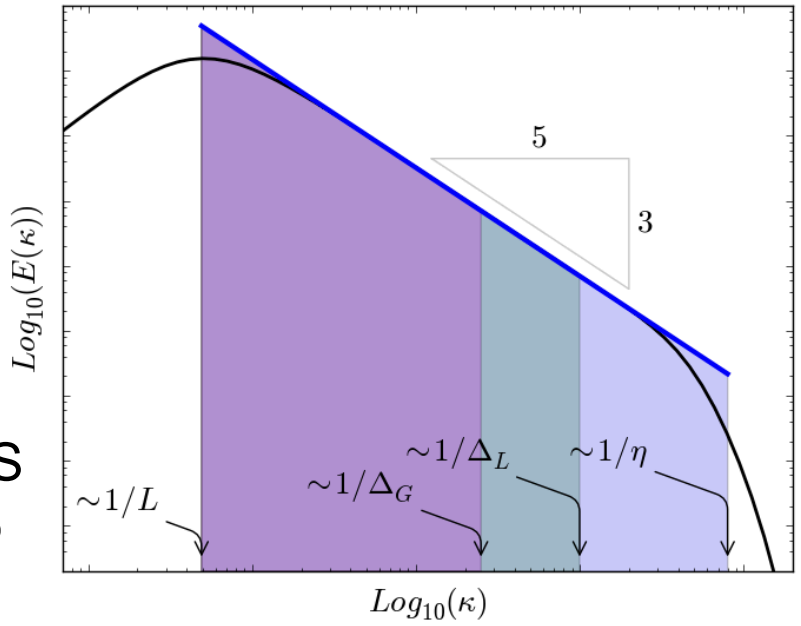

- One of the major advancements in LES is the use of scale similarity to develop the dynamic procedure to estimate the model coefficients.
  - Germano identity:

$$\underbrace{\overline{\overline{\rho}\widetilde{u}_i\widetilde{u}_j} - \frac{\overline{\overline{\rho}\widetilde{u}_i}\;\overline{\overline{\rho}\widetilde{u}_j}}{\overline{\overline{\rho}}}}_{\text{Resolved stress, } L_{ij}} = \underbrace{\overline{\overline{\rho}\mathcal{T}(u_i,u_j)}}_{\substack{\text{Subgrid stress} \\ \text{for } \Delta_G \text{ filter}}} - \underbrace{\overline{\overline{\rho}\tau(u_i,u_j)}}_{\substack{\Delta_G\text{-filtered subgrid} \\ \text{stress for } \Delta_L \text{ filter}}}$$

- Assuming that the Smagorinsky model is applicable at both LES and test filter scales we have:

$$\overline{\overline{\rho}}\mathcal{T}(u_i,u_j)-\frac{1}{3}\overline{\overline{\rho}}\mathcal{T}(u_k,u_k)\delta_{ij}=-\overline{\overline{\rho}}C_s^2\Delta_G^2|\widehat{\widehat{S}}|(2\widehat{\widehat{S}}_{ij}-\frac{2}{3}\widehat{\widehat{S}}_{kk}\delta_{ij}),$$

$$\overline{\overline{\rho\tau(u_i,u_j)}}-\frac{1}{3}\overline{\overline{\rho\tau(u_k,u_k)}}\delta_{ij}=-\overline{\overline{\rho}C_s^2\Delta_L^2|\widehat{S}|(2\widehat{S}_{ij}-\frac{2}{3}\widehat{S}_{kk}\delta_{ij})},$$

$$|\widehat{\widehat{S}}|=\sqrt{2\widehat{\widehat{S}}_{ij}\widehat{\widehat{S}}_{ij}},$$

$$\widehat{\widehat{S}}_{ij}=\frac{1}{2}\left(\frac{\partial\widetilde{\widetilde{u}}_i}{\partial x_j}+\frac{\partial\widetilde{\widetilde{u}}_j}{\partial x_i}\right)=\frac{1}{2}\left(\frac{\partial}{\partial x_j}\left(\frac{\overline{\overline{\rho\widetilde{u}_i}}}{\overline{\overline{\rho}}}\right)+\frac{\partial}{\partial x_i}\left(\frac{\overline{\overline{\rho\widetilde{u}_j}}}{\overline{\overline{\rho}}}\right)\right)\approx\frac{1}{2}\left(\overline{\frac{\partial\widetilde{u}_i}{\partial x_j}}+\overline{\frac{\partial\widetilde{u}_j}{\partial x_i}}\right),$$

- Substituting above into the Germano identity

$$L_{ij}-\frac{1}{3}L_{kk}\delta_{ij}=C_s^2M_{ij}=C_s^2\left(\overline{\overline{\rho}\Delta_L^2|\widehat{S}|(2\widehat{S}_{ij}-\frac{2}{3}\widehat{S}_{kk}\delta_{ij})}-\overline{\overline{\rho}}(\kappa\Delta_L)^2|\widehat{\widehat{S}}|(2\widehat{\widehat{S}}_{ij}-\frac{2}{3}\widehat{\widehat{S}}_{kk}\delta_{ij})\right),$$

- The dynamic procedure relies on minimizing the “square” of the error tensor, which represents the difference between resolved and modeled subgrid stresses

$$E_{ij} = L_{ij} - \frac{1}{3}L_{kk}\delta_{ij} - C_s^2 M_{ij},$$

$$\frac{dE_{ij}E_{ij}}{dC_s^2} = 0, \Rightarrow 2E_{ij}\frac{dE_{ij}}{dC_s^2} = 0, \Rightarrow L_{ij}M_{ij} - \frac{1}{3}L_{kk}M_{ij}\delta_{ij} - C_s^2 M_{ij}M_{ij} = 0,$$

($-M_{ij}$)

$$C_s^2 = \frac{L_{ij}M_{ij} - \frac{1}{3}L_{kk}M_{ij}\delta_{ij}}{M_{ij}M_{ij}} = \boxed{\frac{L_{ij}M_{ij}}{M_{ij}M_{ij}}}.$$

($\frac{1}{3}L_{kk}M_{ij}\delta_{ij} \to 0$)

- We can apply this procedure in a similar fashion to any model coefficient, with the caveat that
  - We need to “test-filter” the resolved field with a filter width greater than the filter scale
  - Additional care must be taken to ensure that Cs is not ill posed

- Another common model for the subgrid viscosity is one utilizing the one equation model for the subgrid kinetic energy

$$\mu_t = \overline{\rho} C_k \Delta_L \sqrt{k}.$$

- The value of the model constant may be computed using the dynamic procedure
- The unclosed form of the subgrid kinetic energy equation is

$$\frac{\partial \overline{\rho} k}{\partial t} + \frac{\partial \overline{\rho} \widetilde{u}_i k}{\partial x_i} = \frac{\partial}{\partial x_i}\left(\widehat{\mu}\frac{\partial k}{\partial x_i}\right) - \overline{\rho}\tau(u_i,u_j)\frac{\partial \widetilde{u}_i}{\partial x_j} - \overline{\rho}\epsilon - \frac{1}{2}\frac{\partial \overline{\rho}\tau(u_j,u_i,u_i)}{\partial x_j} - \left(\overline{u_i\frac{\partial p}{\partial x_i}} - \widetilde{u}_i\frac{\partial \overline{p}}{\partial x_i}\right),$$

- Following closures are commonly used:

$$\begin{aligned}
-\overline{\rho}\tau(u_i,u_j)\frac{\partial \widetilde{u}_i}{\partial x_j} &= \left(2\mu_t\left(\widehat{S}_{ij} - \frac{1}{3}\frac{\partial \widetilde{u}_k}{\partial x_k}\delta_{ij}\right) - \frac{2}{3}k\delta_{ij}\right)\frac{\partial \widetilde{u}_i}{\partial x_j}, \\
-\overline{\rho}\epsilon &= -C_D\overline{\rho}\frac{k^{3/2}}{\Delta_L}, \\
-\frac{1}{2}\frac{\partial \overline{\rho}\tau(u_j,u_i,u_i)}{\partial x_j} &= \frac{\partial}{\partial x_j}\left(\frac{\mu_t}{\sigma_k}\frac{\partial k}{\partial x_j}\right),
\end{aligned}$$

- The velocity-pressure gradient correlation is often neglected, but …

- Wilcox proposed a compressible correction for high speed flows which can be readily adopted to LES

$$\begin{aligned}\left(\overline{u_i\frac{\partial p}{\partial x_i}}-\widetilde{u}_i\frac{\partial \overline{p}}{\partial x_i}\right) &= \overline{(\widetilde{u}_i+u_i'')\left(\frac{\partial \overline{p}}{\partial x_i}+\frac{\partial p'}{\partial x_i}\right)}-\widetilde{u}_i\frac{\partial \overline{p}}{\partial x_i}\\ &= \overline{u_i''}\frac{\partial \overline{p}}{\partial x_i}-\overline{p'\frac{\partial u_i''}{\partial x_i}}+\frac{\partial \overline{u_i'' p'}}{\partial x_i},\end{aligned}$$

- where the last three terms are the pressure work, dilatation, and diffusion
- The compressible correction is then

$$\begin{aligned}\overline{u_i''}\frac{\partial \overline{p}}{\partial x_i} &= \frac{M_t k}{\overline{\rho}\epsilon}\tau(u_i,u_j)\frac{\partial \overline{\rho}}{\partial x_j}\frac{\partial \overline{p}}{\partial x_i},\\ \overline{p'\frac{\partial u_i''}{\partial x_i}} &= \alpha_2 M_t\overline{\rho}\tau(u_i,u_j)\frac{\partial \widetilde{u}_i}{\partial x_j}-\alpha_3 M_t^2\overline{\rho}\epsilon,\\ \frac{\partial \overline{u_i'' p'}}{\partial x_i} &= 0,\end{aligned}$$

- where subgrid turbulence Mach number is $M_t=\sqrt{2k/\widetilde{u}_i\widetilde{u}_i}$

- Final form of the turbulent subgrid kinetic energy transport equation

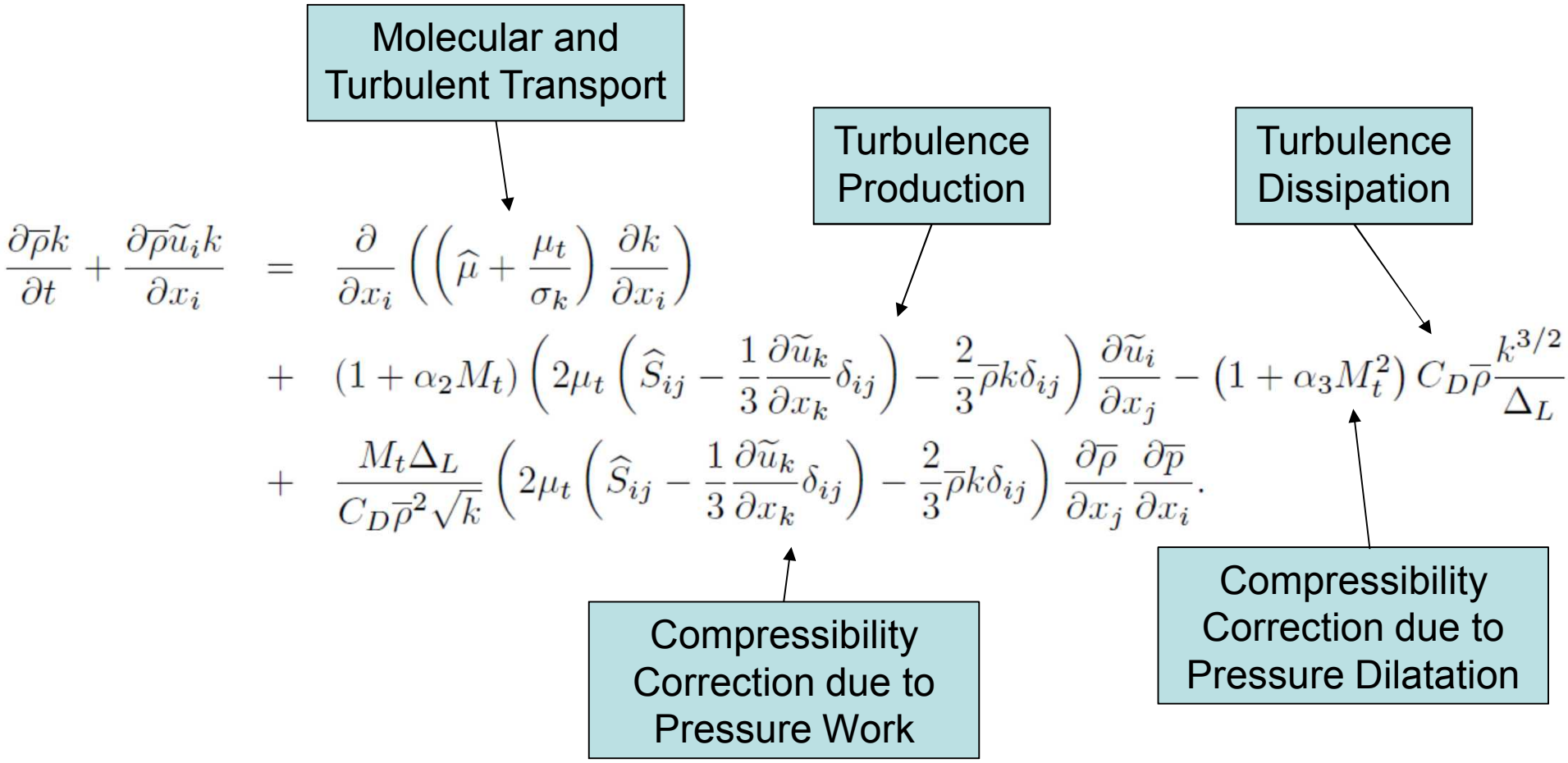

- with M_t=0 the conventional incompressible model is recovered.

- References

Tennekes, H. and Lumley, J.L., *A First Course in Turbulence*, MIT Press, Cambridge, MA, 1972.

Hinze, J.O., *Turbulence*, McGraw Hill Book Company, New York, NY, 1975.

Libby, P.A. and Williams, F.A., eds., *Turbulent Reacting Flows*, Academic Press, London, UK, 1994.

Pope, S.B., *Turbulent Flows*, Cambridge University Press, Cambridge, UK, 2000.

Wilcox, D.C., *Turbulence Modeling for CFD*, DCW Industries, Inc., La Cañada, CA, 2000.

Sagaut, P., *Large Eddy Simulation of Incompressible Flows: An Introduction*, Springer-Verlag, Berlin, Germany, 3rd ed., 2006.

Durbin, P.A. and Reif, B.A.P., *Statistical Theory and Modeling for Turbulent Flows*, John Wiley & Sons, Ltd., New York, NY, 2nd ed., 2011.

Baurle, R.A., "Modeling of High Speed Reacting Flows: Established Practices And Future Challenges," in *42nd AIAA Aerospace Sciences Meeting and Exhibit*, AIAA, Reno, NV, 2004. AIAA-2004-267.

Pope, S., "Small Scales, Many Species and the Manifold Challenges of Turbulent Combustion," *Proc. Combust. Inst.*, **34**:1–31, 2013.

Numerical Methods

- Physical domain discretization (i.e., grid/mesh type):
  - Structured: Cartesian, Generalized Curvilinear Coordinates, Overset
  - Unstructured (hex, tets, prisms, pyramids)
- Equation discretization:
  - Finite Difference (typically only used on structured meshes) (arbitrary order)
  - Finite Volume (cell-centered, cell-vertex, staggered) (typically 2nd order)
  - Finite Element : Discontinuous Galerkin (DG) (high order)
  - Spectral or Pseudo-Spectral (high order)
- Time discretization:
  - Explicit: Runge-Kutta, Predictor-Corrector (e.g., MacCormack), Backward Euler, etc.
  - Implicit: Runge-Kutta, Dual Time-Stepping, ADI, DAF, LU, Sundials, Hypre
- Numerical Approach:
  - Pressure projection : Rhie-Chow (typically for "weakly" compressible reacting flows)
  - Density-based (stiff at low Mach numbers)
- Acceleration Techniques:
  - Local Time-Stepping
  - Multigrid
  - Preconditioning (physical and numerical)
  - Parallelization (MPI, OMP, GPU)

Book available on Science Direct

Blazek, J., *Computational Fluid Dynamics: Principles and Applications*, *Elsevier*, **2005**

- Finite volume scheme in generalized curvilinear coordinates

$$\frac{\partial \mathbf{Q}}{\partial t} + \frac{\partial \mathbf{E}}{\partial x} + \frac{\partial \mathbf{F}}{\partial y} + \frac{\partial \mathbf{G}}{\partial z} = \mathbf{S}$$

$$\iiint_V \frac{\partial \mathbf{Q}}{\partial t} dV + \iiint_V \left(\frac{\partial \mathbf{E}}{\partial x} + \frac{\partial \mathbf{F}}{\partial y} + \frac{\partial \mathbf{G}}{\partial z} \right) dV = \iiint_V \mathbf{S} dV$$

- Applying the divergence theorem to the flux terms

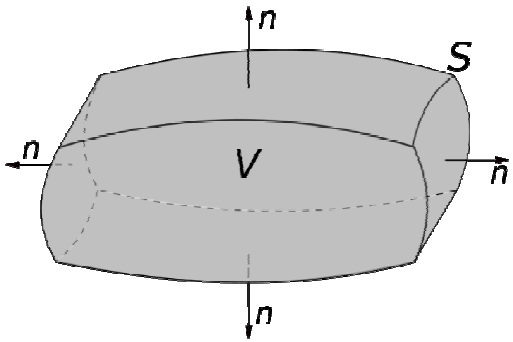

$$\frac{\partial}{\partial t} \iiint_V \mathbf{Q} dV + \oiint_S \left(\mathbf{E} dS_x + \mathbf{F} dS_y + \mathbf{G} dS_z \right) dV = \iiint_V \mathbf{S} dV$$

- Coordinates transformation

$$\xi = \xi(x, y, z)$$
$$\eta = \eta(x, y, z)$$
$$\zeta = \zeta(x, y, z)$$

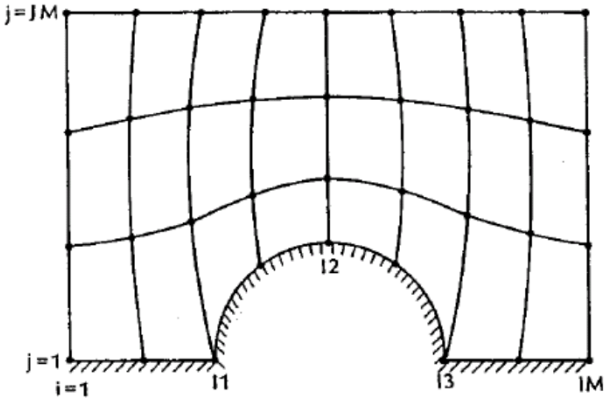

$$\frac{\partial}{\partial x} = \xi_x \frac{\partial}{\partial \xi} + \eta_x \frac{\partial}{\partial \eta} + \zeta_x \frac{\partial}{\partial \zeta}$$
$$\frac{\partial}{\partial y} = \xi_y \frac{\partial}{\partial \xi} + \eta_y \frac{\partial}{\partial \eta} + \zeta_y \frac{\partial}{\partial \zeta}$$
$$\frac{\partial}{\partial z} = \xi_z \frac{\partial}{\partial \xi} + \eta_z \frac{\partial}{\partial \eta} + \zeta_z \frac{\partial}{\partial \zeta}$$

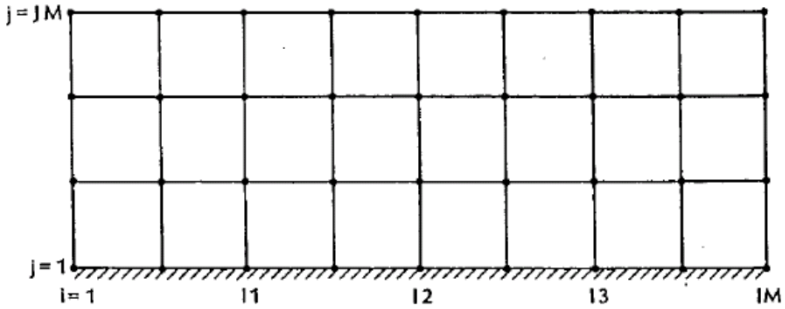

$$J = \det \left| \frac{\partial(\xi, \eta, \zeta)}{\partial(x, y, z)} \right| = \det \left| \begin{pmatrix} \xi_x & \xi_y & \zeta_z \\ \eta_x & \eta_y & \eta_z \\ \zeta_x & \zeta_y & \zeta_z \end{pmatrix} \right| = \det \left| \begin{pmatrix} x_\xi & x_\eta & x_\zeta \\ y_\xi & y_\eta & y_\zeta \\ z_\xi & z_\eta & z_\zeta \end{pmatrix}^{-1} \right|$$

$$= \frac{1}{x_\xi(y_\eta z_\zeta - y_\zeta z_\eta) - x_\eta(y_\xi z_\zeta - y_\zeta z_\xi) + x_\zeta(y_\xi z_\eta - y_\eta z_\xi)}$$

- Transformed governing equation in conservative form

$$\frac{\partial \bar{\mathbf{Q}}}{\partial t} + \frac{\partial \bar{\mathbf{E}}}{\partial \xi} + \frac{\partial \bar{\mathbf{F}}}{\partial \eta} + \frac{\partial \bar{\mathbf{G}}}{\partial \zeta} = \bar{\mathbf{S}}$$

$$\bar{\mathbf{Q}} = \frac{\mathbf{Q}}{J}$$

$$\bar{\mathbf{E}} = \frac{1}{J}(\xi_x \mathbf{E} + \xi_y \mathbf{F} + \xi_z \mathbf{G})$$

$$\bar{\mathbf{F}} = \frac{1}{J}(\eta_x \mathbf{E} + \eta_y \mathbf{F} + \eta_z \mathbf{G})$$

$$\bar{\mathbf{G}} = \frac{1}{J}(\zeta_x \mathbf{E} + \zeta_y \mathbf{F} + \zeta_z \mathbf{G})$$

$$\mathbf{Q} = \frac{1}{J}\begin{bmatrix} \overline{\rho} \\ \overline{\rho}\widetilde{Y}_1 \\ \vdots \\ \overline{\rho}\widetilde{Y}_\alpha \\ \vdots \\ \overline{\rho}\widetilde{Y}_N \\ \overline{\rho}\widetilde{u} \\ \overline{\rho}\widetilde{v} \\ \overline{\rho}\widetilde{w} \\ \overline{\rho}\widetilde{e^t} \\ \overline{\rho}k \end{bmatrix}$$

- Time integration
  - Explicit

$$\Delta\bar{\mathbf{Q}} = \bar{\mathbf{Q}}^{n+1} - \bar{\mathbf{Q}}^{n} = \Delta t \left(-\frac{\partial \bar{\mathbf{E}}}{\partial \xi}\bigg|^{n} - \frac{\partial \bar{\mathbf{F}}}{\partial \eta}\bigg|^{n} - \frac{\partial \bar{\mathbf{G}}}{\partial \zeta}\bigg|^{n} + \bar{\mathbf{S}}^{n} \right)$$

  - Implicit
    - Linearization

$$\bar{\mathbf{E}}^{n+1} = \bar{\mathbf{E}}^{n} + \frac{\partial \bar{\mathbf{E}}}{\partial t}\Delta t + \mathcal{O}(\Delta t^2)$$

$$\bar{\mathbf{E}}^{n+1} = \bar{\mathbf{E}}^{n} + \frac{\partial \bar{\mathbf{E}}}{\partial \bar{\mathbf{Q}}}\frac{\partial \bar{\mathbf{Q}}}{\partial t}\Delta t + \mathcal{O}(\Delta t^2)$$

$$\bar{\mathbf{E}}^{n+1} = \bar{\mathbf{E}}^{n} + \frac{\partial \bar{\mathbf{E}}}{\partial \bar{\mathbf{Q}}}\left(\frac{\bar{\mathbf{Q}}^{n+1} - \bar{\mathbf{Q}}^{n}}{\Delta t} + \mathcal{O}(\Delta t) \right) \Delta t + \mathcal{O}(\Delta t^2)$$

$$\bar{\mathbf{E}}^{n+1} = \bar{\mathbf{E}}^{n} + \frac{\partial \bar{\mathbf{E}}}{\partial \bar{\mathbf{Q}}}\Delta\bar{\mathbf{Q}} + \mathcal{O}(\Delta t^2)$$

$$\left(\frac{\mathbf{I}}{\Delta t} - \frac{\partial}{\partial \xi}\frac{\partial \bar{\mathbf{E}}}{\partial \bar{\mathbf{Q}}}\bigg|^{n} - \frac{\partial}{\partial \eta}\frac{\partial \bar{\mathbf{F}}}{\partial \bar{\mathbf{Q}}}\bigg|^{n} - \frac{\partial}{\partial \zeta}\frac{\partial \bar{\mathbf{G}}}{\partial \bar{\mathbf{Q}}}\bigg|^{n} + \frac{\partial \bar{\mathbf{S}}}{\partial \bar{\mathbf{Q}}}\bigg|^{n} \right) \Delta\bar{\mathbf{Q}}$$

$$= -\left(\frac{\partial \bar{\mathbf{E}}}{\partial \xi}\bigg|^{n} + \frac{\partial \bar{\mathbf{F}}}{\partial \eta}\bigg|^{n} + \frac{\partial \bar{\mathbf{G}}}{\partial \zeta}\bigg|^{n} - \bar{\mathbf{S}}^{n} \right) = -\mathbf{R}^{n}$$

- Discretization of Convective Fluxes
  - Central
  - Flux-vector splitting
  - Flux-difference splitting
  - TVD

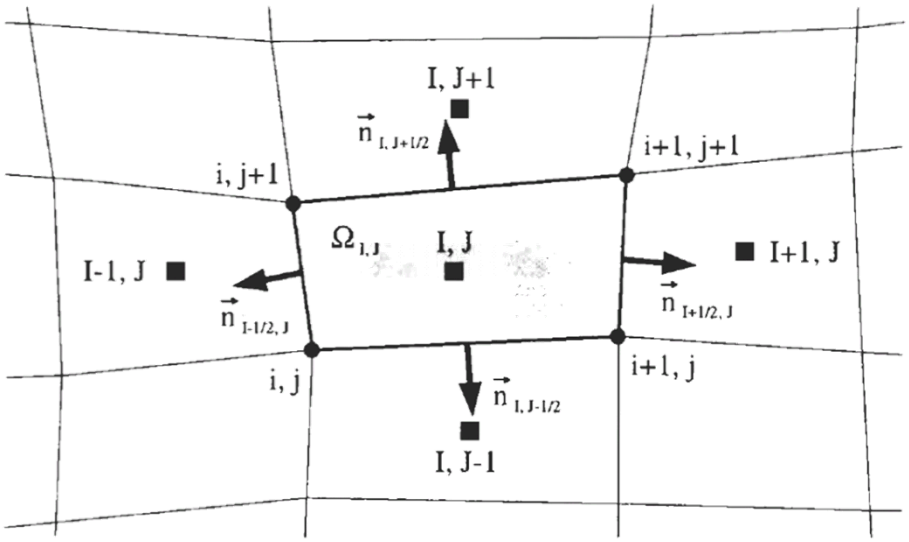

- General spatial discretization for fluxes at cell faces (cell centered scheme)
  - Average of fluxes from adjacent cells

$$(\mathbf{E}\,\Delta S)_{I+1/2,J} \approx \frac{1}{2}\left(\mathbf{E}(\mathbf{Q}_{I,J}) + \mathbf{E}(\mathbf{Q}_{I+1,J})\right)\Delta S_{I+1/2,J}$$

  - Average of variables to cell face

$$(\mathbf{E}\,\Delta S)_{I+1/2,J} \approx \mathbf{E}(\mathbf{Q}_{I+1/2,J})\Delta S_{I+1/2,J} \qquad \mathbf{Q}_{I+1/2,J} = \frac{1}{2}(\mathbf{Q}_{I,J} + \mathbf{Q}_{I+1,J})$$

  - Flux reconstruction from quantities interpolated to left and right side of the face

$$(\mathbf{E}\,\Delta S)_{I+1/2,J} \approx f_{Flux}(\mathbf{Q}_L, \mathbf{Q}_R, \Delta S_{I+1/2,J})$$

$$\mathbf{Q}_L = f_{Interp}(\ldots, \mathbf{Q}_{I-1,J}, \mathbf{Q}_{I,J}, \ldots) \qquad \mathbf{Q}_R = f_{Interp}(\ldots, \mathbf{Q}_{I,J}, \mathbf{Q}_{I+1,J}, \ldots)$$

Numerical Methods

- Verification
  - Richardson extrapolation and Grid Convergence Index (GCI)
  - Method of Manufactured Solutions (strong verification)
  - Comparisons with exact solutions of canonical problems (numerical methods)
  - Comparisons with DNS (for modeling)
  - Uncertainty Quantification (sensitivities)
  - Comparisons with Experiments (weak verification)
- Richardson extrapolation and Grid Convergence Index (GCI)

$$Error = f(\Delta) - f^{exact} = C\Delta^p + H.O.T$$

$$Diff(2\Delta, \Delta) = f(2\Delta) - f(\Delta) = C\Delta^p(2^p - 1)$$

$$Error = C^* \frac{Diff(2\Delta, \Delta)}{2^p - 1}$$

Safety Factor
(1.25 for p=1, 3 for p=2)

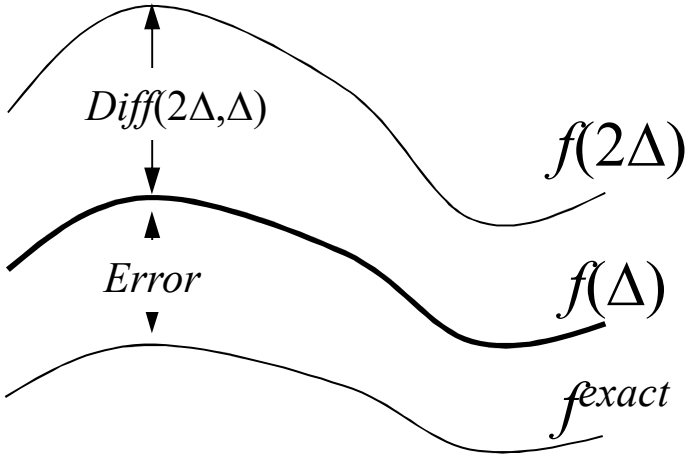

Numerical Methods

- References

★ Masatsuka, K., *I Do Like CFD*, vol. 1, http://www.cfdbooks.com/cfdbooks.html, 2nd ed., 2013.

Pletcher, R.H., Tannehill, J.C., and Anderson, D.A., *Computational Fluid Mechanics and Heat Transfer*, CRC Press, Boca Raton, FL, 3rd ed., 2013.

★ Blazek, J., *Computational Fluid Dynamics: Principles and Applications*, Elsevier, Washington, D.C., 2nd ed., 2005.

Hoffmann, Klaus, A. and Chiang, Steve, T., *Computational Fluid Dynamics, Volume I*, Engineering Education Systems, Wichita, KS, 4th ed., 2000.

Hoffmann, K.A. and Chiang, S.T., *Computational Fluid Dynamics, Volume II*, Endingeering Education System, Wichita, KS, 4th ed., 2000.

★ Free PDF available online

★ Free download from www.sciencedirect.com with organization's subscription

CFD Modeling and Simulation of High Speed Reacting Flows: Applications

Tomasz (Tom) G. Drozda

tomasz.g.drozda@nasa.gov

Hypersonic Airbreathing Propulsion Branch

NASA Langley Research Center

Hampton Virginia

With contributions from Dr. Rob Baurle, Jeff White, and Dr. Phil Drummond.

Outline

- Example Applications
  - (Re)Introduction to Problem Space
  - External Aero of Hypersonic Vehicles
  - Facility Nozzle Simulations for Ground Experimentation
  - Component Simulations
  - Scale Resolving (LES) Simulations vs. Reynolds Average Simulations (RAS)

VULCAN-CFD Overview

- VULCAN-CFD is a hybrid Structured/Unstructured 3-D compressible flow solver
  - Solves the Reynolds-averaged or spatially filtered (LES) equations governing thermal equilibrium/non-equilibrium gases with chemical reactions
  - Supports any combination of FNS and/or PNS solution procedures
  - Parallelized via domain decomposition using portable MPI libraries
  - Currently supports 36 boundary conditions
  - Arbitrary C0 and non-C0 block to block connectivity supported
  - Variety of turbulence closure models (LEVMs, ARSM, hybrid RAS/LES, dynamic SGS closures)
  - Generalized chemistry treatment (finite rate with allowances for arbitrary reaction orders and pressure-dependent kinetics, CARM)
  - Collaborative development environment with continuous regression testing
  - Portable to a wide class of Unix/Linux architectures
  - Suite of post-processing tools specific to high-speed propulsion

- VULCAN-CFD is available to US Nationals (Export Controlled) and a reasonable level of support is offered as well
  - VULCAN-CFD is used extensively by government, industry and academia for external and internal hypersonic flow analysis
  - On the order of 10 new requests per year are processed

Problem Space Addressed by the CFD

Flight

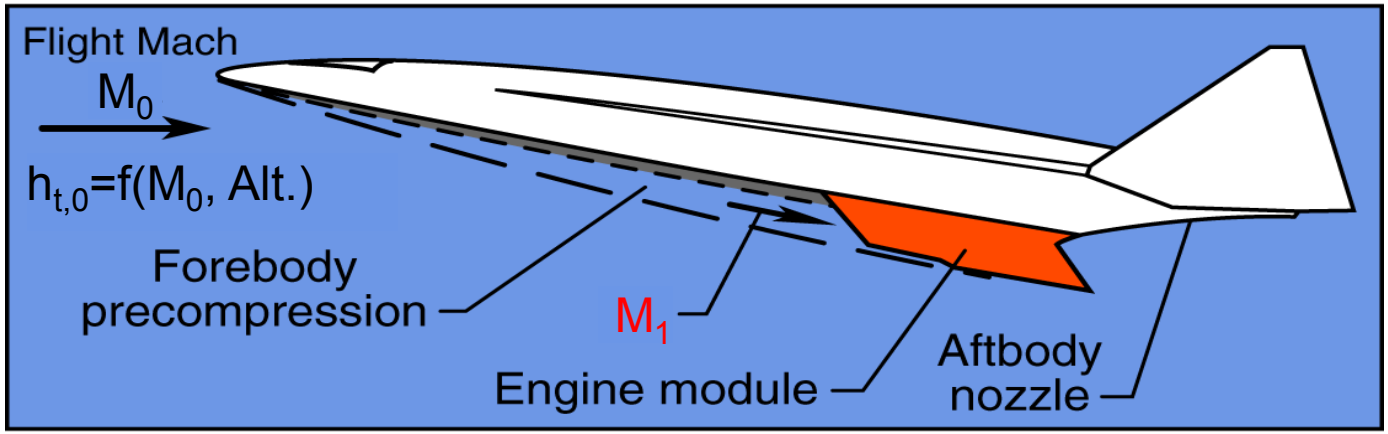

Simulation in ground facility

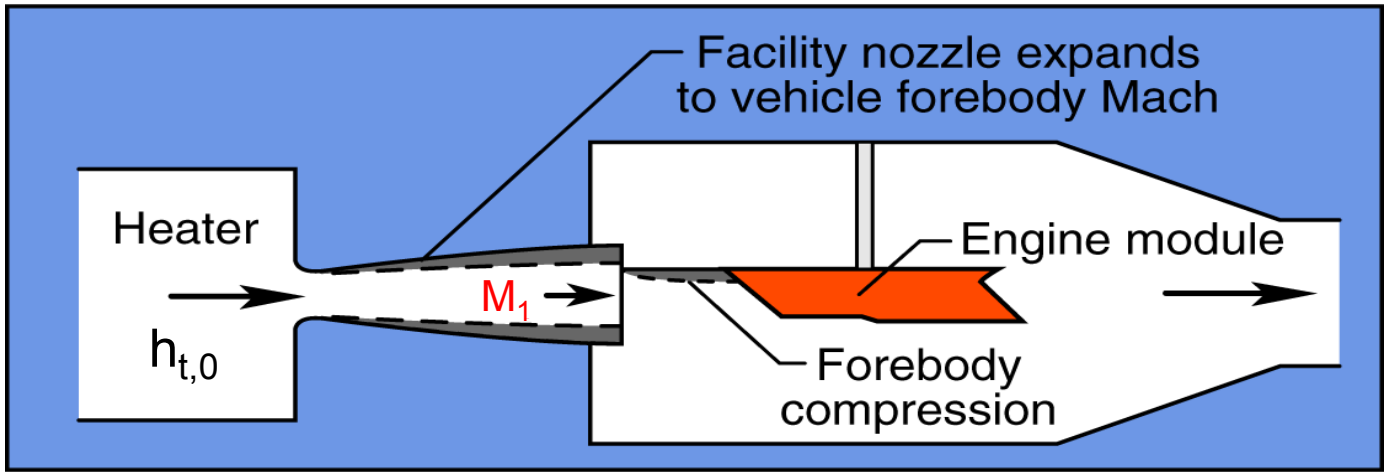

Current Coupled Numerical-Experimental Approach

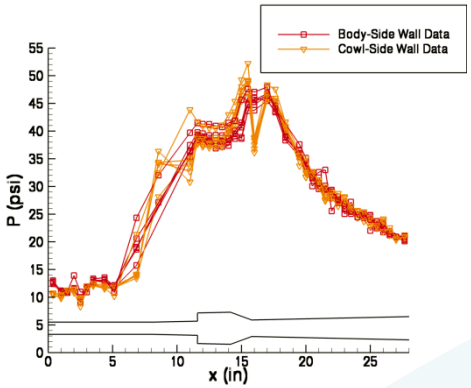

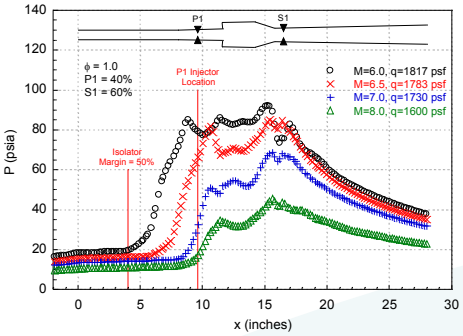

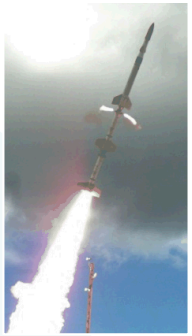

Make pre-flight operability predictions with quantified margin

Collect flight data, perform post-flight analyses

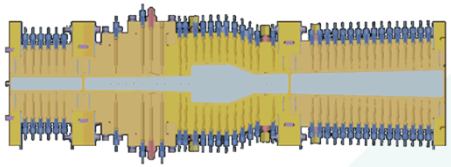

Quantify uncertainties: test condition variations and physics modeling

Verify robust combustor operation and calibrate analysis tools to ground test data

Design flowpath components

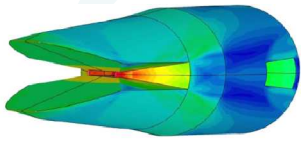

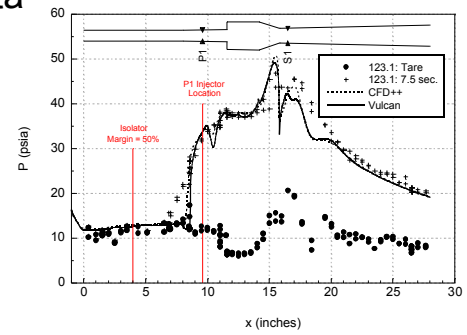

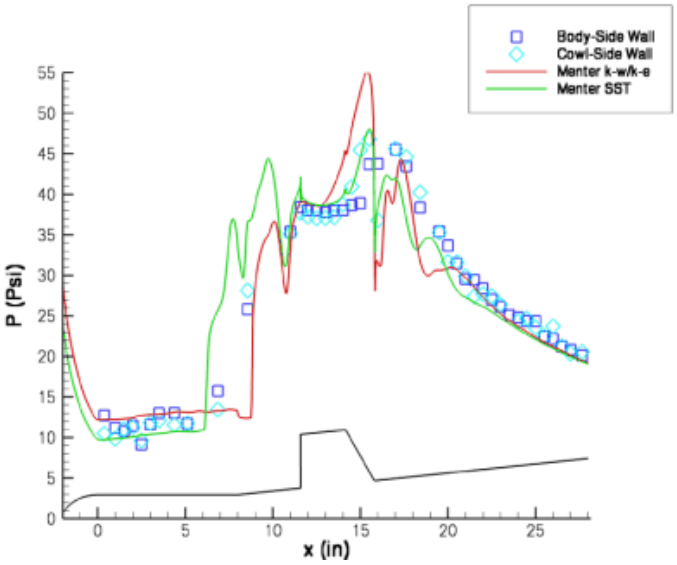

Problem Space Addressed by the CFD

Flight

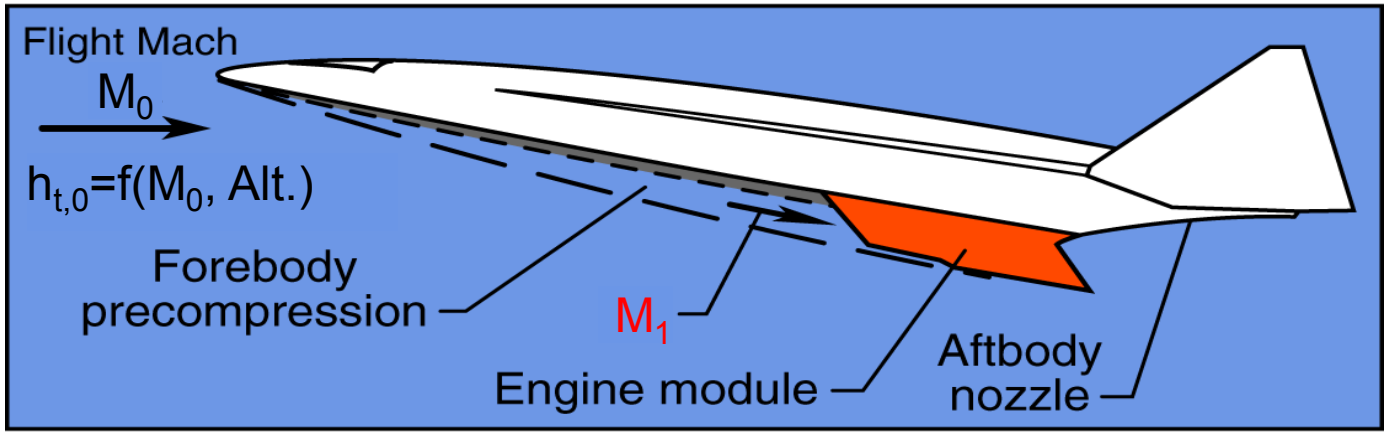

Simulation in ground facility

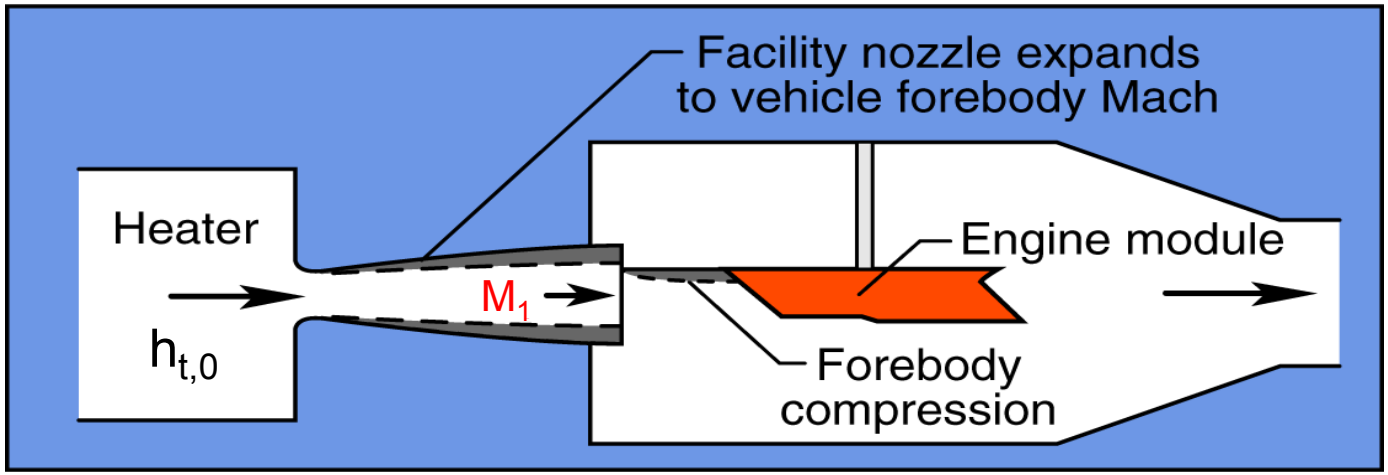

External Aero of Hypersonic Flight Vehicles

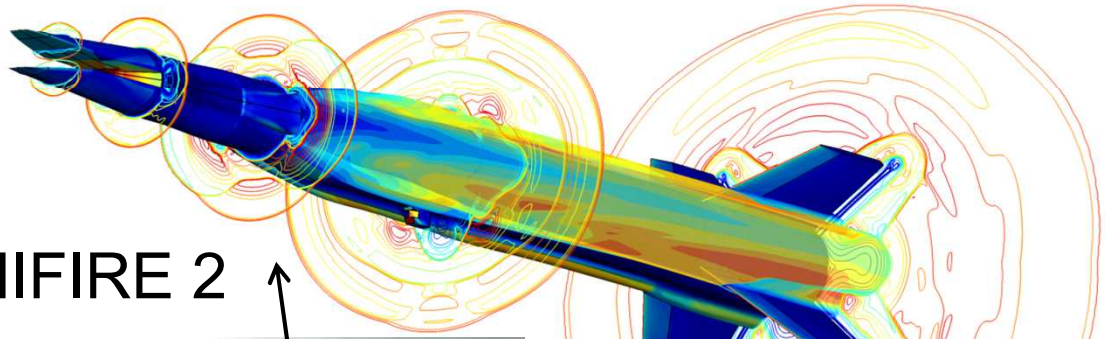

HIFIRE 2

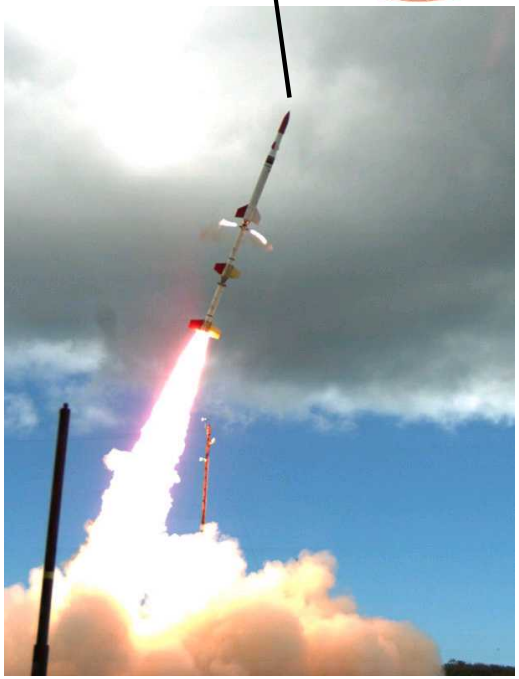

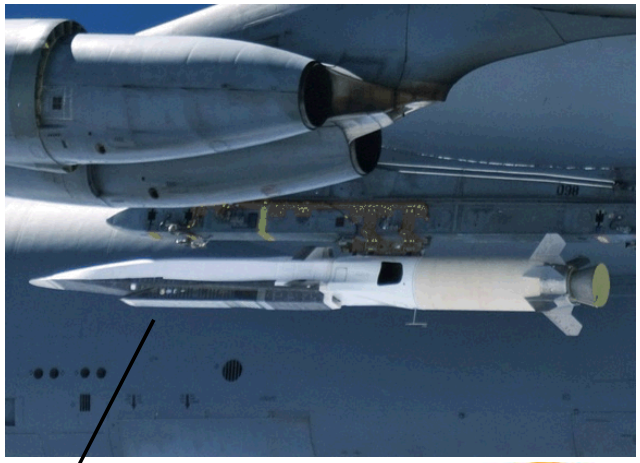

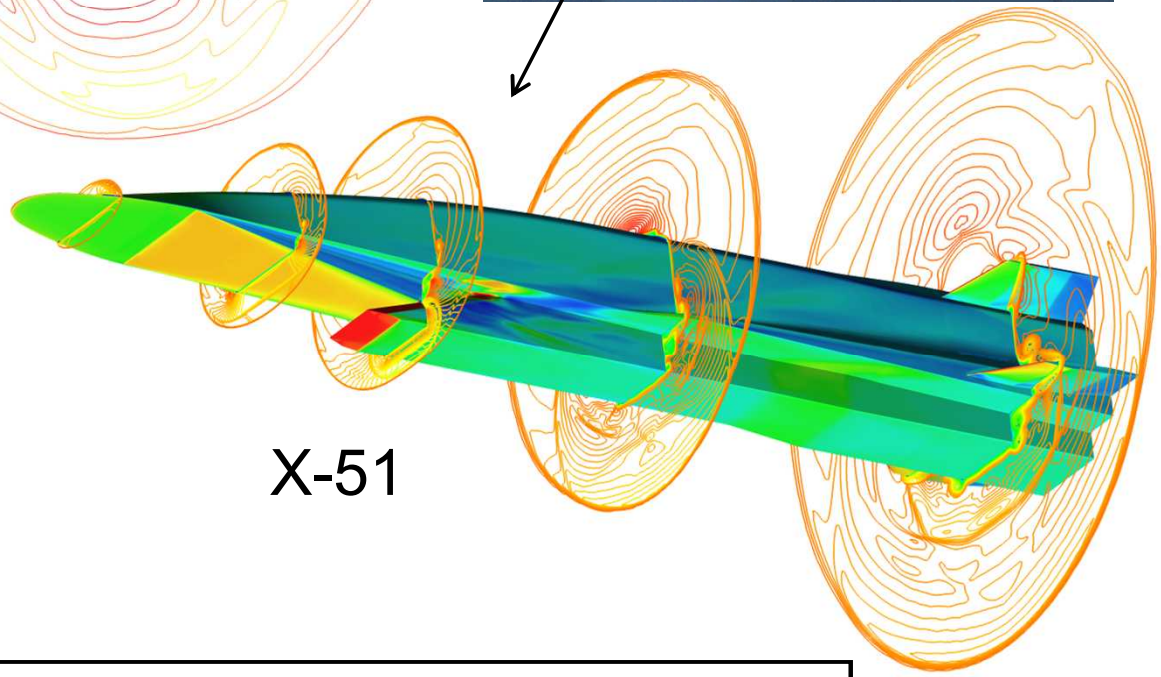

X-51

Both external aero and engine flowpaths can be simulated

External Aero of Hypersonic Flight Vehicles

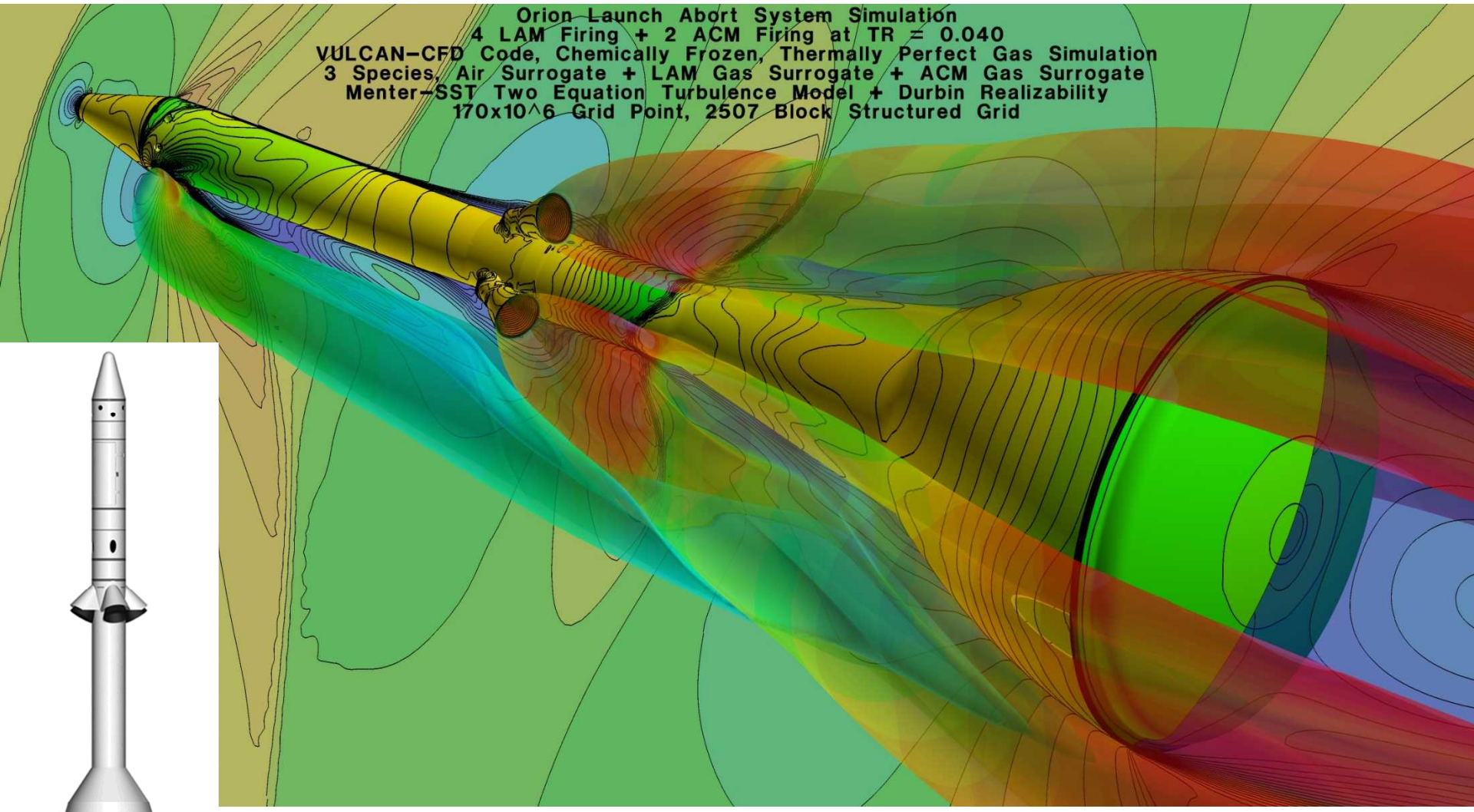

[NASA Video Collection: Orion Pad Abort-1 Launch Abort System Flight Test (YouTube)]

Problem Space Addressed by the CFD

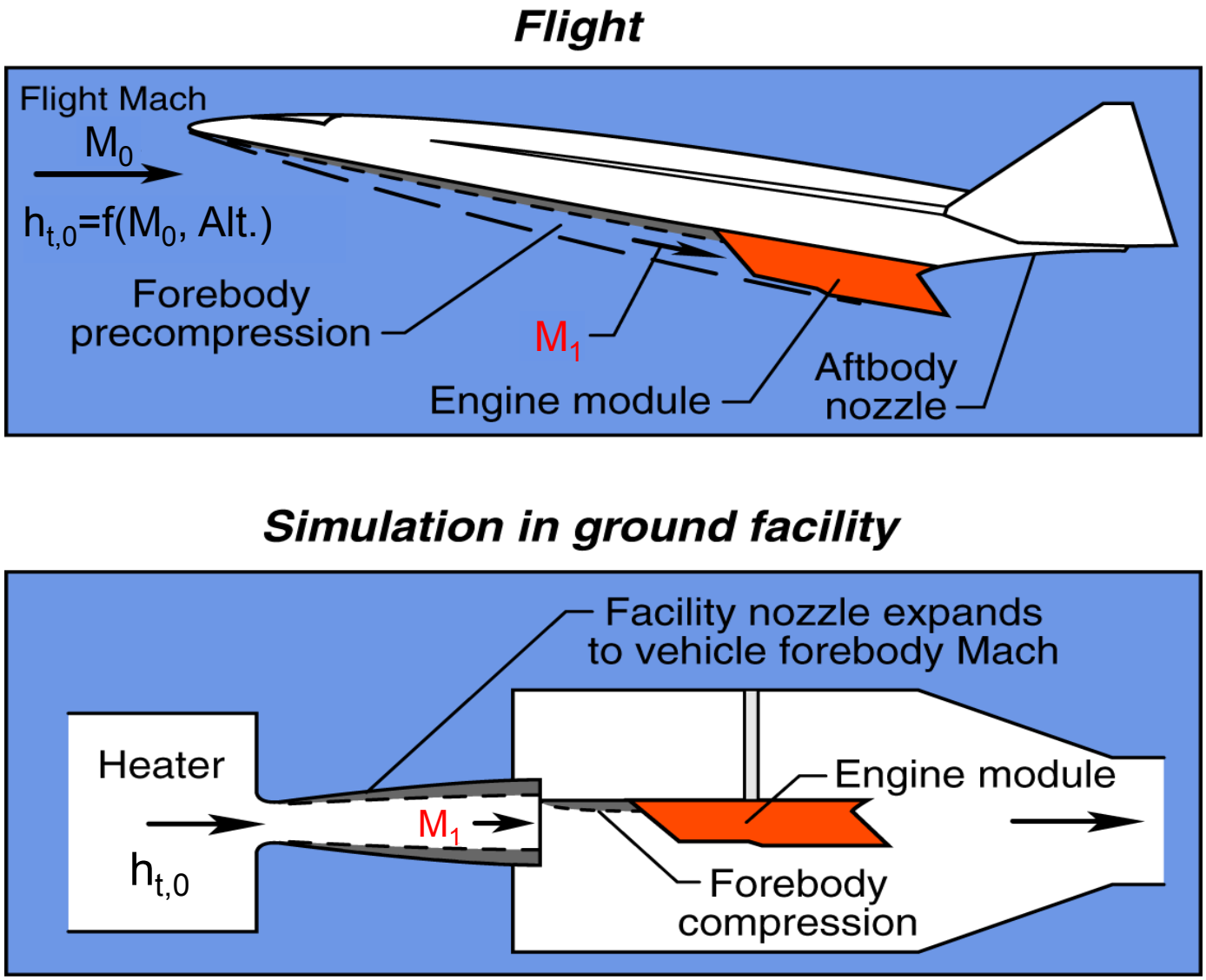

Simulations of Experimental Facility Nozzle

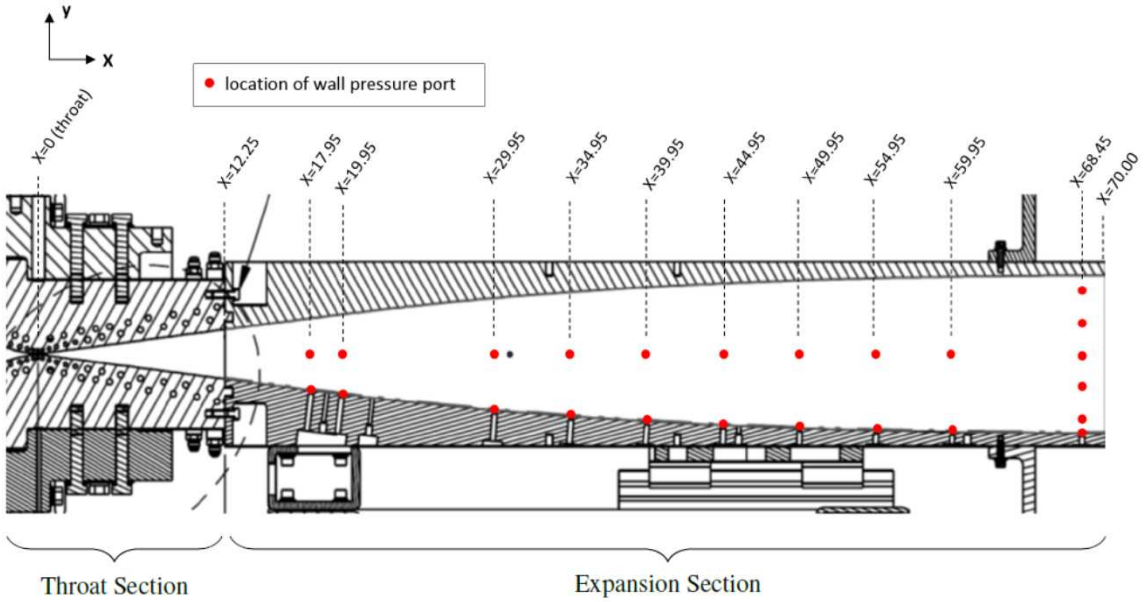

Total Temperature

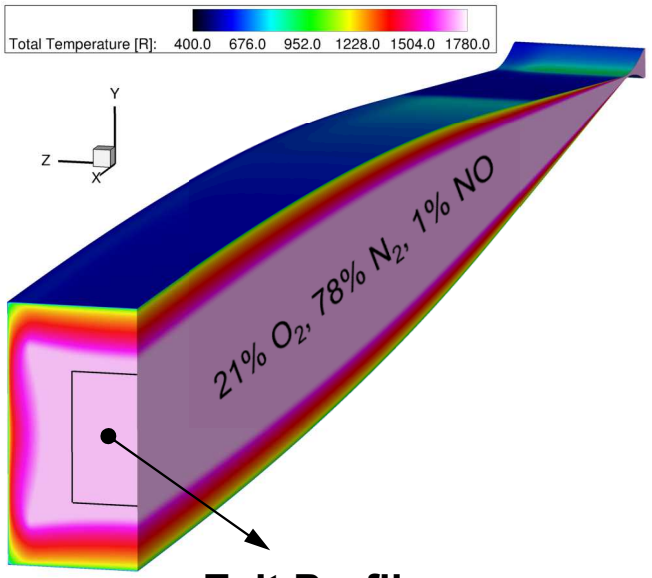

Exit Profile

Impact of thermodynamic nonequilibrium on nozzle exit

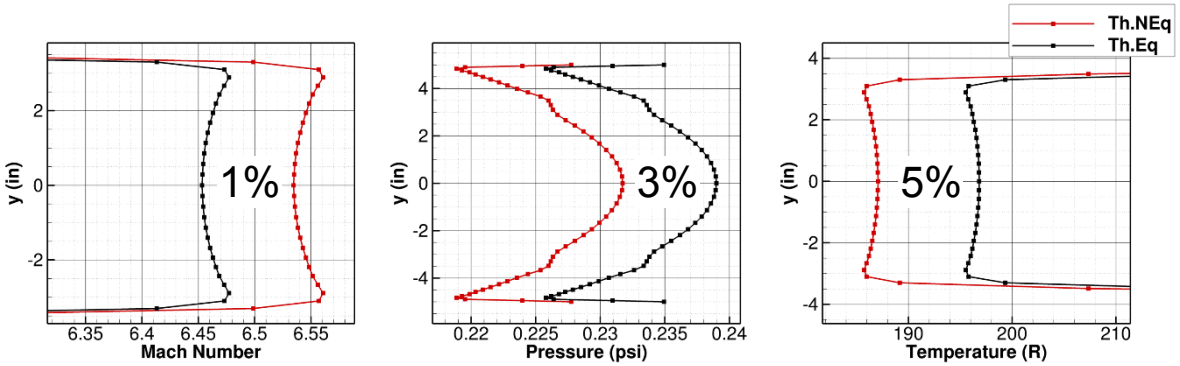

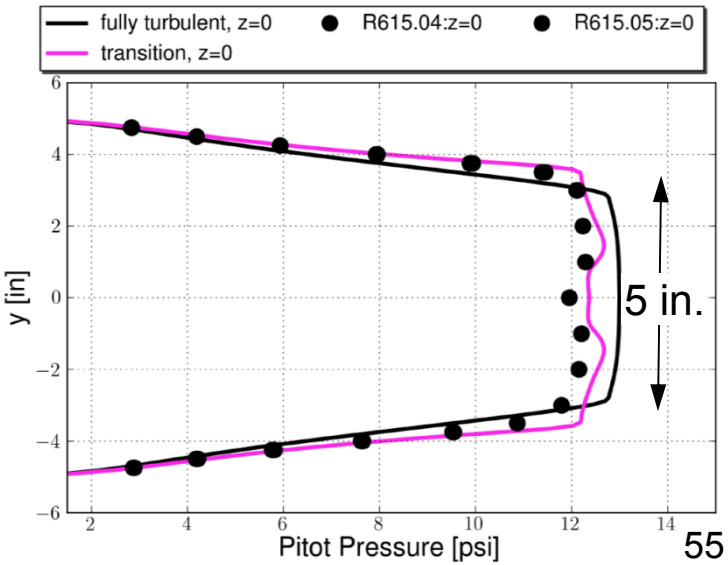

Injector Geometries

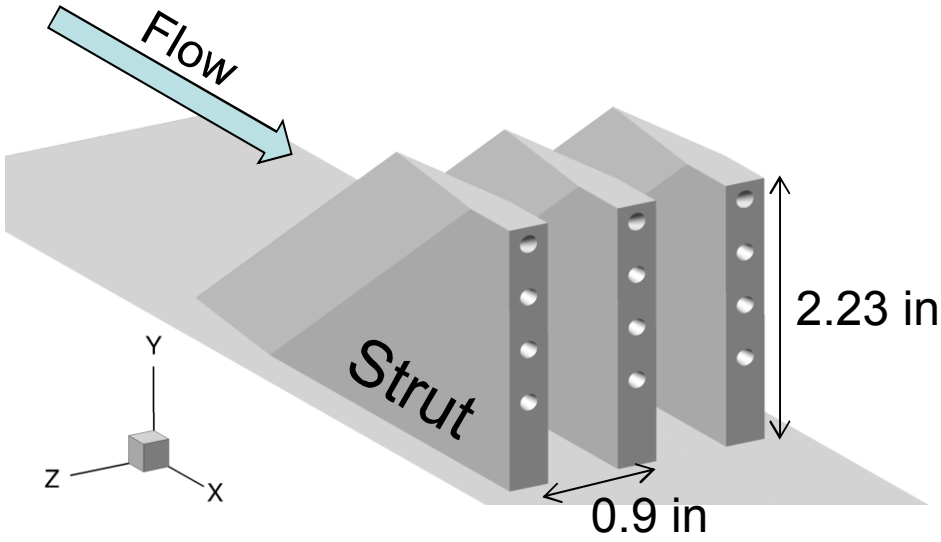

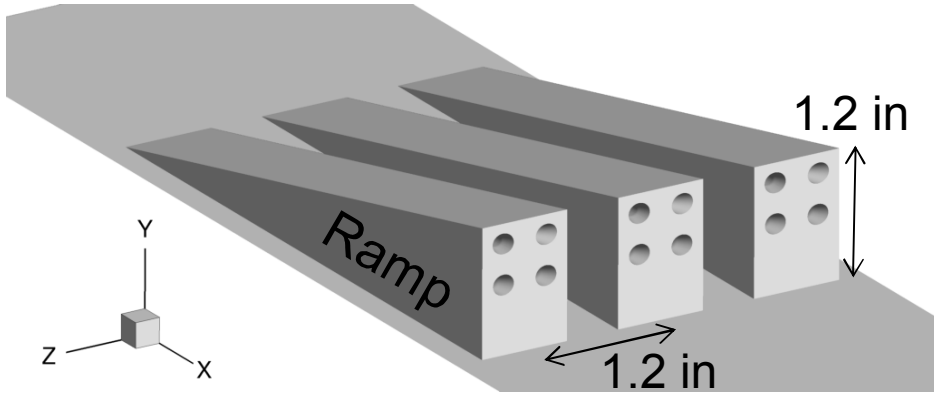

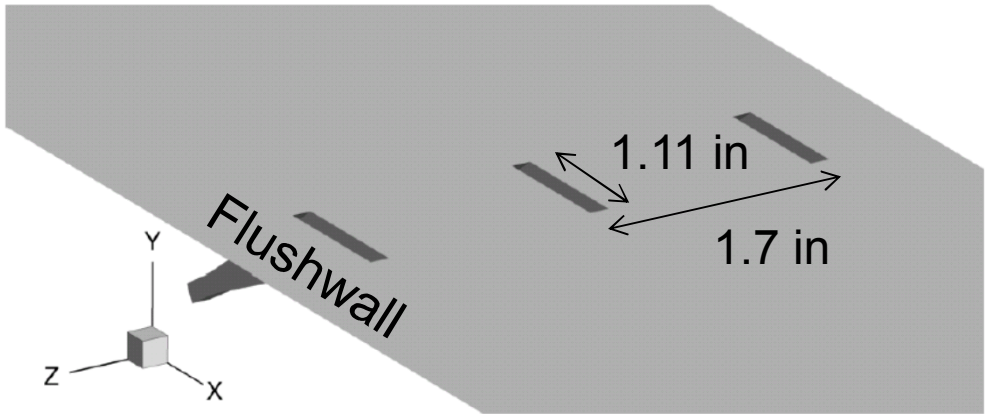

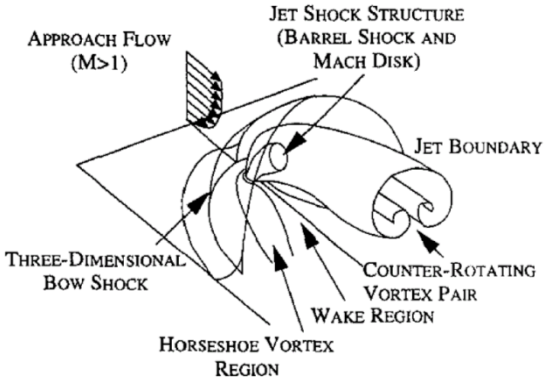

Injector Geometry and Grid Topology

- High quality grids are as important as turbulence modeling selection
  - Hex elements are most efficient and accurate
  - Grid alignment with shock features desired but in practice only achievable for the vehicle bow shock
  - Orthogonality and uniformity (gradual stretch rates of less then 10-15%) preferred
- Awareness of general flow features and their resolution requirements is needed (matter of experience)
  - Near-wall resolution requirements for wall-resolved (y+ < 1) vs. wall-modeled (y+ ~ 20) simulations
  - Increased grid densities near shear layers

Strut

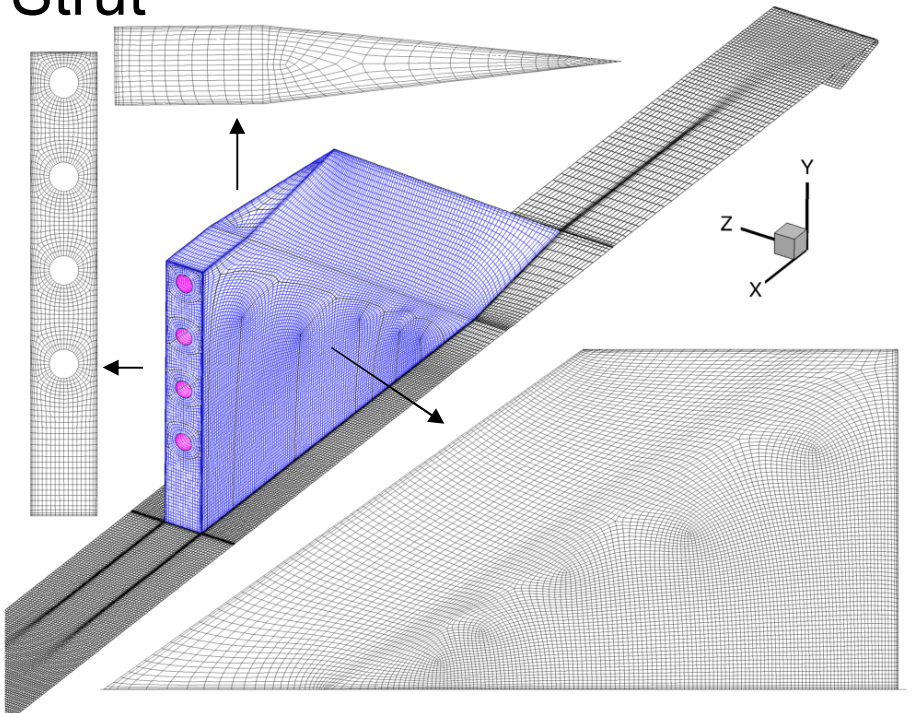

Ramp

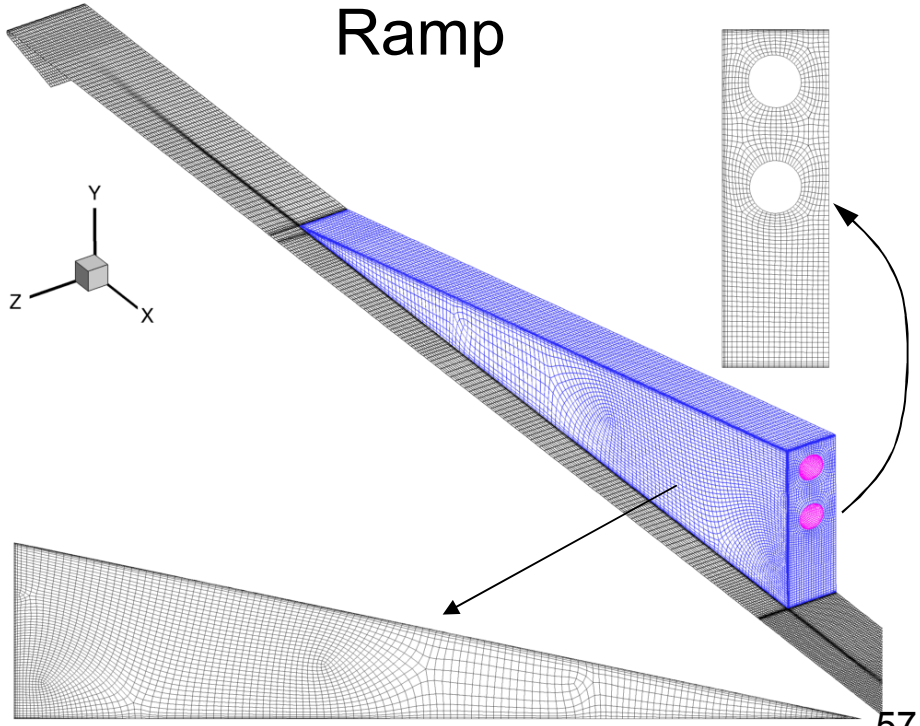

Numerical Simulation Errors (Grid Dependence)

Contours of the Mach number through the centerline of the strut injector obtained on coarse, medium, and fine meshes

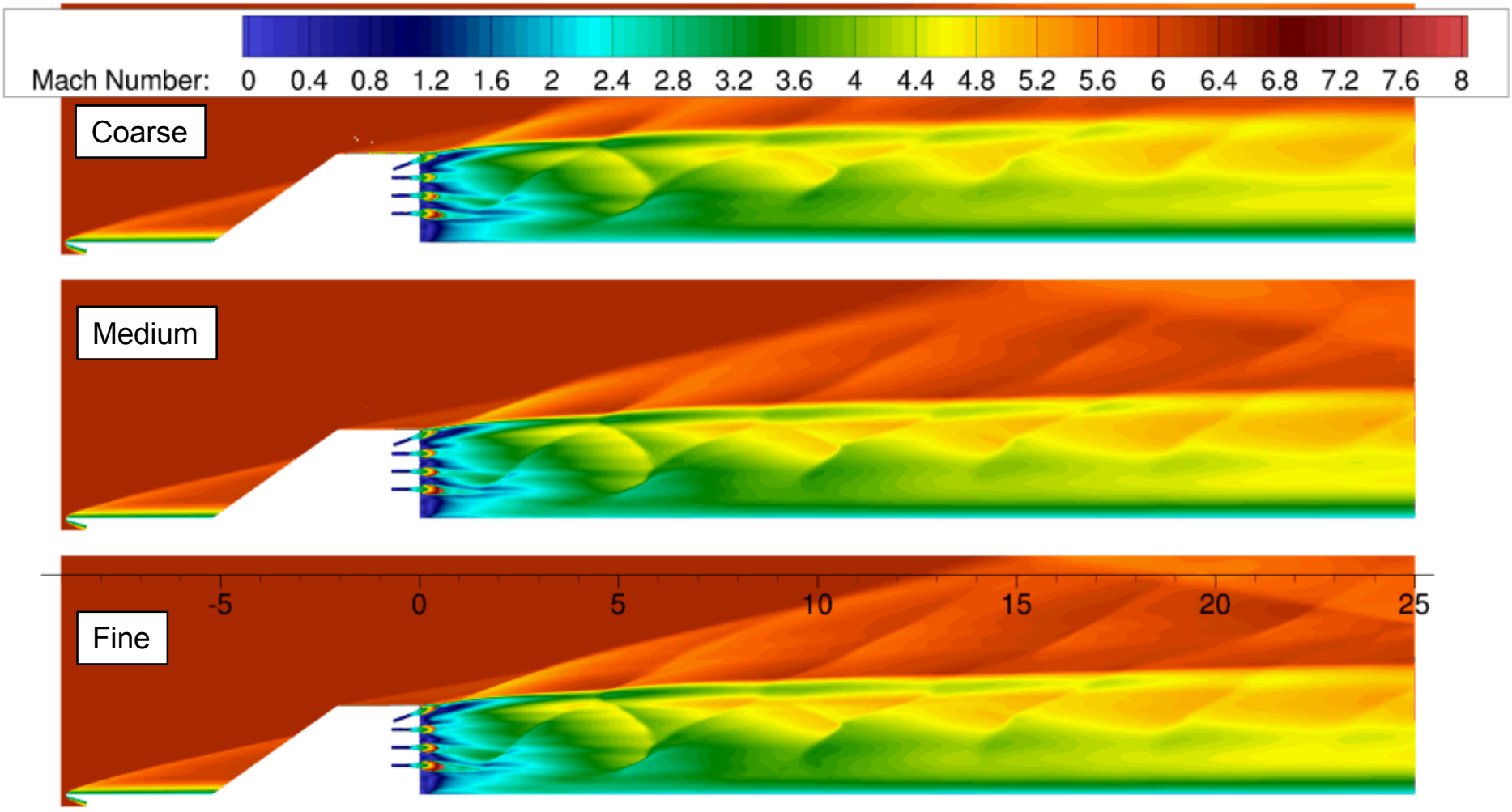

1D profiles of total pressure and mixing efficiency vs. distance

- Order of accuracy (rate of convergence)
  - One for the mixing efficiency
  - ~1.5 for the total pressure recovery
- Error bars represent the Grid Convergence Index (GCI) obtained using the Richardson Extrapolation:

$$Error = C^* \frac{Diff(2\Delta, \Delta)}{2^p - 1}$$

Safety Factor
(1.25 for p=1, 3 for p=2)

- Mixing efficiency appears more sensitive to the grid resolution than other 1D quantities (e.g., total pressure, Mach, thrust potential)

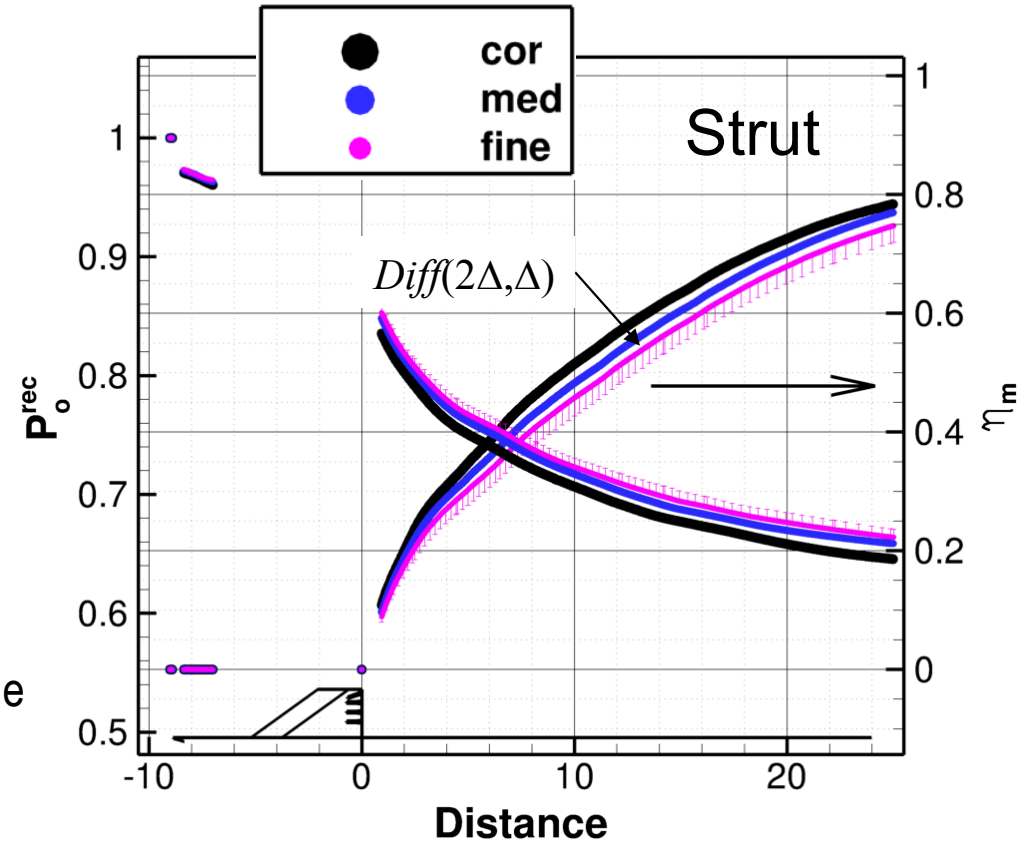

Baurle, R. and Gaffney, R., "**Extraction of One-Dimensional Flow Properties From Multidimensional Data Sets**", J. Propul Power, Vol. 24, No. 4, 2008, pp. 704–714.

	Strut	Ramp	Flushwall
Coarse	4,921,682	4,057,382	4,356,936
Medium	39,373,456	32,459,056	34,855,488
Fine	314,987,648	259,672,448	278,843,904

Strut

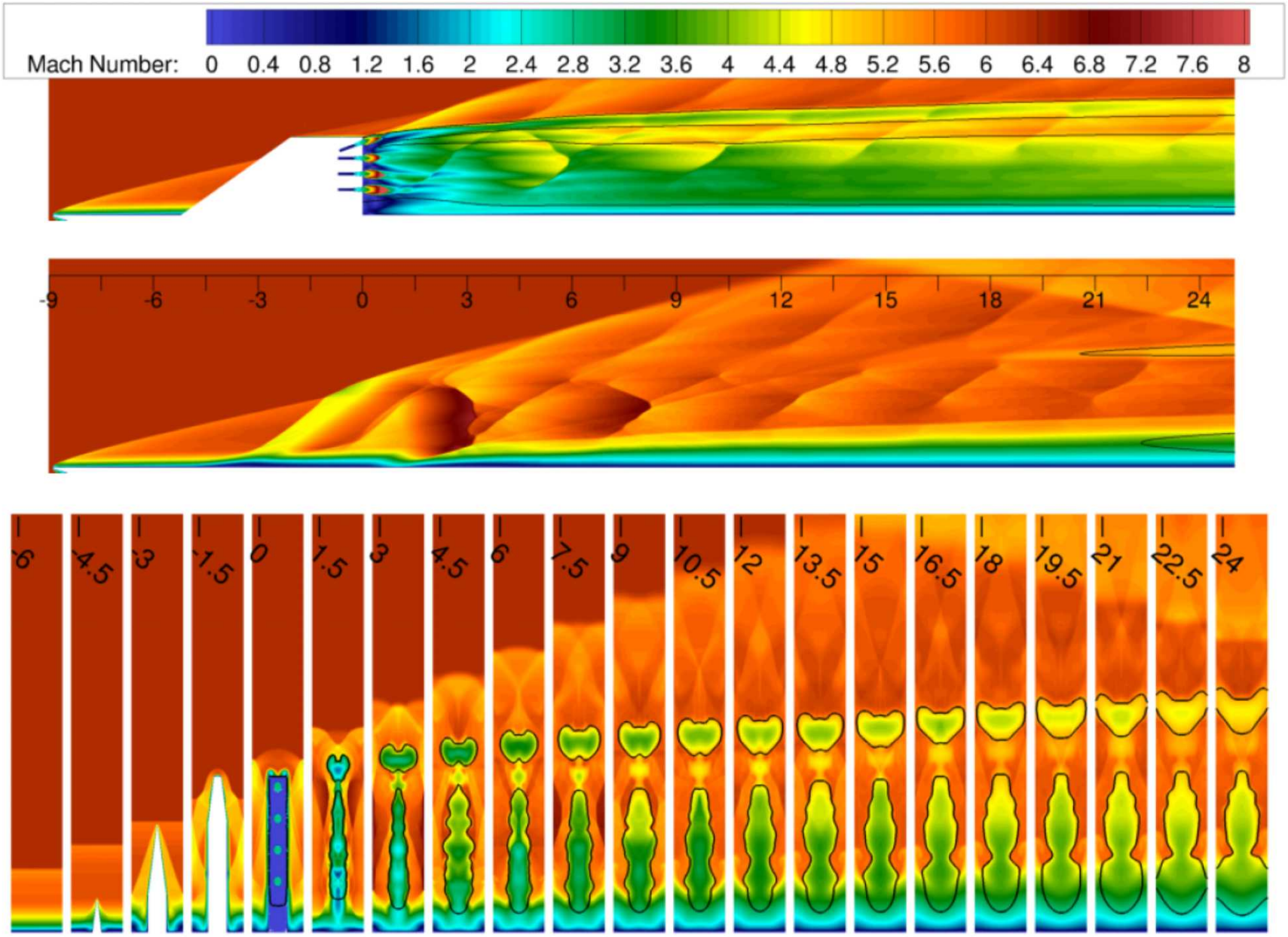
Mach Number: 0 0.4 0.8 1.2 1.6 2 2.4 2.8 3.2 3.6 4 4.4 4.8 5.2 5.6 6 6.4 6.8 7.2 7.6 8
-9 -6 -3 0 3 6 9 12 15 18 21 24
-6 -4.5 -3 -1.5 0 1.5 3 4.5 6 7.5 9 10.5 12 13.5 15 16.5 18 19.5 21 22.5 24

One-Dimensional Integrated Quantities

- All 1-D averages are mass-flux weighted

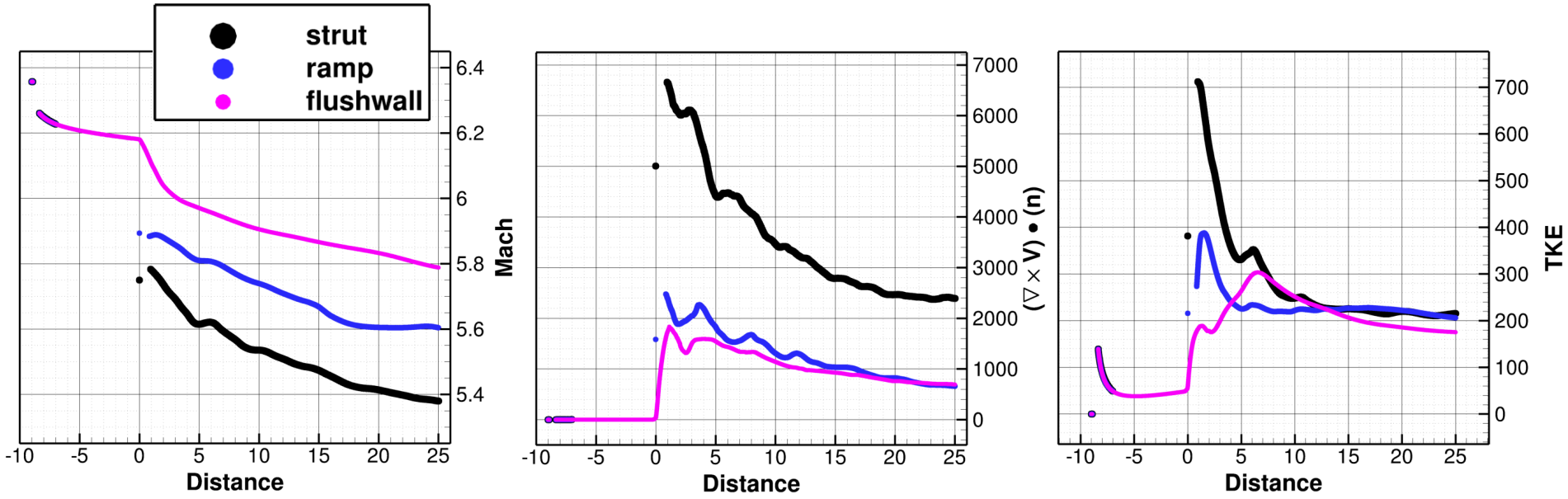

- Strut injectors induce largest decrease in the Mach number and largest increase in the vorticity (or circulation) and turbulence kinetic energy (TKE)
- Ramp and flushwall injectors induce comparable levels of vorticity and TKE
- TKE is comparable among the three injectors in the far field

Reduction in the Mach number is a result of both the viscous drag on the injector bodies (for the strut and ramp) and the induced shock waves. What about injector mixing performance?

One-Dimensional Integrated Quantities

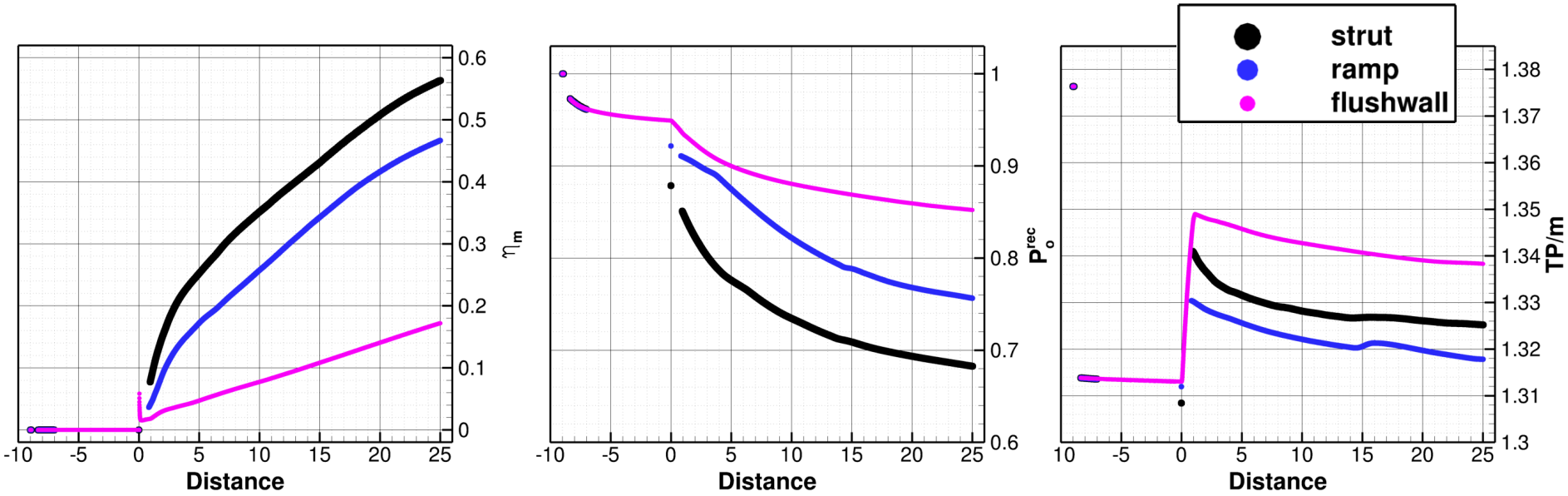

- Strut Injectors
  - have highest mixing efficiency but also the largest total pressure loss (smallest recovery)
  - exhibit rapid mixing in the strut wake region x=0 to 3
- Ramp Injectors
  - despite comparable vortical and TKE features, exhibit better mixing than the flushwall …
  - albeit at the expense of the lower total pressure recovery
- Flushwall
  - have lowest mixing, highest total pressure recovery, and …
  - highest specific thrust potential? (least total pressure loss + largest momentum flux ratio)

Skin Friction and Heat Flux Along Ascent Trajectory

- Injector flat plate was numerically “flown” along a constant-Q ascent trajectory from subsonic to Mach 16 free stream conditions
- As the Mach number increases the skin friction decreases but heat flux increases (heat flux predictions typically require y+ < 0.1)
- Numerically-induced boundary layer transition can be observed
- Flow transition is one of the hardest phenomena to predict accurately (trips)

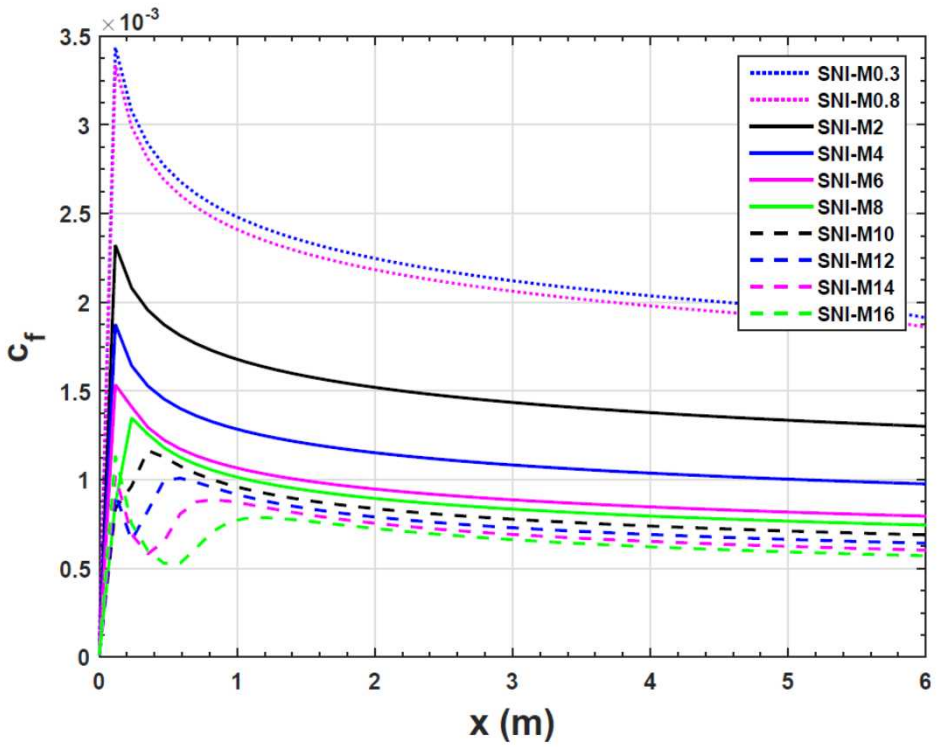

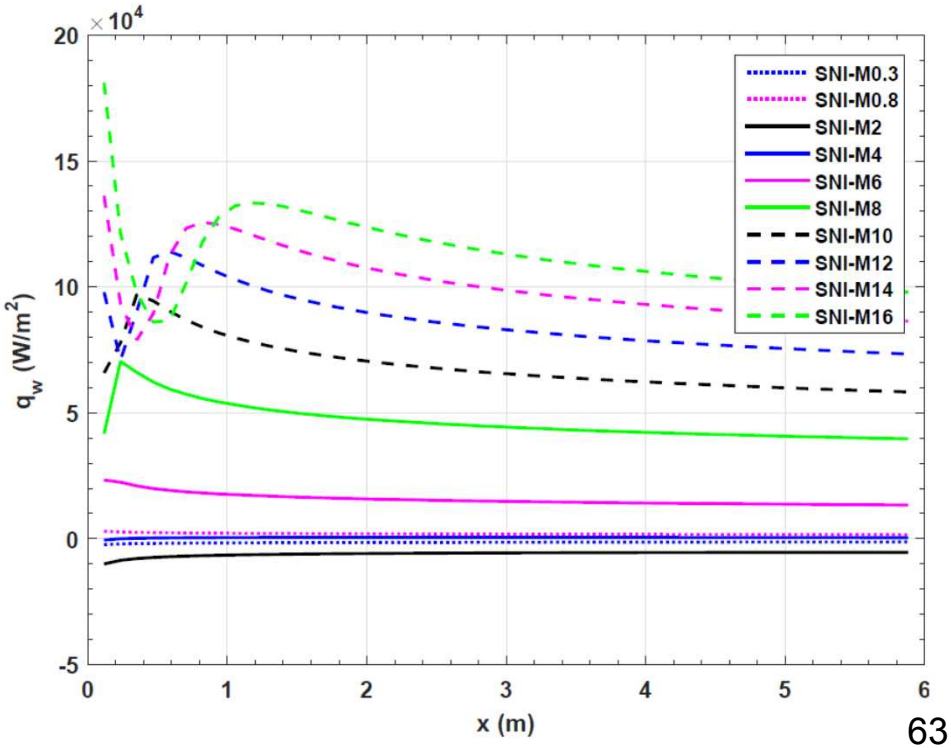

Cross-Stream PLIF and CFI: Strut Injector

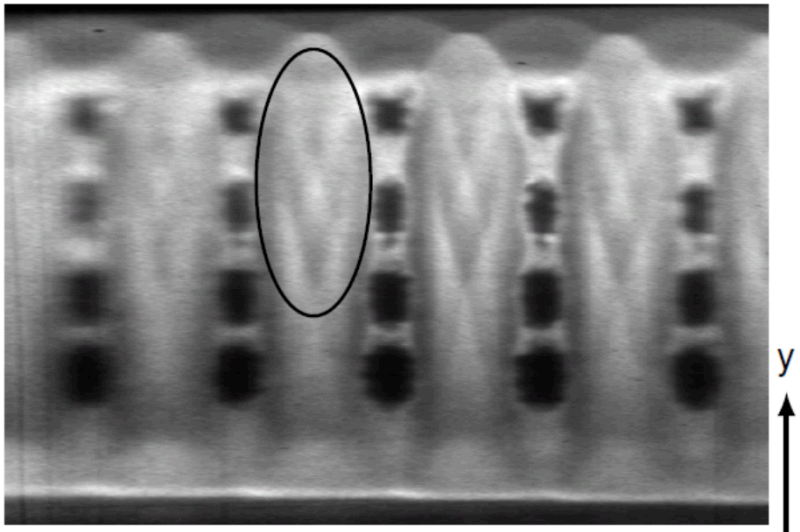

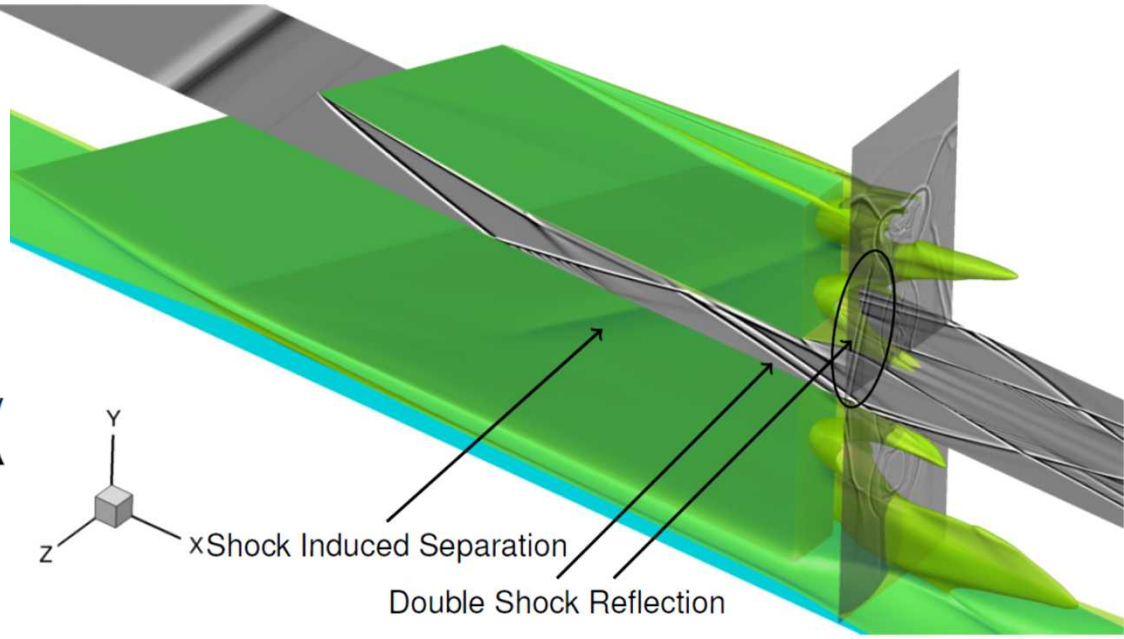

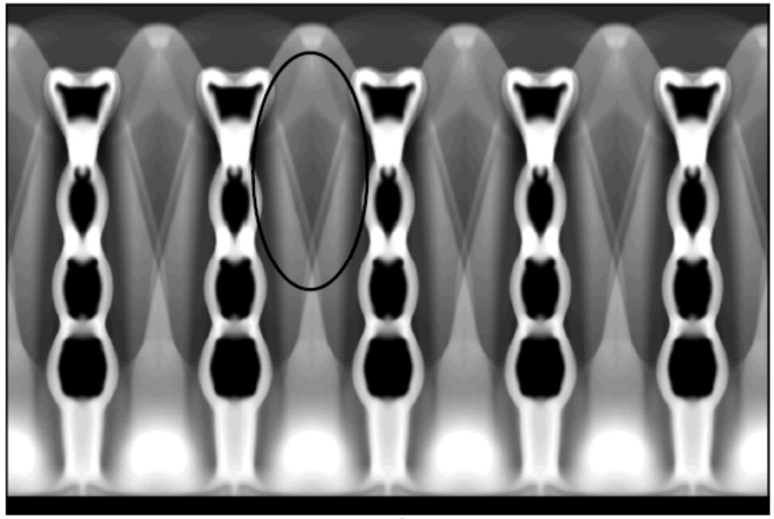

Turbulent Simulation

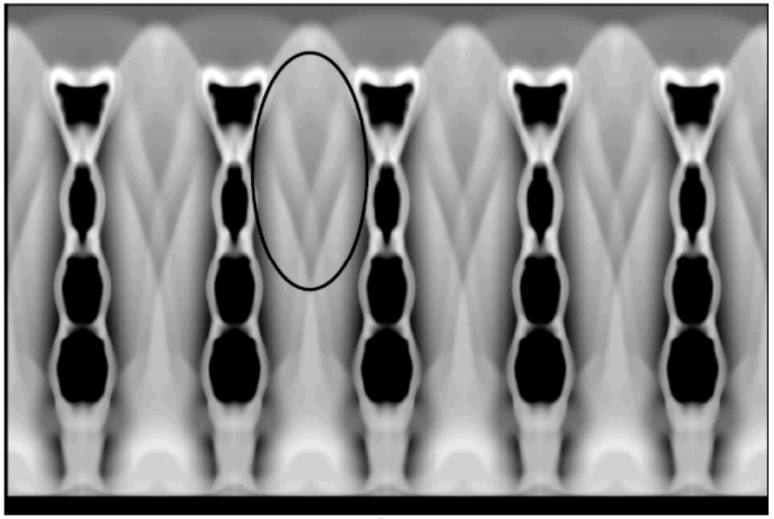

Laminar Simulation

Problem Space Addressed by the CFD

Flight

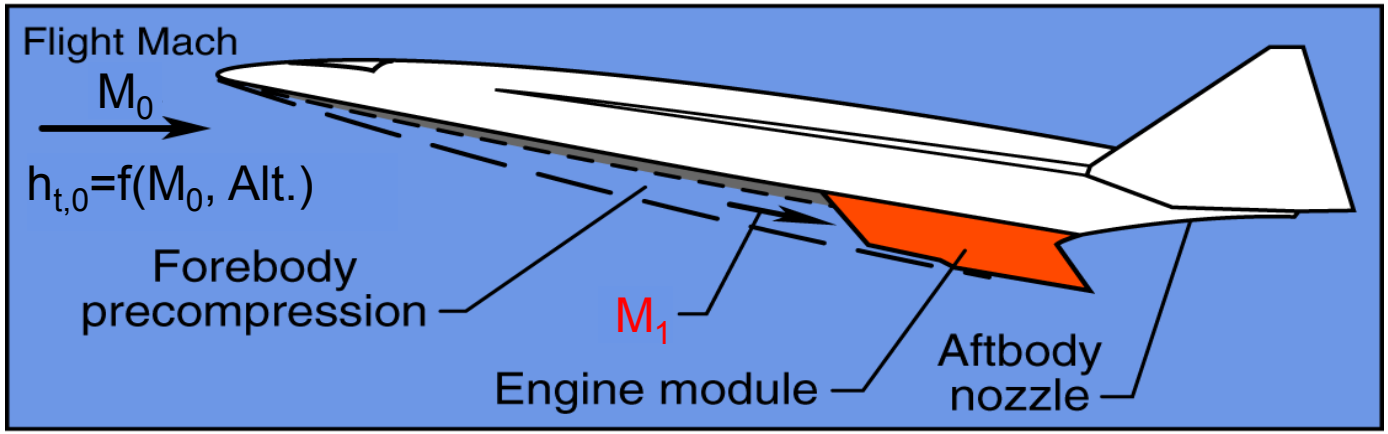

Simulation in ground facility

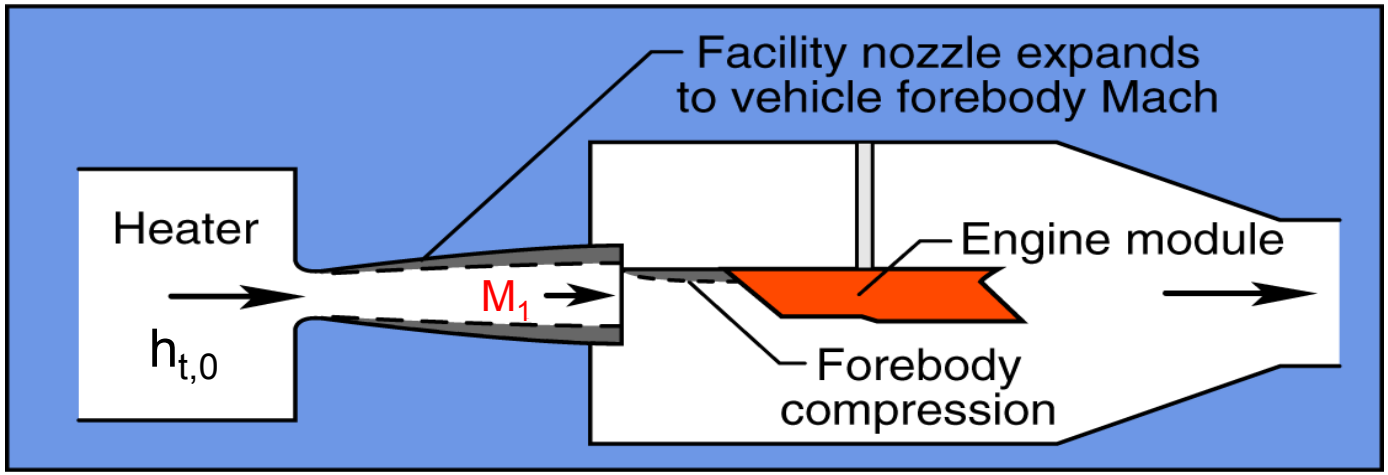

LES Study of Dynamics in the Supersonic Cavity Flow

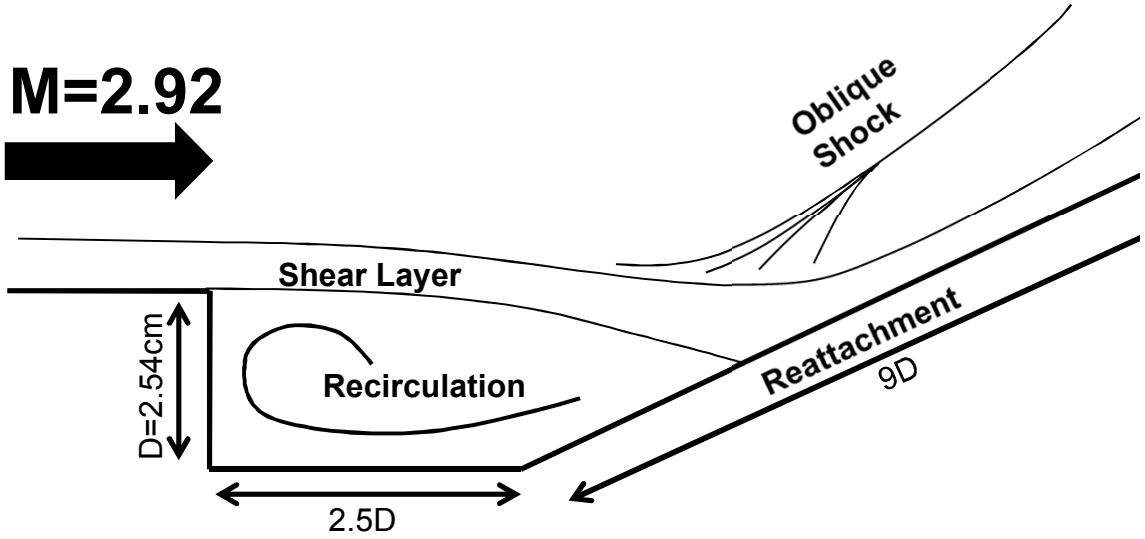

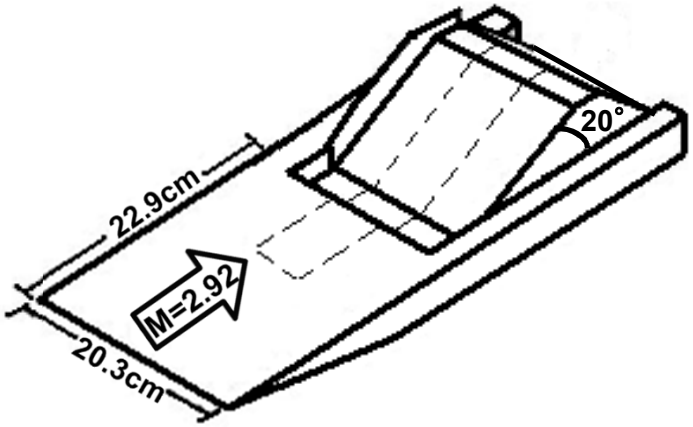

Major flow features of supersonic flow over cavity.

Nominal Test Conditions	
Mach	2.92
Total Temperature	258K
Total Pressure	0.69MPa
Freestream Unit Re	6.7×10^7/m

Microsecond spark shadowgraph. *Settles, et al. (1980)*

Boundary Conditions

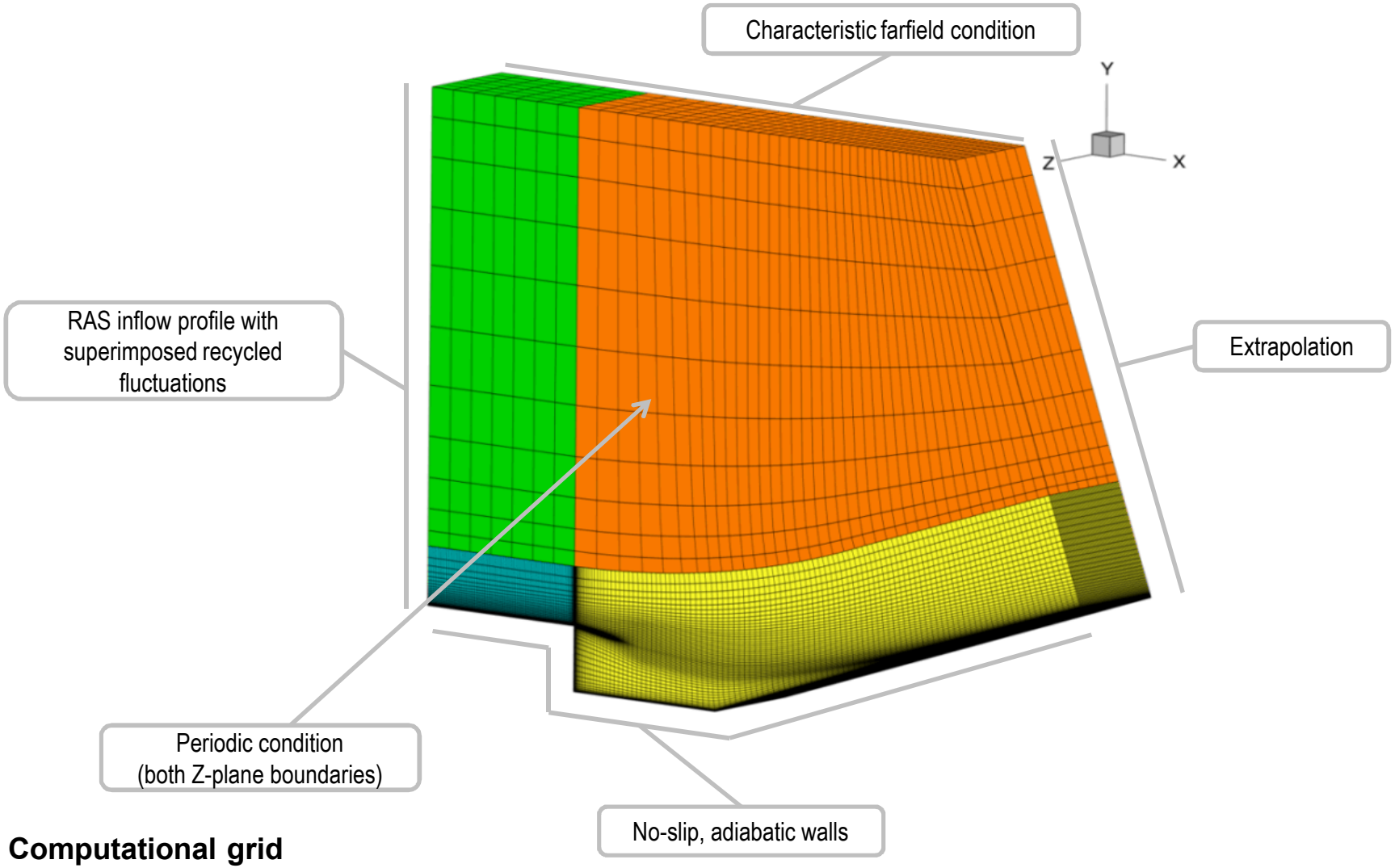

Computational grid coarsened twice for visual clarity.

LES Study of Dynamics in the Supersonic Cavity Flow

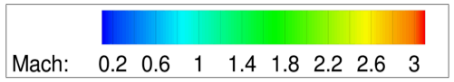

Mach Number

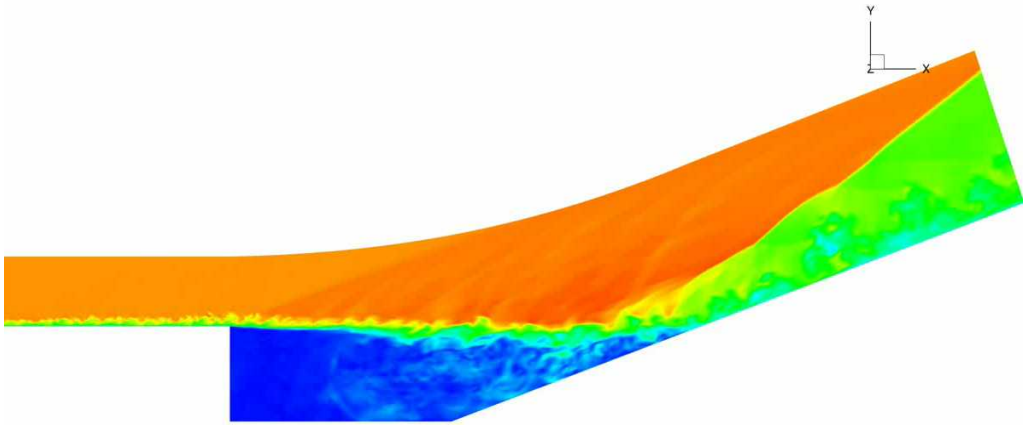

Red: $|\nabla \times V| = 1 \times 10^5 \left[\frac{1}{s}\right]$

Orange: $|\nabla \times V| = 5 \times 10^4 \left[\frac{1}{s}\right]$

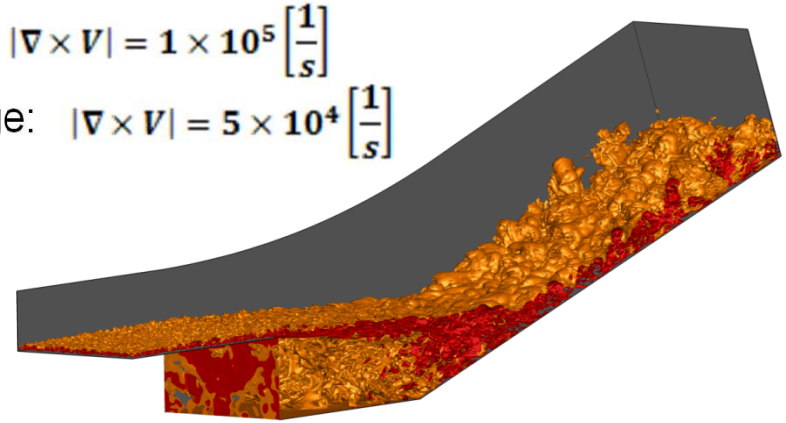

Blending Function

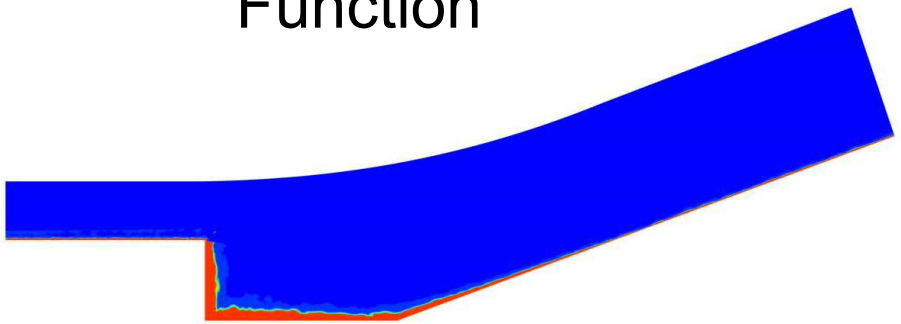

LES Study of Dynamics in the Supersonic Cavity Flow

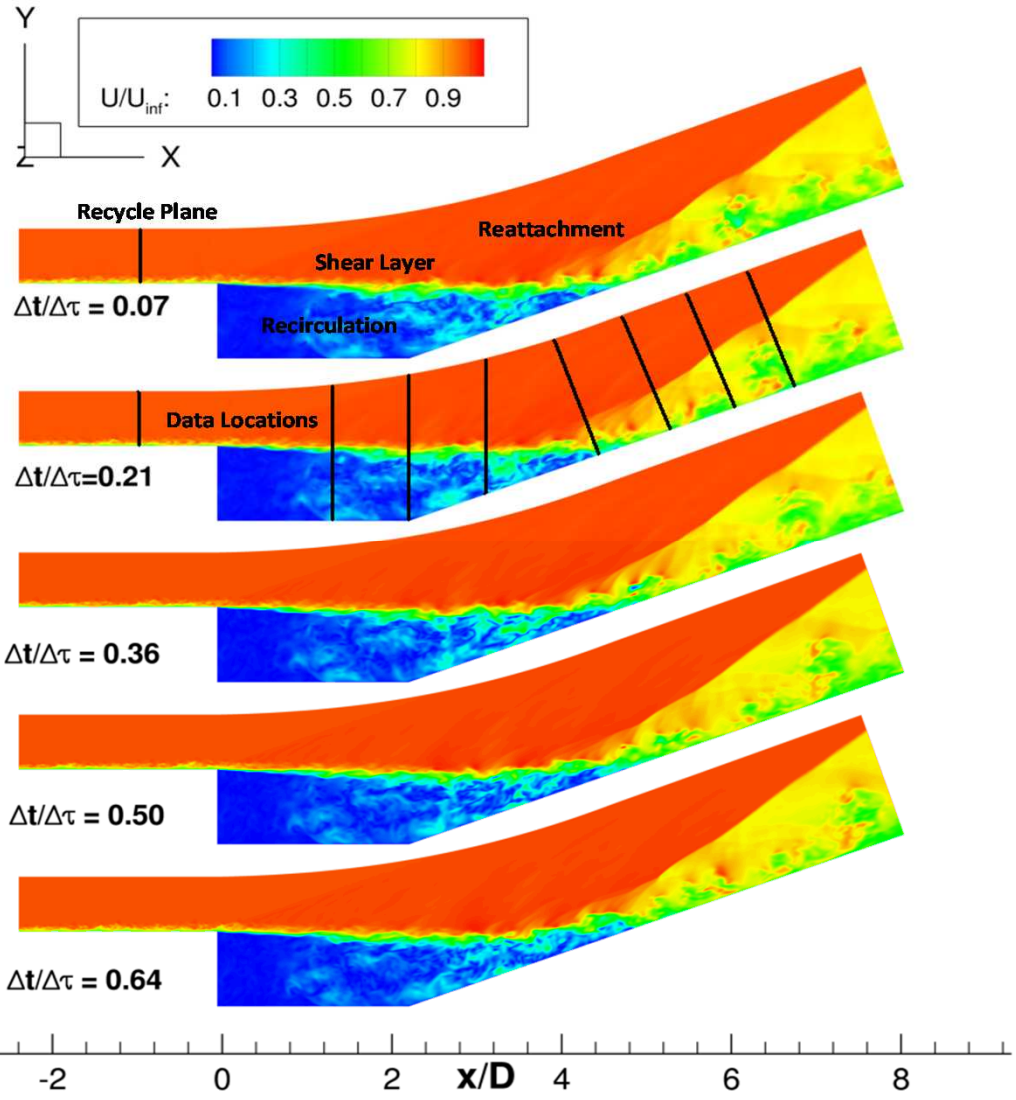

Instantaneous snapshots of velocity with data locations highlighted

Shear Layer Growth Rate

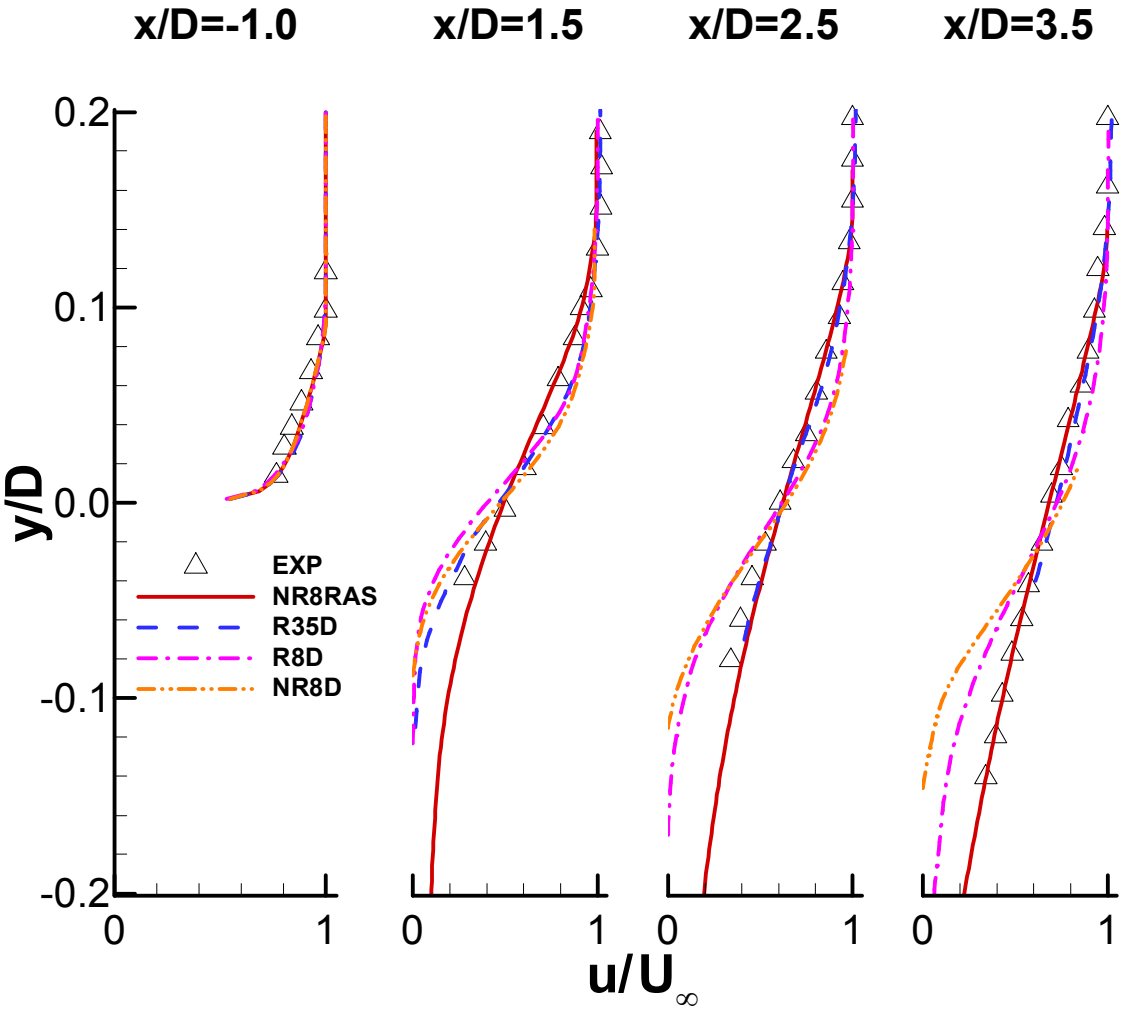

Shear layer velocity profiles shifted to emphasize growth rate.

Grid Refinement

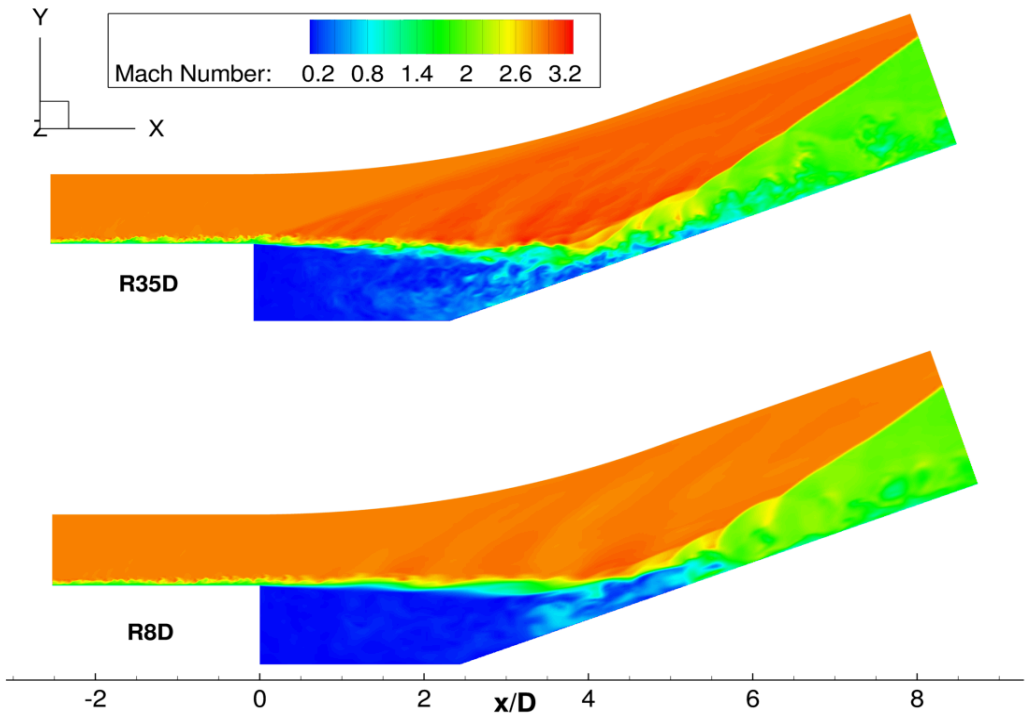

Instantaneous snapshot of Mach number for cases R35D and R8D.

Resolved Turbulent Kinetic Energy (%)			
CASE ID	x/D = 0.7	x/D = 1.1	x/D = 1.9
R35D	*71*	*80*	*85*
R8D	*30*	*36*	*50*

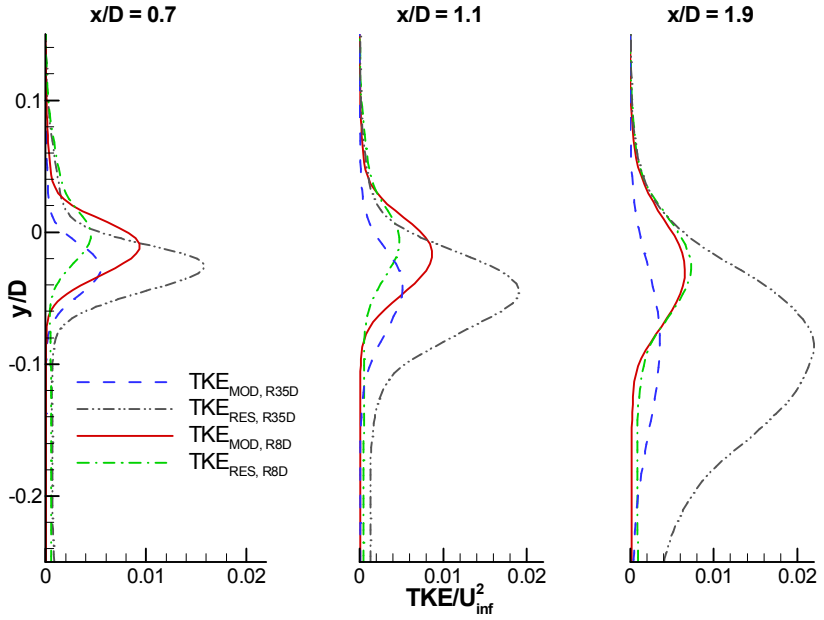

Comparison of TKE contributions for cases R35D and R8D.

Problem Space Addressed by the CFD

Flight

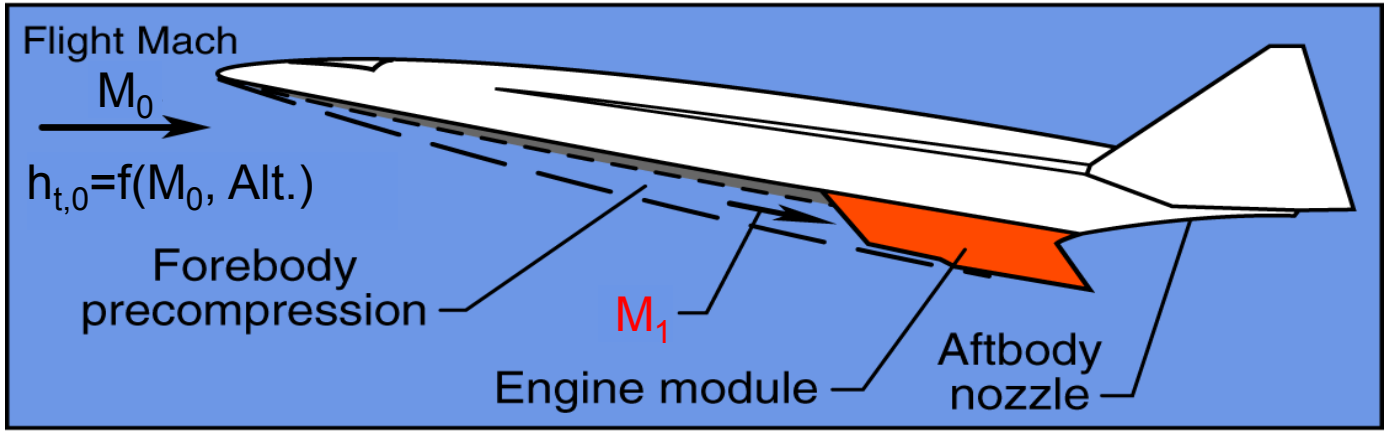

Simulation in ground facility

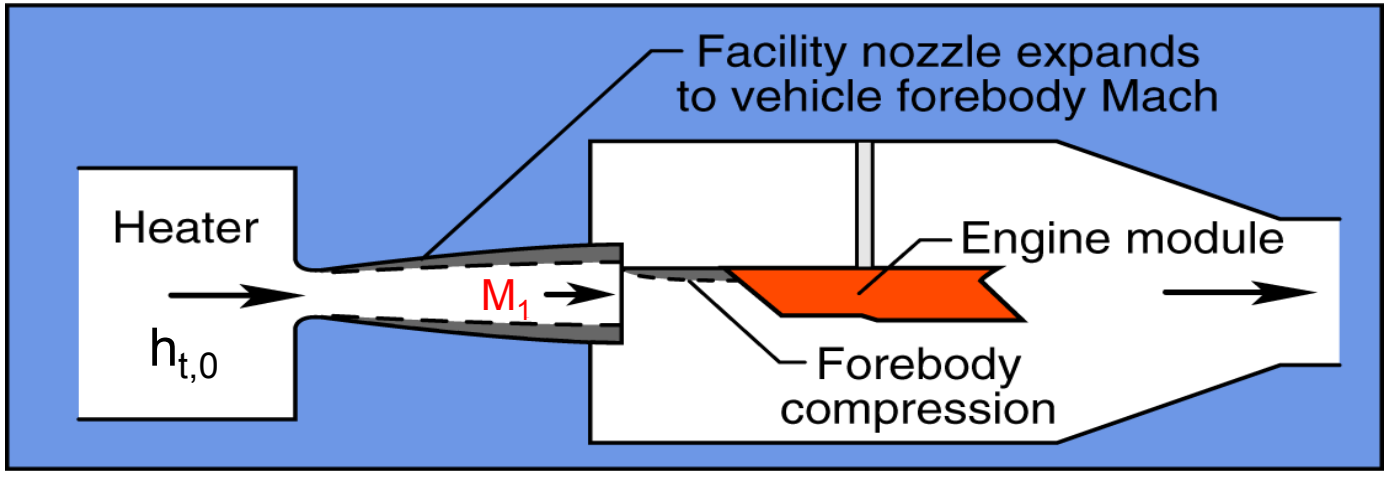

Cavity-Based Flameholder Application

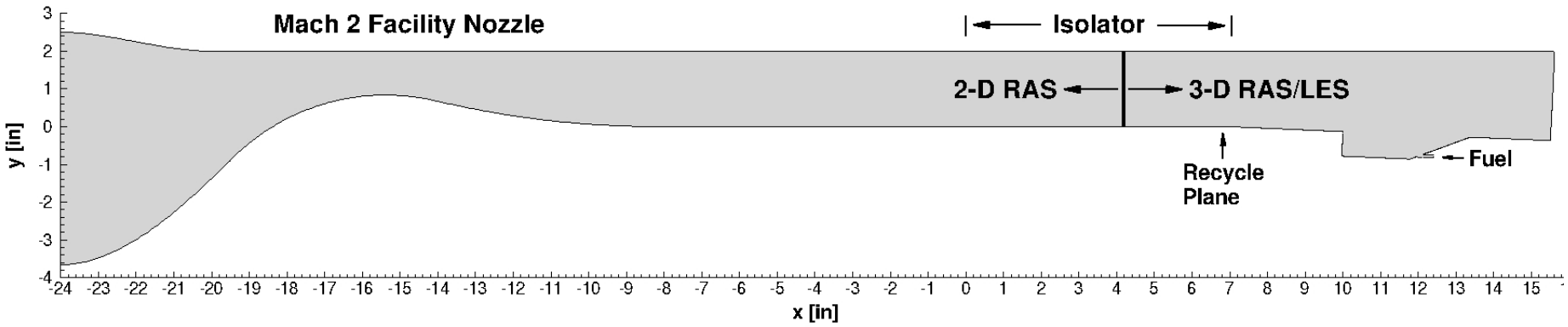

Nominal Conditions	Case 1	Case 2	Case 3
Facility Mach No.	2.0	2.0	2.0
Facility T_o [K]	589.0	589.0	589.0
Facility P_o [kPa]	483.0	483.0	483.0
C2H4 Flow Rate [SLPM]	0.0	56.0	99.0
C2H4 T_o [K]	N/A	310.0	310.0

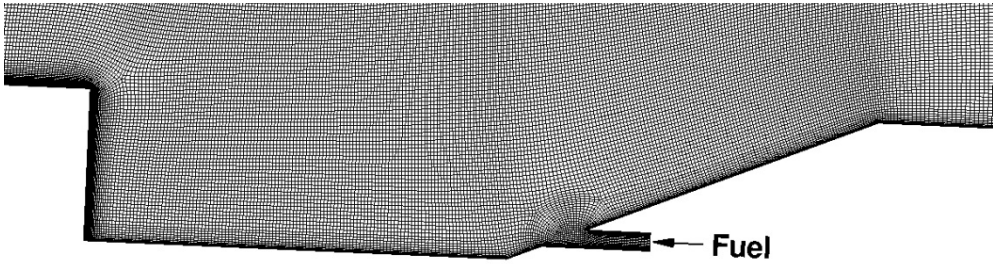

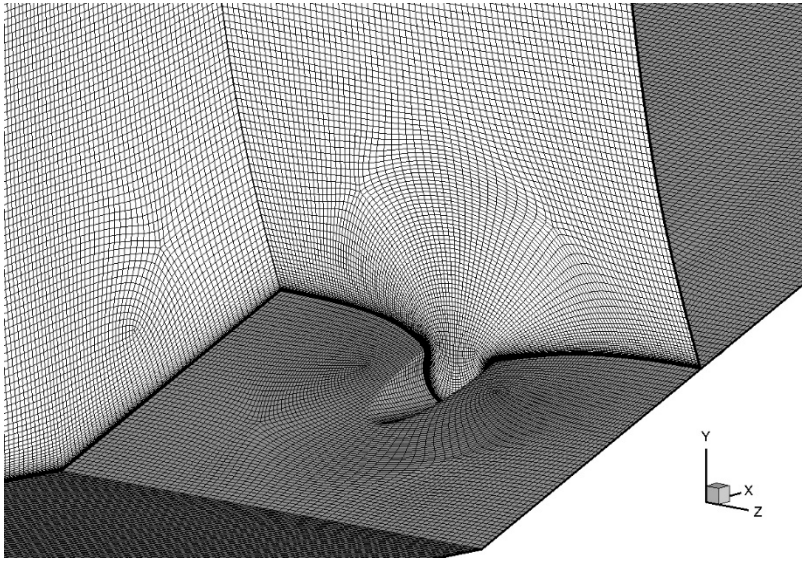

Sensitivity to RAS Turbulence/Mixing Model

Menter-SST

Gatski-EAS

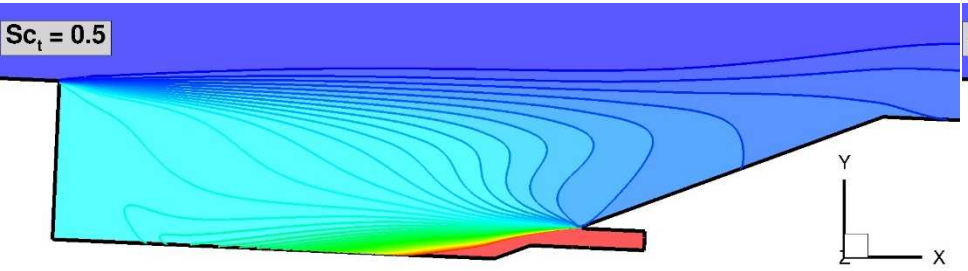

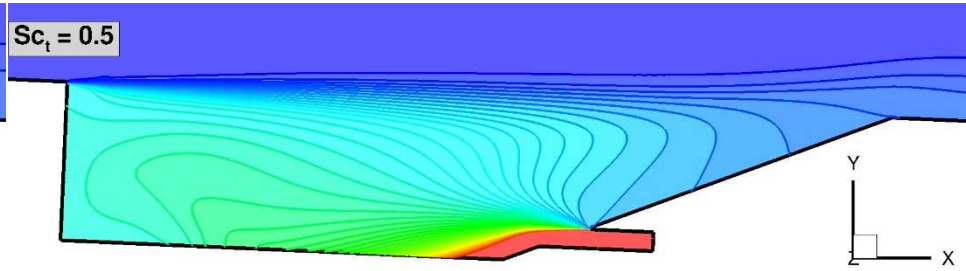

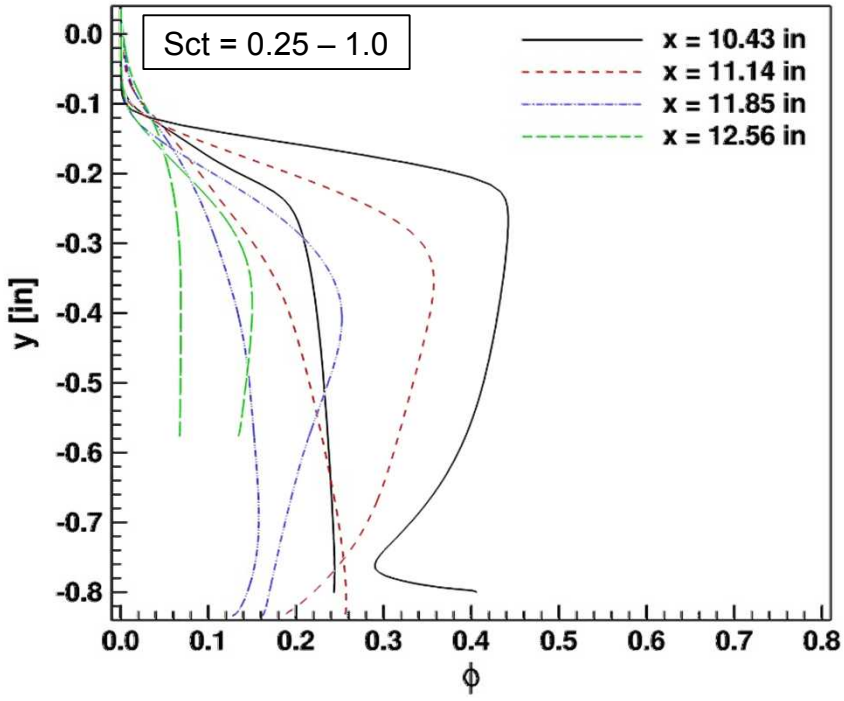

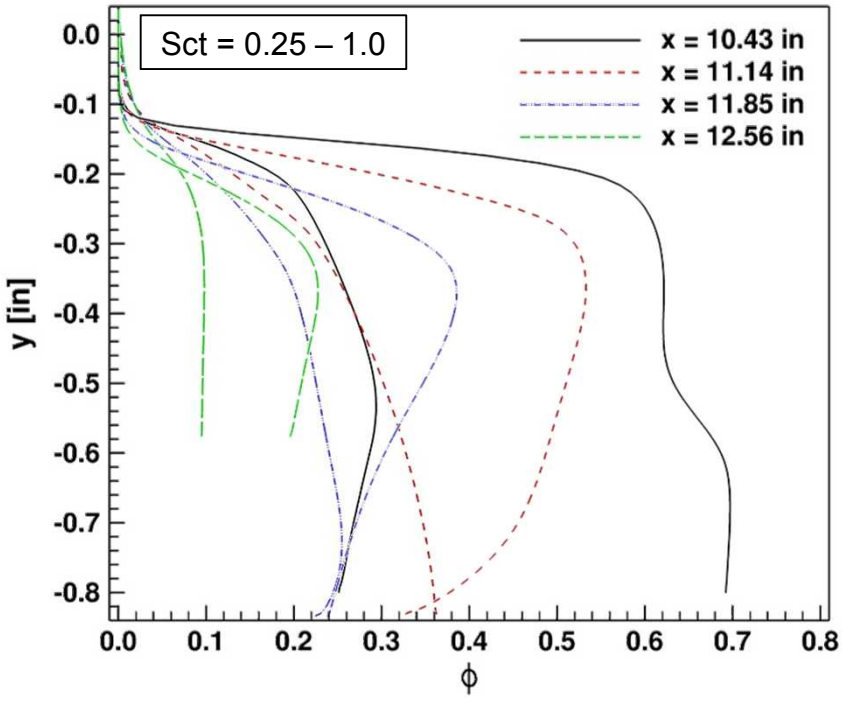

Hybrid RAS/LES Sensitivity to SGS Closures

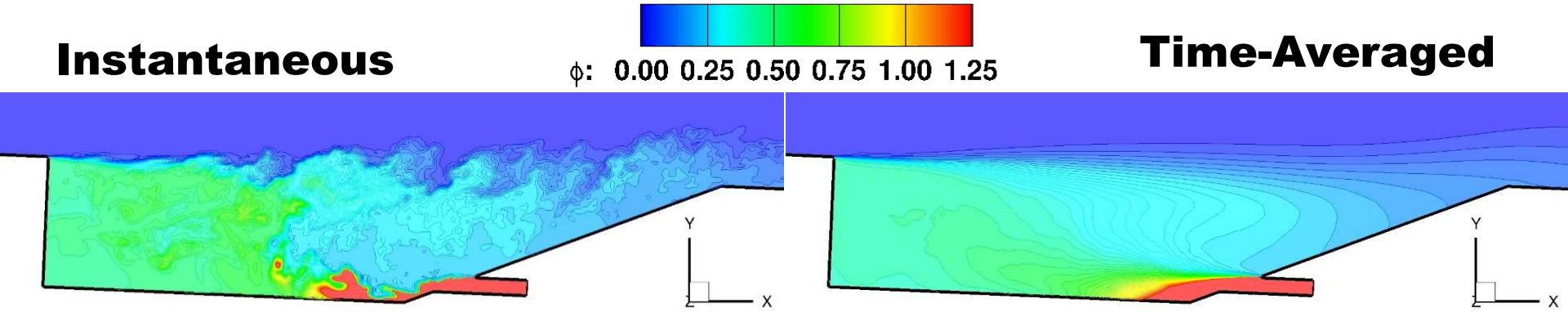

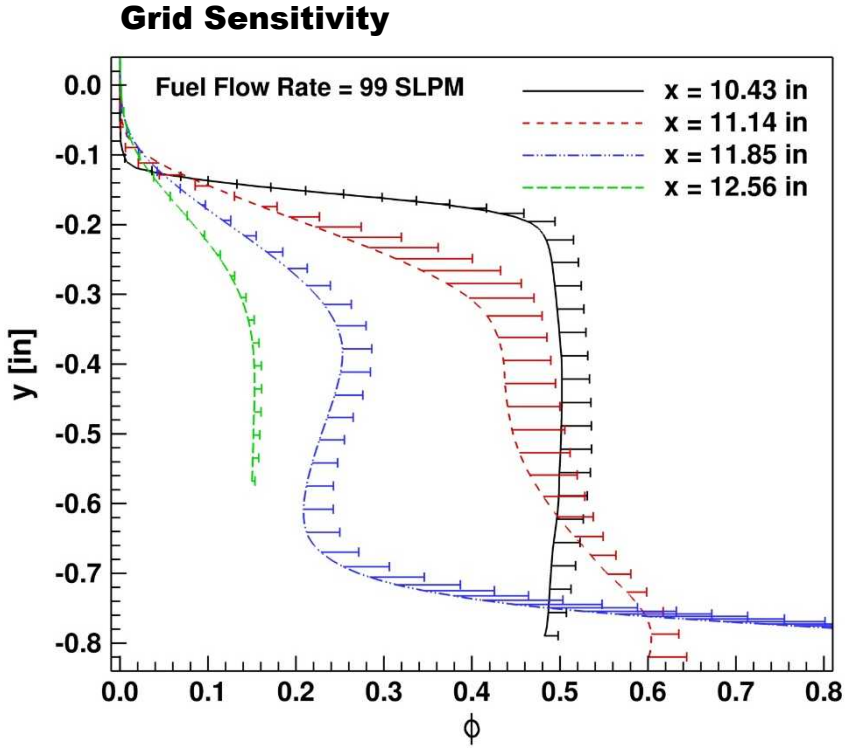

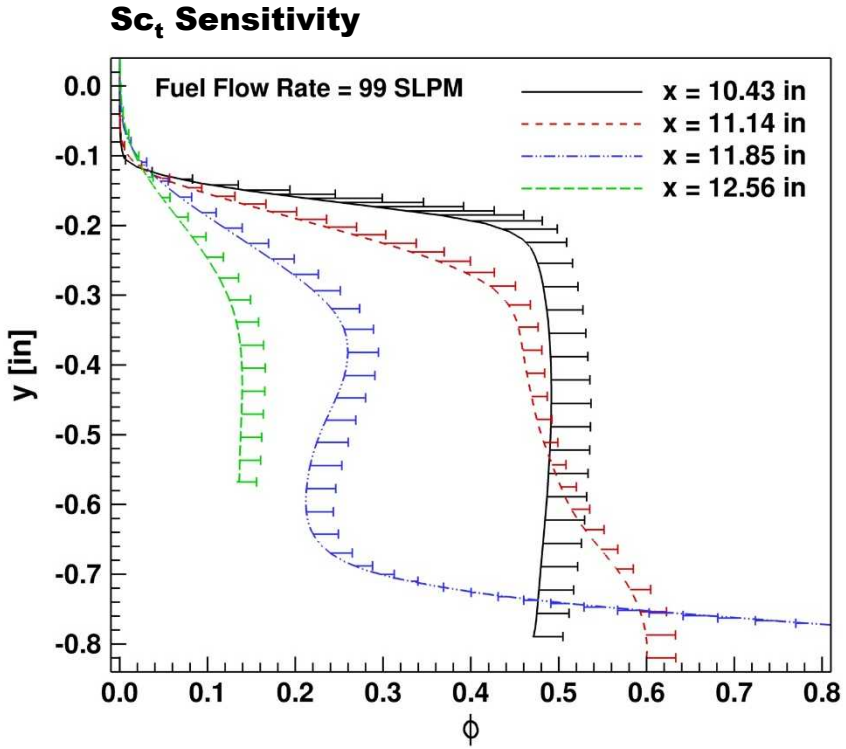

Scramjet Propulsion System

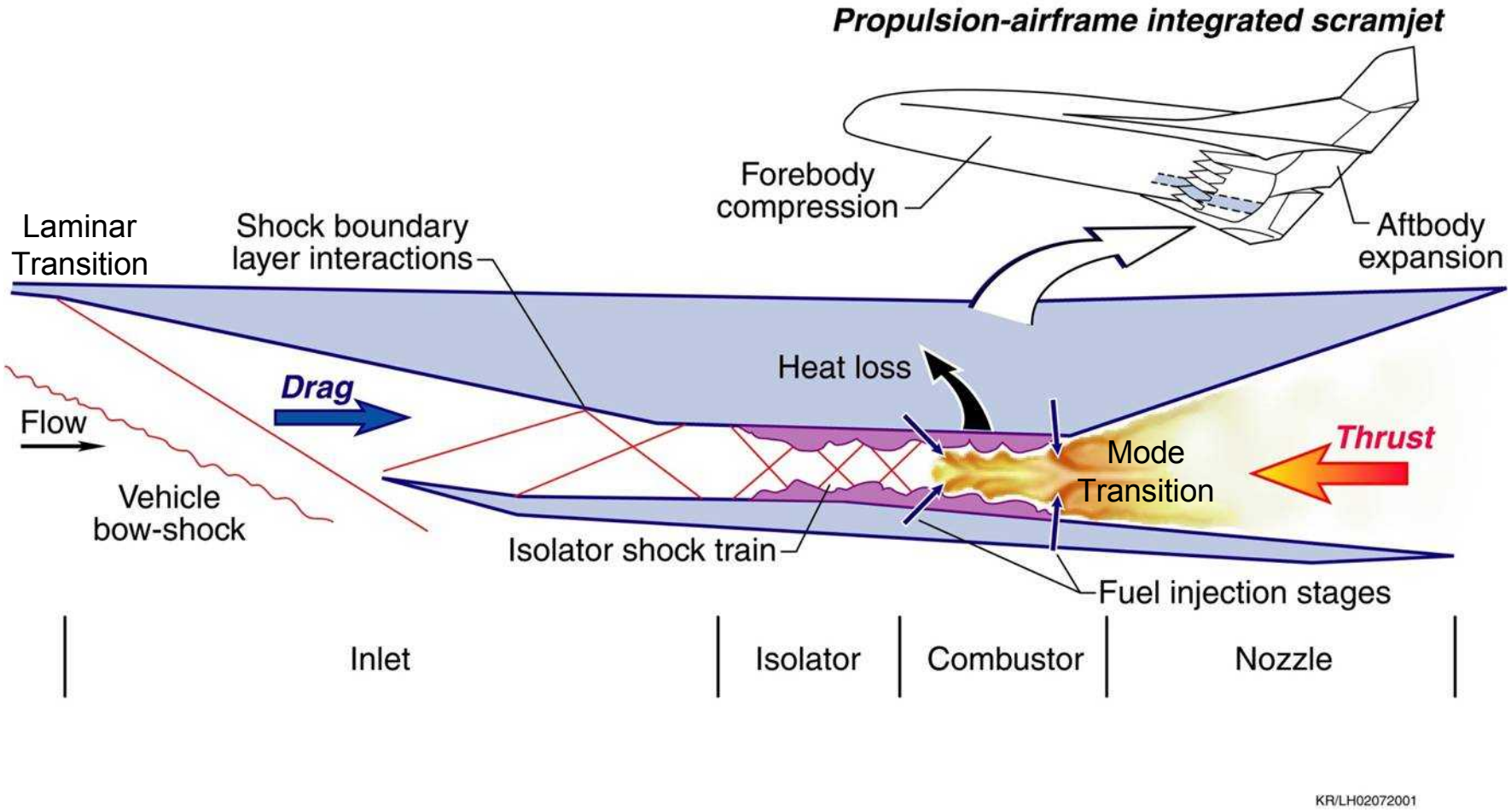

Why CFD?

Question: Don't we have enough practical design experience and physics knowledge to build robust devices?

Answer: Most designers and experienced staff think so … until there are unforeseen difficulties that require detailed (beyond what relevant experiments can provide) understanding of complex multiphysics interactions.

How should CFD be used:

- *At the least,* CFD analysis offers a risk-mitigating strategy that can potentially confirm and/or raise questions about some design well before difficulties are encountered
  - Current state-of-the-art allows CFD to be used effectively in this context because only qualitative accuracy is required
- *At the most,* CFD analysis will be the only tool available and used to evaluate a particular design's performance. This can occur if the experimental and/or design space for practical device are beyond our current capability and experience.

- **Current SoA for CFD analysis of high-speed propulsion flow paths are Reynolds-Averaged Simulations**
  - All scales of turbulence are modeled → often leading source of uncertainty
    - Boussinesq approximation with LEVM
    - Gradient diffusion assumption with constant Pr_t and Sc_t
    - Turbulence-Chemistry interactions neglected (or crudely modeled)
  - Modeling strategy is relatively mature with only "evolutionary" improvements documented over the past 15-20 years → Current focus is primarily on UQ
  - Even vehicle-scale simulations (or matrices of simulations) are computationally affordable for problems of programmatic interest on current supercomputers (typically 1-2 weeks to solution)

- **Scale-Resolved Simulations (LES) have the potential to substantially reduce turbulence model uncertainty (for some models)**
  - Only the smaller turbulence scales are modeled (larger scales resolved)
  - Model form uncertainty (related to turbulence) can be reduced with grid resolution
  - Computational cost about 100 times that of above RAS

Path Forward

- Continue to leverage RAS capabilities in design and analysis of high-speed reacting flows while systematically investigating modeling sensitivities on a case-by-case basis
  - Higher-order closures for the Reynolds stress tensor may prove beneficial for the shock-dominated internal flows prevalent in high speed propulsion devices
- Utilize LES (keeping large computational costs in mind):
  - to improve understanding of physical interactions (universities are doing this)
  - to investigate impact of unsteady effects
  - for cases (configurations and operating conditions) exhibiting high sensitivities
  - for isolated key flight conditions near operability bounds (we need to know these)
  - to reduce model-form uncertainty with RAS
- Improvements in predictive fidelity of LES over RAS must still be demonstrated
  - Are current LES SGS models sufficient for simulations of highly compressible flows?
  - Can we utilize LES as “truth” when experiments are unavailable?
- Questions?

RAS continues to be the dominant tool for high-speed reacting flow analysis


AIAA
Shaping the Future of Aerospace
NASA
HAPB

Additional Slides

Branch Mission & Functional Disciplines

Branch Mission: **perform multidisciplinary research to develop advanced technology for hypersonic airbreathing propulsion systems for aerospace vehicles. Focus on airframe-integrated engine concepts having high performance over a wide Mach range.**

Physics Model Development: **develop, implement, and validate Computational Fluid Dynamics (CFD) models for the design, prediction and assessment of the performance of hypersonic air-breathing propulsion systems and system components.**

Numerical Methods and Code Development: **develop and implement enhanced numerical methods appropriate for the simulation of highly compressible flows with shocks and finite-rate chemistry.**

Code Application: **provide state-of-the-art hypersonic airbreathing propulsion system design, analysis, and optimization capability in support of NASA's high speed full-scale vision vehicle development, subscale flight demonstrators, and associated ground tests**

Experimental Airbreathing Propulsion: **develop and apply state-of-the-art hypersonic airbreathing propulsion test techniques for the NASA Langley Scramjet Test Complex and advance facility flight simulation capabilities. Develop comprehensive development, demonstration and verification test plans for national flight demo programs utilizing the national test infrastructure and capability.**

Vehicle Configuration Development & Optimization: **design, development and optimization of ramjet/scramjet flowpaths for a given vehicle and mission, flowpath/engine performance analysis and operability assessments, design and analysis tool development, and the projection of ground test data assessments to the requisite flight environments.**

Flight Test: **PI role on flight experiments and support major flight demonstrations, develop flight test approach, ensure science and/or demonstration objectives are met, develop flowpath and subsystem requirements to ensure operability and performance goals/requirements are met, develop measurement and instrumentation requirements.**

Scramjet Propulsion System

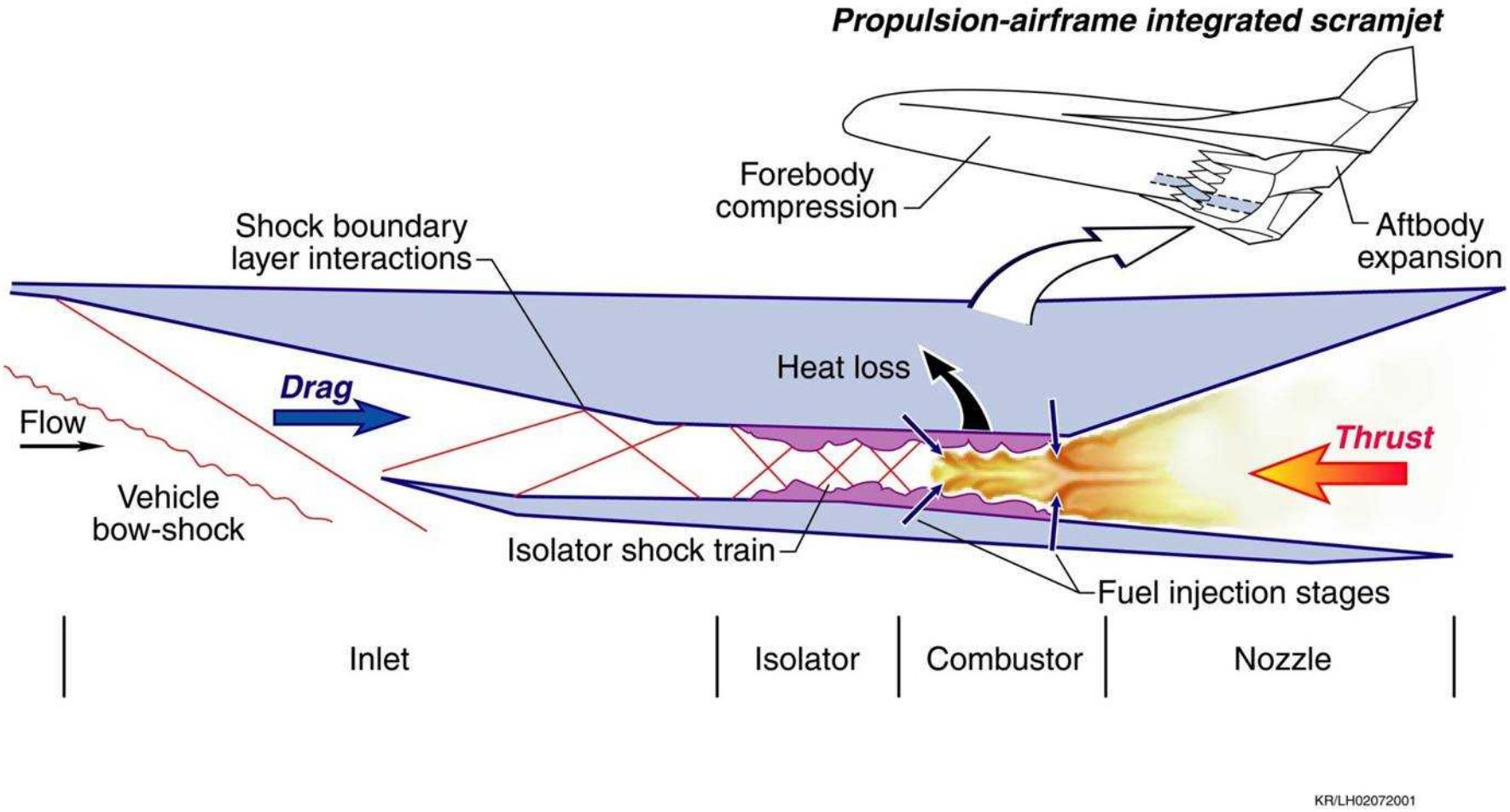

Scramjet Propulsion System

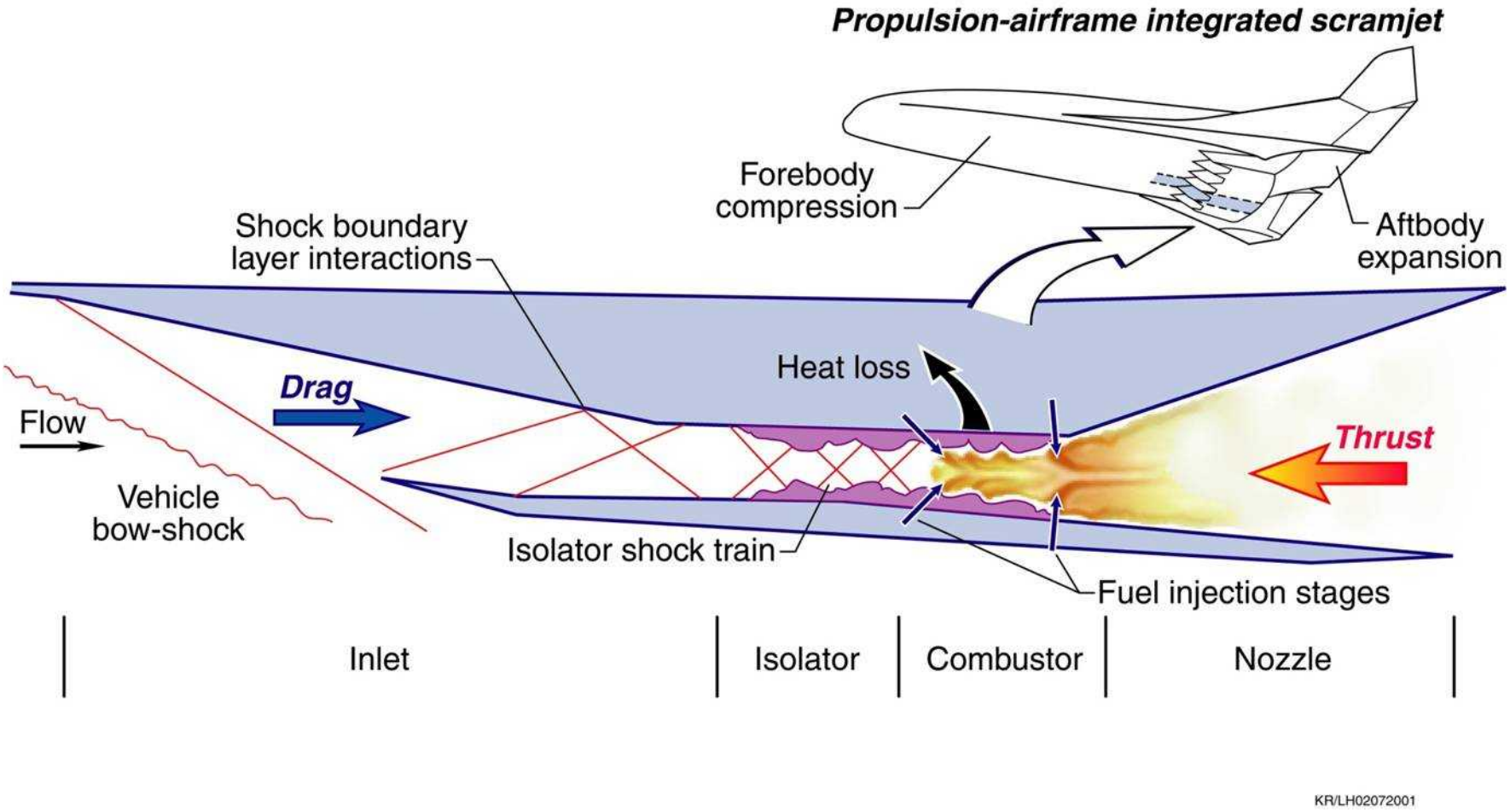

HIFiRE2 Direct Connect Rig (HDCR) Experiment

Sounding rocket used for HIFIRE flight

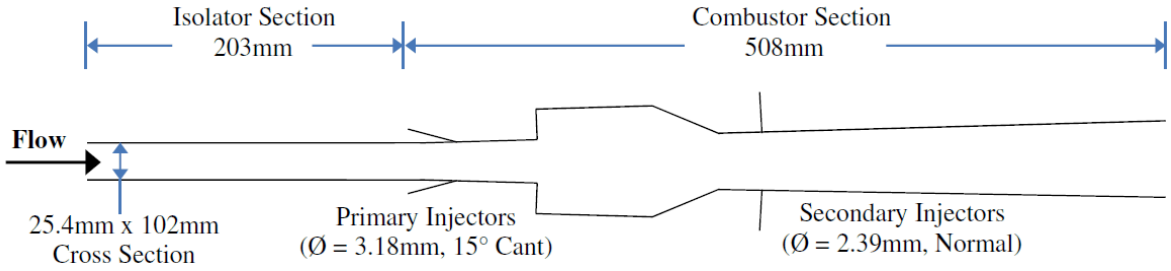

HDCR combustor mold line.

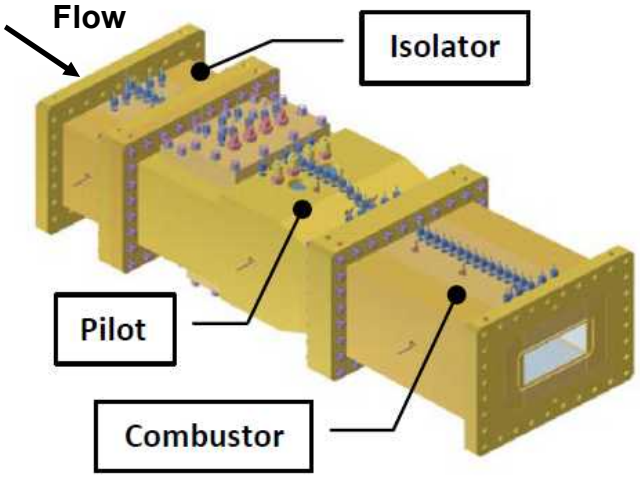

HDCR combustor experimental rig

- Tested in the NASA LaRC Arc-Heated Scramjet Test Facility [10] in support of HIFiRE flight experiment
- Primary test objectives included developing fuel splits for:
  - Sufficient unstart margin
  - Successful dual-mode transition
  - Scram-mode operation at $\phi > 0.7$
- Employed 144 static pressure ports and 19 surface thermocouples
- Data collected at numerous test points spanning simulated flight Mach numbers 5.84-8.0

HIFiRE2 Direct Connect Rig (HDCR) Experiment

Dual Mode

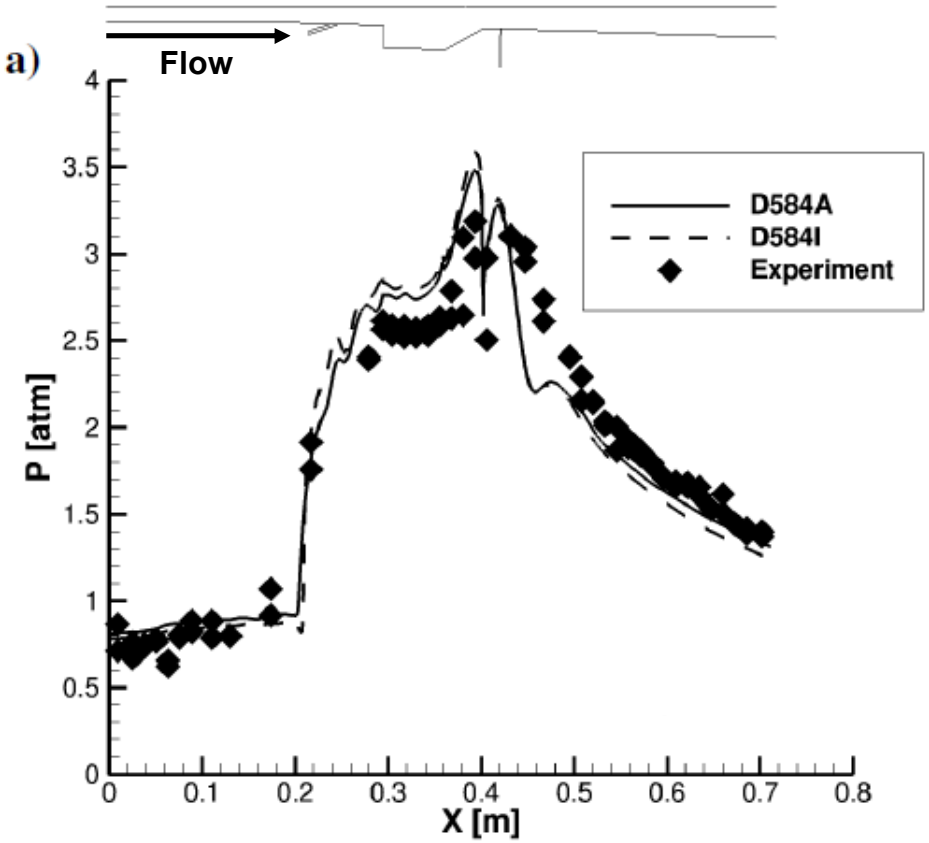

Scram Mode

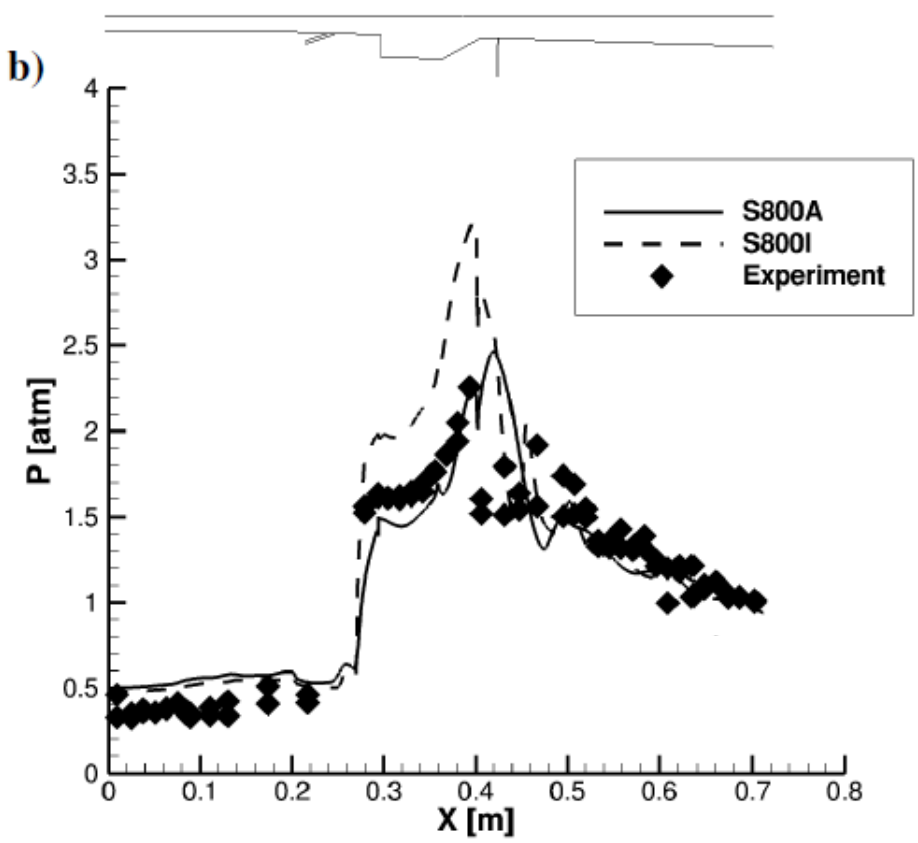

Current RAS appear to correctly model the heat release in the flowpath since the heat release is responsible for the pressure rise

HIFiRE2 Direct Combustor Rig (HDCR)

Mach Number

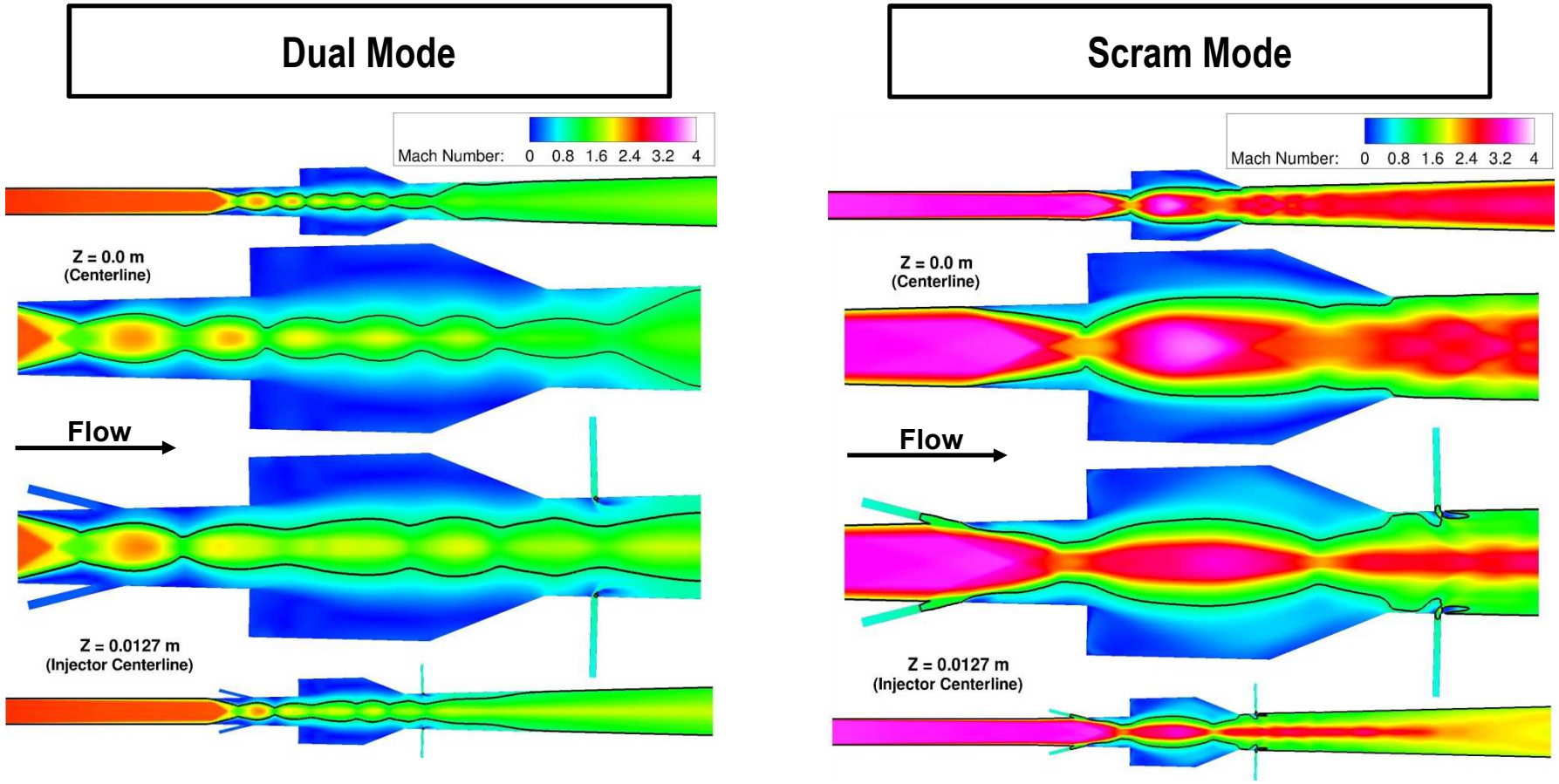

The position of the leading shock shifts downstream from the primary injector after transition from dual to scram mode

HIFiRE2 Direct Combustor Rig (HDCR)

Heat Release Rate

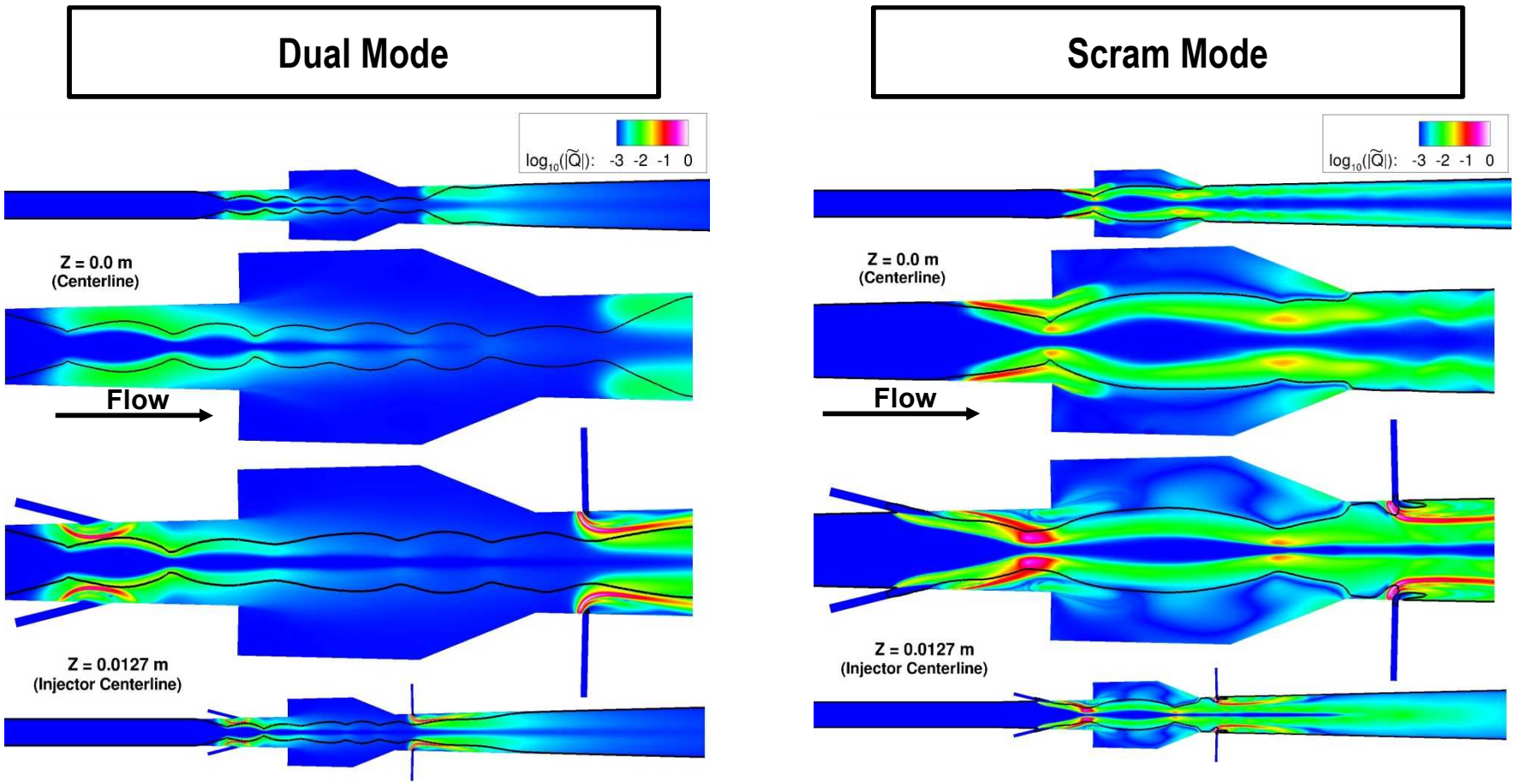

Contours of the normalized heat release rate suggest dominance of subsonic combustion for dual mode operation and supersonic combustion for scram mode

HIFiRE Direct Combustor Rig (HDCR)

Flame Index

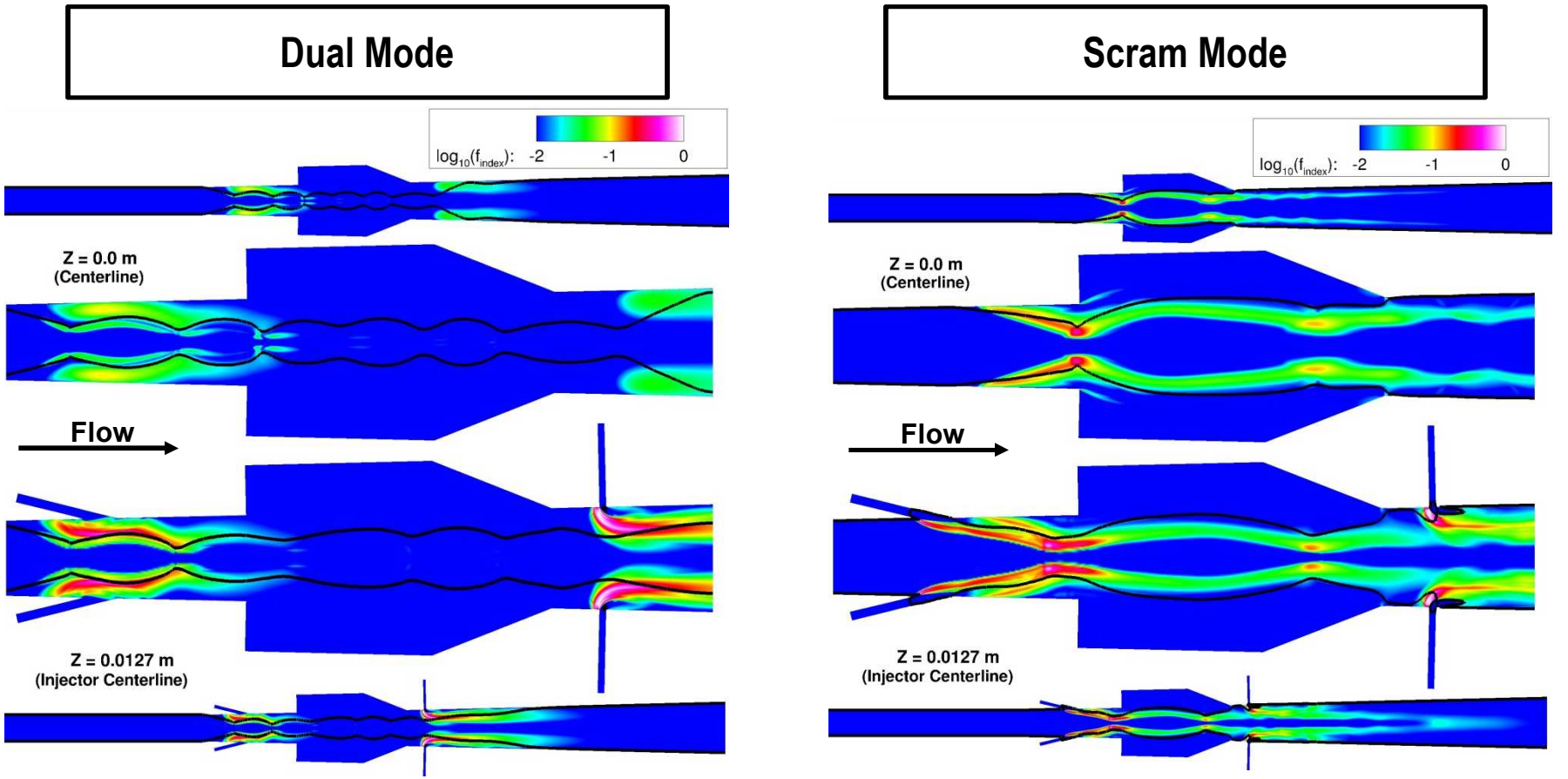

Flame index contours are consistent with the normalized heat release rate suggesting dominance of subsonic combustion for dual mode operation and supersonic combustion for scram mode

Injector Testing for Hypervelocity Mixing

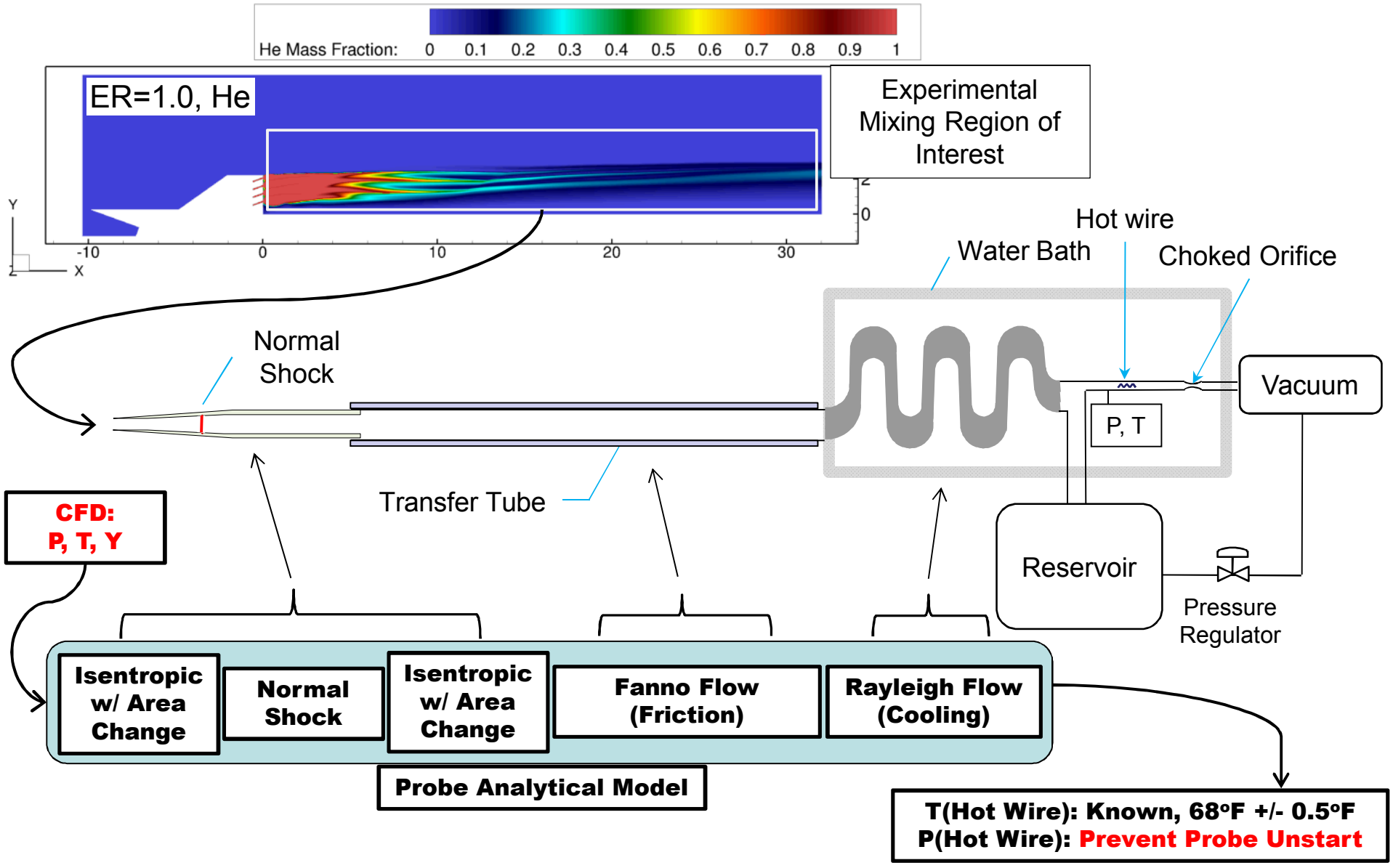

Durable Combustor Rig (DCR)

Carbon Matrix Composite (CMC) Panel Testing for Scramjets:

X-43C Engine (GDE-2) and Forebody in the 8ft HTT

Toward Predictive Use of CFD for Design and Development of Propulsion Devices

Large Eddy Simulation (LES)

Submodel Research and Development

Device Validation Experiments

Direct Numerical Simulation (DNS)

Submodel Validation Experiments

Turbulent Flame Experiments

Unsteady Laminar Flame Simulations

Mechanism Reduction

Ab Initio Chemical Kinetics Simulations

Mechanism Development

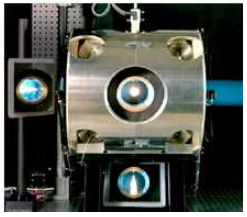

Detailed Device Models

- e.g., Gas Turbines, IC Engines, Rockets, SCRAMJET

Mechanistic Experiments

Kinetic Experiments

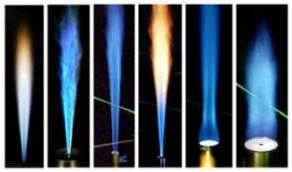

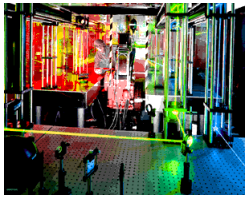

Chemical Dynamics Theory

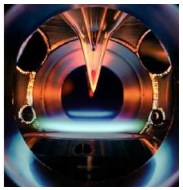

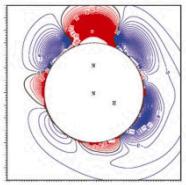

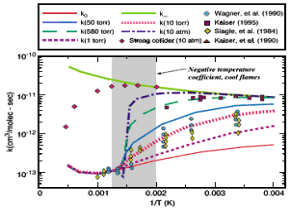

Questions?